

## JOURNAL ARTICLES

Adsorption of Carbaryl by River Sediment from an Acetone Solution: Apparent Thermodynamic Properties

*M. F. Zaranyika<sup>1</sup> and P. Ncube*

Creation of the Universe from a non classical space-time state

*M.G. Okeyo, M. N Maonga, M. J Otieno*

Electron Transfer Properties of 2-acetylferrocenyl-2-thiophenecarboxylsemicarbazone and its Copper (II) Complex

*P.M. Guto, J. M. Kiratu, L. S. Daniel, Enos M. R. Kiremire, G. N. Kamau*

Model for the Estimation of Initial Conditions in a Conflict Environment

*V.O. Omwenga, M.M. Manene and C.B. Singh*

Initial Correlations among the Levels of Various Nutrient Species in Water from Nairobi Dam, Kenya

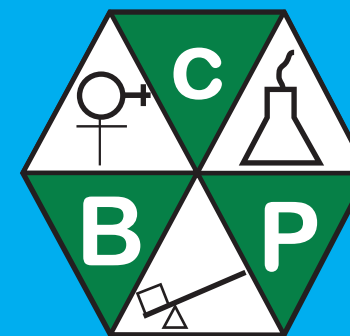
*P.G. Muigai, P. M. Shiundu, F. B. Mwaura and G. N. Kamau*

Estimation of Binding Ratio between Colloidal Gold Particles and Thiourea from Surface Studies

*S. A. Mbogo, A.Y. Ngenya and L.L. Mkyayula*

## REFEREES

Dr. K.AL - Sabati (Canada), Prof. J. Barongo (Kenya), Prof. C.R. Das(India), Prof. T.C. Davies (Nigeria), Dr. S. Derese (Kenya), R.O. Genga (Kenya), De. L.N. Gwaki (Kenya), Prof. S.M. Kagwanja (Kenya), Prof. C.N. Warui (Kenya), Prof. E.M.R. Kiremire (Namibia), Prof. M. Kishimba (Tanzania), Dr. M. Kumar (Kenya), Dr. H.M. Kwaambwa (Botswana), Prof. M. Mammino (South Africa), Dr. S.A. Mbogo (Tanzania), Dr. G. Morris (U.S.A), Dr. B. Munge (U.S.A), Prof. J.B. Mwaura (Kenya), Dr. J.C. Ngila (South Africa), Prof. L.W. Njenga (Kenya), Dr. N.C. Njoroge (Kenya), Prof. W.M. Njue (Kenya), Dr.F.Njui (Kenya), Dr. S. Nyanzi (Uganda), Dr. J.B. Sreekanth (South Africa), Prof. A.H.S. El-Busaidy (Kenya), Prof. H. Ssekaalo (Uganda), Prof. Dr. A.K. Yagoub (Sudan), Dr.A.O. Yusuf (Kenya), Prof.A. Yenesew (Kenya), Prof. M. Zaranyika (Zimbabwe) and Prof. H. Zewdie (Ethiopia).



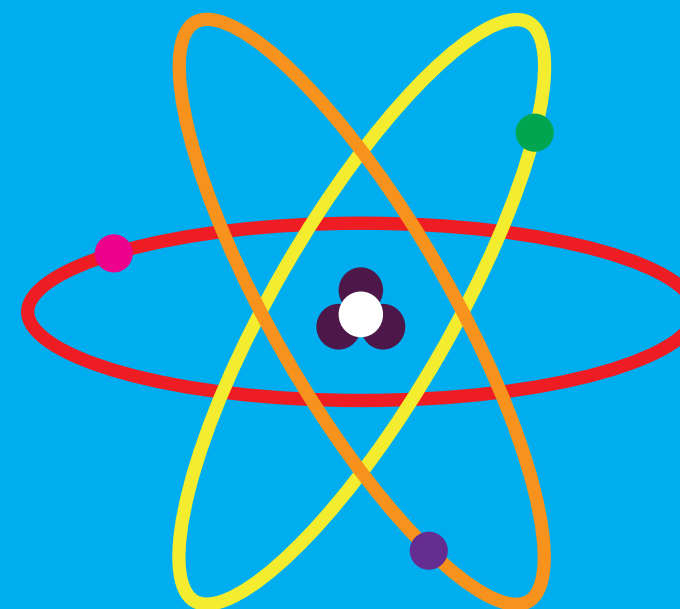
# International Journal of BioChemistryPhysics

Volume 19

ISSN 1019-7648

July 2011

## ATOMIC ENERGY



The atom contains a central heavy mass, called the nucleus, which in turn is surrounded by lighter particles (electrons).

Everything, including ourselves, in the Universe is made up of the same building block, that is the atom, and all forms of life has energy, demonstrating that we are ALL Atomic Energy.

Most of the energy is stored in central mass, called the nucleus, compared to that associated with the electrons, orbiting the nucleus.

This nuclear energy can be tapped for peaceful purposes for the benefit of the entire human race.

## EDITORIAL

### **‘Tapping Nuclear Energy for peaceful purpose’**

Have you ever considered a case, like that of the city of Nairobi, in terms of the many activities taking place? What makes it possible for so many people (about 3 million) to reside and work ‘comfortably’ in such a city, containing many tall buildings, factories, residential houses and providing an enabling environment for transport and related services? A city such as Nairobi must need a large amount of energy in the form of electricity in order to operate all types domestic lighting devices, traffic and street lights, radio and television stations, various types of machines in different industries, instruments in research institutions, airport control devices, lifts, air conditioners, land line and mobile telephone exchange units and all other types of gadgets which require electricity. Considering all the above energy requirements for the city of Nairobi, it is clear that there is not enough electricity all of the time to meet the demands of the ever increasing activities which need electricity for their operations. Power outage and rationing is a common feature in the city of Nairobi and the problem is escalating as more structures (residential and industries), which need electrical energy, come up. The shortage of electrical energy is not only a problem in the city of Nairobi but rather a nationwide problem as the population continue growing. The power shortage scenario is even more compounded by the fact the Kenya government has taken measures to have the country become industrialized by year 2030 (vision 2030). This calls for more power output than ever before. The question is how do we get more electrical power for this country, apart from hydro, geothermal, diesel burning, wind, biomass and solar.

Over the years science and technology has played a significant role in making life better for the human beings and at the same time creating some side effects or problems. Currently, if we make efforts to solve electrical power needs by building more power plants, fuelled by coal and oil, the net result will be increased air pollution and green house effects. We already know the effects of polluted air. Some people have had their life time shortened due to polluted air, not just by lung cancer but from many other air related pollution. In addition, the supply of oil in the World is limited and the supply of coal is not infinite, let alone the resultant menace of global warming. Therefore,

scientists, engineers, entrepreneurs and managers must explore ways of generating and conserving power, methods which will not pollute the atmosphere and at the same time provide human beings with urgently needed energy when we run out of oil and coal. Some of the methods which have been investigated and being optimized in some cases include: energy conservation, conversion of sun's rays into electrical energy, geothermal energy (from the Earth's core), ocean tides and winds. These alternate energy sources are promising, but significance advances in technology must be developed before major contributions can be realized. However, there is already available, possibly non ending, supply of energy, **the Nuclear Energy**. The necessary technology for nuclear energy exploitation is available and a number of developed countries are currently using it. A major positive aspect of nuclear power plant is the fact that one kilogram of uranium 235 (U-235) can produce as much energy as 4 million kilograms of coal, and does it without creating soot and many pollutants of the atmosphere, such as oxides of carbon and sulphur. This provides a highway in tapping nuclear energy for peaceful purposes and at the same time keeping the gates of global warming closed. In the next issue of the journal of BioChemiPhysics we will give more information on nuclear energy.

Geoffrey N. Kamau

**International Journal of Biochemphysics**

**EDITOR-IN-CHIEF**

Prof. ANTONY M. KINYUA  
I.N.S., College of Architecture and  
Engineering, University of Nairobi,  
P.O. Box 30197, NAIROBI, KENYA.

**EDITOR**

Prof. G.N. KAMAU  
Dept. of Chemistry, College of  
Biological & Physical  
Sciences, University of Nairobi,  
P.O. Box 30197, NAIROBI, KENYA.

**Deputy Editor**

Dr. J.P. Kithinji  
Dept. of Chemistry, College of  
Biological & Physical  
Sciences, University of Nairobi,  
P.O. Box 30197, NAIROBI, KENYA.

**CIRCULATION MANAGER**

Prof. J.N. Muthama  
Dept. of Meteorology, College of  
Biological and Physical  
Sciences, University of Nairobi,  
P.O. Box 30197, NAIROBI, KENYA.

**PUBLIC RELATIONS**

**MANAGER**

D. Maina, I.N.S., College of  
Architecture and  
Engineering, University of Nairobi,  
P.O. Box 30197, NAIROBI, KENYA.

**ADVERTISING MANAGER**

J. T. PATEL  
Xpress Colour & Screen  
P.O. Box 31920 NAIROBI, KENYA,

**CONSULTING EDITORS**

Prof. R.M. MUNAVU  
(University of Nairobi)  
Prof. P.N. NYAGA  
(University of Nairobi)  
Prof. S.O. WANDIGA  
(University of Nairobi)  
Prof. W. LORE  
(Moi University)  
Prof. D. K. KOECH  
(Kenya Medical Research Institute-  
KEMRI)

**REGIONAL EDITORS**

**THE NETHERLANDS**

Dr. H. VAN WILGENBURG  
Dept. of Pharmacology, University  
of Amsterdam, Academic Medical  
Centre, Meibergdreef 15,  
1105 AZ AMSTERDAM.

**NEW ZEALAND**

Dr. RAVI GOONERATNE  
Dept. of Animal and Veterinary  
Sciences Group, Lincoln University,  
P.O. Box 84, CANTERBURY.

**CANADA**

Dr. J. M. MOLEPO  
1707 Meadowbrook Road,  
Gloucester, Ontario, K1B4W6.

**WEST AFRICA**

Dr. C.O. DIRIBE  
Anambra State University of  
Technology, Enugu  
Campus, Independence Layout,  
P.M.B. 01660, ENUGU, NIGERIA.

**SOUTHERN AFRICA**

Prof. J. B. SREEKANTH  
School of Chemistry, University of  
KwaZulu-Natal, Durban, South  
Africa.

**GERMANY**

Prof. Dr. B. MARKERT  
Internationales Hochschulinstitut  
Zittau Markt 2302763 Zittau

**SLOVENIA**

Dr. KABIL AL-SABATI  
Jozef Stefan Institute P.O. Box 100,  
Jamova 39, 61111 Ljubljana,  
SLOVENIA (YUGOSLAVIA)

**ASIA**

PROF. C.R. Das  
Utkal University of Culture,  
Bhubaneswa, India

**EDITORIAL BOARD**

Dr. W. Kofi-Tsekpo,  
Kenya Medical Research Institute  
(KEMRI), Kenya  
Dr. L. Mammino

Dept. of Chemistry, University of  
Venda, South Africa

Dr. F. Njui  
School. of Mathematics, University  
of Nairobi, Kenya

Prof. N.K. Olembo  
Dept. of Biochemistry, University of  
Nairobi, Kenya

Dr. W.M. Njue  
Dept. of Chemistry, Kenyatta  
University, Kenya

Prof. A.H. El-Busaidy  
Dept. of Chemistry, University of  
Nairobi, Kenya

Dr. M. Schaible  
Rochester, New York, U.S.A.

Dr. A.K. Yagoub  
Dept. of Chemistry, University of  
Juba, Sudan

Prof. T. Mukiyama  
School of Biological Sciences,  
University of Nairobi, Kenya

Prof. S.M. Kagwanja,  
Egerton University, Kenya

Prof. M. Kishimba,  
Dept of Chemistry University, Dar es  
Salaam, Tanzania

Dr. S. Mbogo,  
Dept of Chemistry University, Dar es  
Salaam, Tanzania

Prof. F.D. Juma  
Dept. of Clinical Pharmacology,  
University of Nairobi, Kenya

Prof. J. Boeyens,  
Dept of Chemistry  
University of Pretoria, South Africa

Prof. E.N.M. Njagi  
Dept. of Biochemistry, Kenyatta  
University

Prof. A. Gachanja,  
Dept. of Chemistry, JKUAT, Kenya

Dr. C. Ngila,  
School of Chemistry,  
University of KwaZulu-Natal,  
Durban, 4041, South Africa

**TYPSETTING:** Dr. P. M. Guto, Department of Chemistry, P.O. Box 30197 - 00100, Nairobi, Kenya. Tel: (254) 713 887854

**PRINTING:** Department of Chemistry, University of Nairobi, P.O. Box 30197 - 00100, Nairobi, Kenya

**ADVERTISING:** For details contact: Editor or Editor-In-Chief, International Journal of BioChemPhysics

**Subscription**

Please enter subscription for one year as marked below:

Airmail		Student Rates
Kenya	Kshs 2000	KShs. 800
East Africa	US \$ 80	US \$ 50
Rest of World	US \$ 150	US \$ 80

The maximum subscription period is one year renewable annually. Six months subscription is available at 50% of the above rates. Payments in Kenya shillings for foreign subscriptions should be calculated at current exchange rates

I enclose payment of \_\_\_\_\_

Please charge to Visa/Mastercard/American Express/Diners Club International

My Card Number is \_\_\_\_\_ Expiry Date \_\_\_\_\_

Signature \_\_\_\_\_

Last Name (BLOCK LETTERS) Prof/Dr/Mr/Mrs/Ms \_\_\_\_\_

First Names \_\_\_\_\_

Address \_\_\_\_\_

All Requirements should be made payable to the: Department of Chemistry,  
University of Nairobi, P.O. Box 30197, Nairobi, Kenya

## TABLE OF CONTENTS

<b>Editorial</b> .....	i
<b>JOURNAL ARTICLES</b> .....	1-55
Adsorption of carbaryl by a river sediment from an acetone solution: Apparent thermodynamic properties <b>M. F. Zaranyika and P. Ncube</b> .....	1-9
Estimation of binding ratio between colloidal gold particles and thiourea from surface studies <b>S. A. Mbogo; A.Y. Ngenya; L. L. Mkayula; J. M. Pratt Ramón Vilar-Compte</b> .....	11-18
Model for the estimation of initial conditions in a conflict environment <b>V.O. Omwenga, M.M. Manene and *C.B. Singh</b> .....	19-24
Initial correlations among the levels of various nutrient species in water from nairobi dam, kenya <b>P. G. Muigai, P. M. Shiundu, F. B. Mwaura and G. N. Kamau</b> .....	25-36
Creation of the universe from a non classical space-time state <b>M. G. Okeyo, M. N. Maonga, M. J. Otieno</b> .....	37-46
Electron transfer properties of 2-acetylferrocenyl-2-thiophenecarboxylsemicarbazone and its copper (ii) complex <b>P. M. Guto, J. M. Kiratu, L. S. Daniel, E. M. R. Kiremire, G. N. Kamau</b> .....	47-55
Information to Contributors.....	56-57
Publishing Agreements.....	57-58
Notices.....	58-69

# ADSORPTION OF CARBARYL BY A RIVER SEDIMENT FROM AN ACETONE SOLUTION: APPARENT THERMODYNAMIC PROPERTIES

M. F. Zaranyika<sup>1</sup> and P. Ncube

<sup>1</sup>Chemistry Department, University of Zimbabwe, P. O. Box MP 167, Mount Pleasant, Harare, Zimbabwe.

## ABSTRACT

The apparent thermodynamic properties for the adsorption/desorption of carbaryl by a river sediment were studied using a modified Freundlich isotherm. The values of the apparent adsorption/desorption equilibrium constant,  $K'$ , apparent adsorption free energy,  $\Delta G'$ , apparent rate constant for the desorption reaction,  $k_d$ , and the apparent lifetime of the adsorbed state,  $\tau_{ad}$ , obtained were  $43 \pm 10$ ,  $-9.3 \pm 0.6 \text{ KJ.mole}^{-1}$ ,  $(3.0 \pm 0.7) 10^9 \text{ s}^{-1}$  and  $(3.5 \pm 0.7) 10^{-10} \text{ s}$  respectively. Possible implications of these properties on the environmental persistence of the pesticide in the aquatic environment are discussed.

**Key Words:** Adsorption, pesticide, carbaryl, adsorption rate constant, Freundlich isotherm.

## INTRODUCTION

Carbaryl [1-naphthyl-N-methylcarbamate] is a broad spectrum contact insecticide used against many insect pests of fruits, vegetables, cotton and other crops [1]. Carbaryl is also used for dermal treatment of most livestock and domestic animals. Like most carbamates, carbaryl acts as an inhibitor of cholinesterase. Carbaryl is considered non-toxic to mammals, although it can temporarily inhibit acetylcholinesterase [2,3]. Its rat acute oral lethal dose is 850 mg/kg [1]. However, carbaryl is toxic to most aquatic organisms.  $LC_{50}$  values for crustacean range from 5 to 9  $\mu\text{g/L}$  (waterfleas, mysidshrimps), 8 to 25  $\mu\text{g/L}$  (scud), and 500 to 2500  $\mu\text{g/L}$  (crayfish) [4]. Aquatic insects have similar range of sensitivities. Plecoptera and ephemeroptera (stoneflies and mayflies) are the most sensitive groups. Molluscs are less sensitive with  $EC_{50}$  values in the range of a few mg/L. For fish, most  $LC_{50}$  values are between 1 and 30 mg/L, with salmonids being the most sensitive group [5-16].

The use of carbaryl to treat fruits, vegetables and crops means that the pesticide will find its way into surface and underground water. However very few studies have been carried out to determine its fate in the aquatic environment. Duell et al. [17] reported that carbaryl was dissipated from flood water through photodecomposition and biological degradation. Laboratory studies showed that the stability of carbaryl and its primary metabolite, 1-naphthol, was greatest in weakly acidic solutions, and that increasing pH and temperature resulted in marked decrease in stability. 77% carbaryl was recovered from solutions exposed to 96 hours of direct sunlight, while higher recoveries (92.5%) were obtained when the pesticide was exposed to laboratory light [17].

The fate and persistence of pesticides in the aquatic environment were reviewed by Edwards [18]. In natural waters such as lakes, rivers and ponds, most of the pesticides are strongly adsorbed onto particulate matter in suspension, which may sink to the bottom, or are taken up by living organisms. Adsorption of

pesticides onto soil and sediment colloids is also important in determining pesticide volatility, bioavailability, mobility and rate of degradation in the soil or sediment [19,20]. Adsorption/desorption experiments can give quantitative information on sorption equilibria in soils and sediments [21]. This information is important in understanding the environmental fate of pesticides in the aquatic environment [22].

The characterization of the adsorption of pesticides by soils is usually described in terms of the Freundlich isotherm:

$$C_{ads} = K_F C_e^n \quad (1)$$

where  $K_F$  is the Freundlich constant,  $C_{ads}$  is the concentration of pesticide adsorbed (in mg/g of soil/sediment),  $C_e$  is the concentration of pesticide in solution (in mg/mL) at equilibrium [23,24]. The Freundlich constant,  $K_F$ , is regarded as an index of sorption capacity, and may be used to compare sorption of different chemicals on different soils, while the exponent  $n$  is regarded as a measure of sorption non-linearity between solution concentration and adsorption [25-27].

Zaranyika and Mandizha [21] pointed out that, while the Freundlich isotherm gives useful information about the initial and final adsorption equilibrium conditions, it cannot be used to arrive at the adsorption/desorption equilibrium constant, and as such will not give any information about the kinetic aspects and nature of the adsorption interaction. These workers suggested a modification of the Freundlich isotherm to

$$\ln[X]_{ads} = \ln(nK') + n \ln([X]_e + [SX_n]_w) \quad (2)$$

where  $[X]_{ads}$  is the concentration of the pesticide X in the adsorbed state in suspension found in the sediment after settling,  $[X]_e$  is the concentration of X in solution at equilibrium,  $[SX_n]_w$  is the concentration of the pesticide-adsorption site complex in suspension at equilibrium,  $K'$  is the apparent adsorption/desorption equilibrium constant, and

$n$  is the number of pesticide molecules associated with a single adsorption site. Zaranyika and Mandizha [21] used the modified Freundlich isotherm to determine the apparent thermodynamic properties  $K'$ ,  $n$  and  $\Delta G$  (the apparent adsorption free energy) for the adsorption of the pesticide amitraz by a river sediment.

The aim of the present work is to determine the apparent thermodynamic properties for the adsorption of carbaryl by a river sediment from acetone solution using the modified Freundlich approach. Because of the low solubility of carbaryl in water (0.005g/100g at 20°C [28]), its dissolution/precipitation equilibrium may interfere with the adsorption/desorption equilibrium. Acetone was chosen as solvent because carbaryl is moderately soluble in acetone, and because acetone is completely miscible with water. The use of acetone will therefore minimize interference from precipitation equilibria.

## EXPERIMENTAL

### Materials

The following materials were used: carbaryl (analytical standard, 99.5%, Dr. Ehrenstorfer, GmbH); acetone, methanol, glacial acetic acid, potassium hydroxide, vanillin [4-hydroxy-3-methoxybenzaldehyde], orthophosphoric acid, (A.R. grade, Merck, Germany). The stream sediment used in these experiments was collected from the portion of upper Marimba River that lies within the University of Zimbabwe grounds in Harare.

### Equipment

UV-Visible spectrophotometer (UV-3101PC, UV-VIS-NIR Scanning Spectrophotometer, Shimadzu, Japan); Flask shaker (Type Thys 2, VEB MLW Labortechnik, ILMENAU, Germany); centrifuge (Kokusan H-103N series (speed 50 Hz), Kokusan Corporation, Tokyo, Japan); glassware: 50 mL conical flasks, test tubes.

**Procedures: Sediment sample collection and pre-treatment.**

Six sediment samples were collected just below the flowing stream at distances of about 5 m apart along the stream using a stainless steel scooper into plastic bags, and immediately taken to the laboratory, where they were blended into one composite sample by quartering. The composite sample was mixed thoroughly, oven dried at 50°C overnight [29], then sieved through a 2 mm sieve to remove gravel particles. About half of the composite sediment sample was ground using a mortar and pestle and then sieved through a 500 µm sieve (9ASTME 11-81, 0.5 mm). The sediment was then characterized with respect to pH, clay, silt, sand and organic matter content using standard methods [30,31], after which they were kept in a desiccator until required. The ground portion of the sediment was used for the determination of pH and organic matter content, and in the adsorption experiments. The unground portion was used for particle size determination. The properties obtained for the sediment are shown in Table 1

**Table 1: Properties of the sediment used in adsorption experiments**

PH (0.01M CaCl <sub>2</sub> )	7.88
Organic carbon (%)	0.9
Sand (%)	74.5
Silt (%)	6.0
Clay (%)	19.5

**Adsorption experiments.**

To demonstrate the existence of the adsorption/desorption equilibrium, 0.0, 0.1, 0.5, 1.0, 1.5 and 2.0 g of the dried ground sediment were added to six conical flasks, followed by 10 ml solution of 40 µg/ml carbaryl in acetone. The flasks were shaken for 5 h on the mechanical shaker and left to settle overnight, after which the supernatants were decanted and filtered. The

supernatants were decanted and filtered through a 0.45 µm filter paper for analysis.

To determine the values of n and “nK”, to each of four sets of five flasks were added 0.5g of dried sediment, followed by 10 mL of 10, 20, 30, 40 and 50 µg/mL carbaryl solution in acetone. The flasks were shaken on a mechanical shaker for seven hours and left to settle overnight. The supernatants were decanted and filtered through a 0.45 µm filter paper for analysis.

Carbaryl was determined by UV-Visible spectrophotometry after derivatization with vanilin (Figure 1) [32]. The method is based on a quantitative colour reaction of vanillin with 1-naphthol in acidic solution following hydrolysis of the carbaryl molecule. 1 mL of filtered supernatant acetone solutions were transferred to test tubes and the solvent evaporated by warming slightly. Into each test tube was pipetted 0.2 mL of 0.5M methanolic KOH solution. The tubes were rotated on the centrifuge for 5 minutes and the methanol evaporated off. 1 mL Vanillin solution (0.6 g vanillin in 100 mL glacial acetic acid) and 4 mL orthophosphoric acid were then added to each test. The test tubes were then heated in a water bath at 60°C for 30 minutes, cooled in water, and the absorbance read on the spectrophotometer at 575 nm [32]. Carbaryl concentrations obtained for the equilibration experiments, after adjusting for blank readings, are plotted as a function of mass of sediment in Figure 2. Carbaryl concentrations obtained for the adsorption experiments, are shown in Table 2.  $[X]_{ads}$  was calculated as the difference between the pre-equilibrium and post-equilibrium concentrations of carbaryl in the suspension and supernatant solution [25,29,33-35]. The regression plots of  $\ln [X]_{ads}$  versus  $\ln([X]_e + [SX_n]_w)$  are shown in Figure 3. The values of n and K' obtained from the regression plots, as well as the values of  $\Delta G$  and  $k_d$ , the desorption rate constant, calculated from them, are shown in Table 3.



**Table 2: Aqueous phase concentration ( $[X]_e + [SX_n]_w$ ) and sediment phase concentration ( $[X]_{ads}$ ) of carbaryl following equilibration of 0.5 g sediment with different concentrations of the pesticide**

Spike level ( $\mu\text{g/mL}$ )			10	20	30	40	50
Analysis ( $\mu\text{g/mL}$ )	(a)	$[X]_e + [SX_n]_w$	2.903	4.058	9.305	14.961	16.637
		$[X]_{ads}$	7.097	15.942	20.695	25.039	33.343
	(b)	$[X]_e + [SX_n]_w$	3.253	3.789	9.359	15.439	16.565
		$[X]_{ads}$	6.747	16.211	20.641	24.561	33.435
	(c)	$[X]_e + [SX_n]_w$	3.358	3.905	8.015	14.235	16.308
		$[X]_{ads}$	6.642	16.095	21.985	25.765	33.692
	(d)	$[X]_e + [SX_n]_w$	3.086	3.738	8.316	13.201	15.961
		$[X]_{ads}$	6.914	16.262	21.684	26.799	34.039

**Table 3: Values of Apparent Thermodynamic Properties**

Expt	n	K	$\Delta G$ (Kj.mole <sup>-1</sup> )	$k_d$ (s <sup>-1</sup> )	$\tau_{ad}$ (s)	1/n
a)	0.701	41.5	-9.23	$2.90 \times 10^9$		1.43
b)	0.582	38.0	-9.01	$2.65 \times 10^9$		1.72
c)	0.636	57.5	-10.40	$4.02 \times 10^9$		1.57
d)	0.761	34.1	-8.74	$2.38 \times 10^9$		1.31
Mean	0.67 $\pm 0.07$	43 $\pm 10$	-9.3 $\pm 0.6$	$(3.0 \pm 0.7) \times 10^9$	$(3.5 \pm 0.7) \times 10^{10}$	1.5 $\pm 0.2$

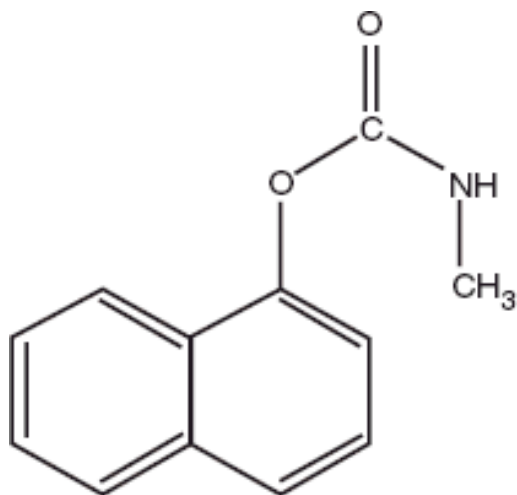


**Figure 1:** Carbaryl (1-naphthyl-N-methyl carbamate)

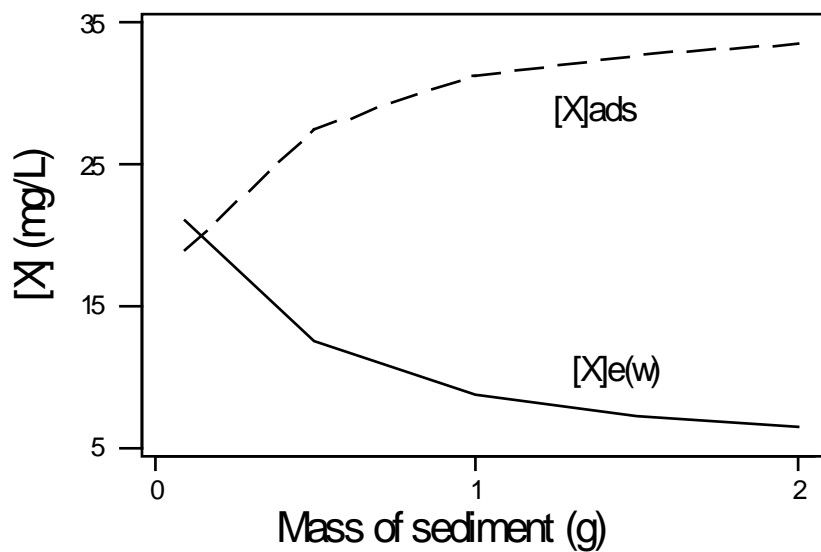


**Figure 2:** Adsorption of carbaryl, X, by upper Marimba river sediment from acetone solution:  $[X]_e$  and  $[X]_{ads}$  versus mass of sediment after 5 h equilibration time. (Subscripts e = solution equilibrium concentration; ads = adsorbed concentration).

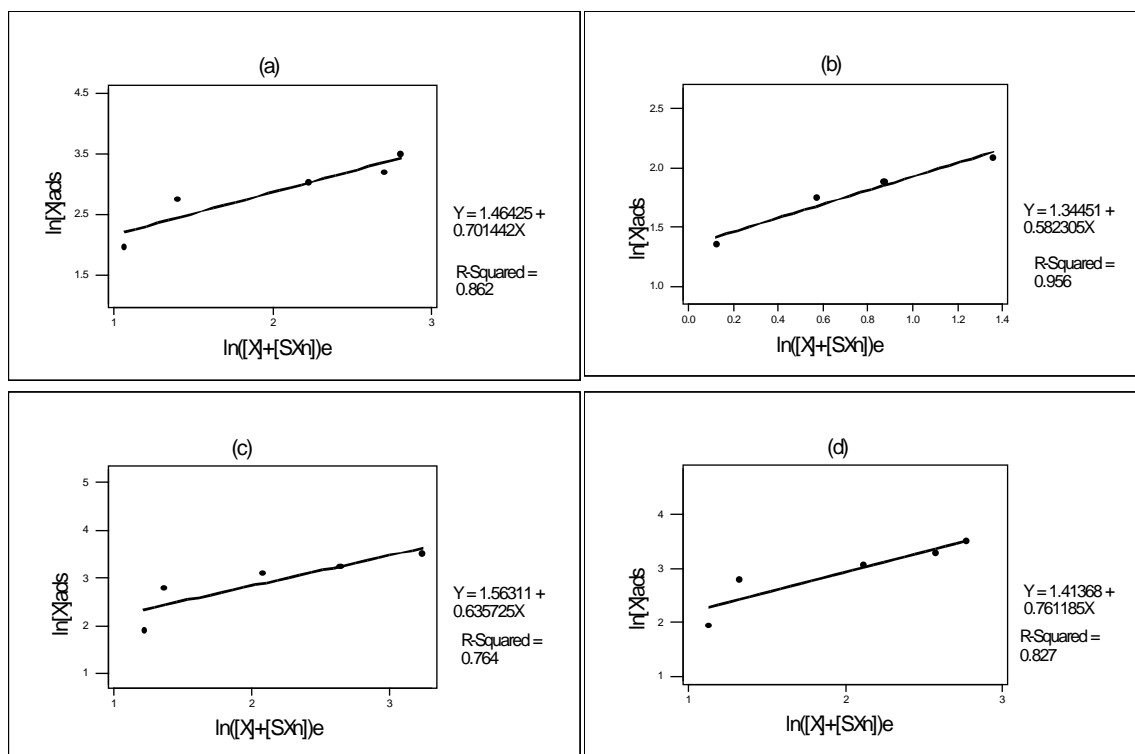


**Figure 3:** Modified Freundlich Isotherm regression curves for the adsorption of carbaryl by Marimba River sediment from an acetone solution.

## RESULTS AND DISCUSSION

From Figure 2 it is apparent that when a 40  $\mu\text{g/mL}$  solution of carbaryl in acetone is equilibrated with increasing amounts of sediment, the concentration of carbaryl remaining in solution and/or suspension shows an exponential drop as the mass of sediment increases, while the concentration of carbaryl adsorbed increases exponentially in a mirror image fashion, confirming the existence of an adsorption/desorption equilibrium in the system.

Table 3 shows the values of  $n$ ,  $K'$ ,  $\Delta G$ , and  $k_d$  obtained for the adsorption/desorption of carbaryl by the sediment collected from the portion of upper Marimba River that lies within the University of Zimbabwe grounds in Harare. As the major

adsorption interactions which bind small organic molecules in the soil environment involve soil particles of colloidal dimensions, 1 nm to 1 mm, it has been suggested that  $1/n$  represents the number of such colloidal particles associated with a single pesticide molecule [21,36]. The values of  $1/n$  in Table 3 suggest that in the system studied, two molecules of carbaryl are associated with three colloidal particles. This number may vary depending on the number density of molecules of the pesticide, relative to the number density of colloidal particles in the system.

Atkins [37] estimates the rate of desorption of gaseous organic molecules from surfaces to be about  $10^8 \text{ s}^{-1}$ . The  $k_d$  value of  $(3.0 \pm 0.7)10^9 \text{ s}^{-1}$  in

Table 3 obtained for carbaryl is therefore reasonable, and points to physi-sorption [21,37]. The values of “K” and  $k_d$  in Table 3 lead to a value for the rate constant for the adsorption reaction,  $k_{ad}$ , of  $1.3 \times 10^{11} \text{ s}^{-1}$ . The negative value for  $\Delta G$  and the high value of  $k_{ad}$  confirm that the adsorption reaction is both thermodynamically feasible and kinetically favourable. In addition the high value for  $k_{ad}$  shows that the lifetime of carbaryl in the desorbed state,  $\tau_d$ , is extremely short at  $8 \times 10^{-12} \text{ s}$ , much shorter than its lifetime in the adsorbed state,  $\tau_{ad}$ , of  $(3.5 \pm 0.7) 10^{-10} \text{ s}$ . Degradation of pesticides in sediments has been attributed to microbial action [17,38]. If we assume that microorganisms will attack molecules of the pesticide only in the desorbed state, then the life-time data for the sorbed and desorbed states above suggest that carbaryl will be 40 times more persistent in the adsorbed state than the desorbed state. Acetone is found in most waste streams from industry [39]. Because carbaryl is moderately soluble in acetone [28], the desorption rate constant obtained in the present experiments represents the upper limit for the rate of desorption of carbaryl from sediments in streams contaminated by acetone. Thus based on the  $k_{ad}$  and  $k_d$  data above, carbaryl will be at least 40 times more persistent in Marimba river type sediment than in the river water phase.

Adsorption of organic molecules by soils and sediments depends on the properties of the soil or sediment, especially those listed in Table 1 [29,40]. Extrapolation of the values of  $n$ ,  $K'$ ,  $\Delta G$ , and  $k_d$  obtained for carbaryl above to other sediment ecosystems should take into account the fact that the data will vary depending on the nature of the sediment.

## CONCLUSIONS

From the foregoing discussion we conclude that adsorption of carbaryl by upper Marimba river sediment from an acetone solution occurs via a physi-sorption equilibrium mechanism in which the adsorption rate constant is higher than the desorption rate constant. For the system studied the life-time of carbaryl in the adsorbed state forty times longer than in the desorbed state.

## ACKNOWLEDGEMENTS

This work was supported by a grant from the Research Board of the University of Zimbabwe.

## REFERENCES

1. Worthing, C.R. (Ed) (1979). The Pesticide Manual, 6<sup>th</sup> ed., British Crop Protection Council.
2. Carpenter C.P., Well C.S., Palm P.E., Woodside M.W., Nair J.H. and Smyth H.F. (1961). Mammalian toxicity of 1-Naphthol-N-methyl carbamate (Sevin insecticide). *J. Agric Food Chem.*, 9(1), 30 -39.
3. Crammer, MF Jr. (1986). Carbaryl: A toxicological review and risk analysis, *Neurotoxicol.*, 7(1): 247-332.
4. WHO (1994) Environmental health Criteria 153: Carbaryl, Draft Report prepared for the WHO International Programme on Chemical Safety, WHO 1994 (ISBN 92 4 157153 s) ([www.inchem.org/documents/ehc/ehc/ehc153.htm](http://www.inchem.org/documents/ehc/ehc/ehc153.htm))
5. Statham CN, Lech J J (1975). Potentiation of the acute toxicity of several pesticides and herbicides in trout by carbaryl. *Toxicol. Applied Pharmacol.*, 34(1), 83-87.
6. Arunachalan, S., Jeyalakshusi K., and Aboobucker S (1980). Toxic and sublethal effects of carbaryl on freshwater catfish, *Mystus vittatus* (Bloch). *Archives Environ. Contam. Toxicol.*, 9(3), 307-316.
7. McKim JM, Schmeider PK, Niemi GJ, Carlson RW, Henry TR (1987). Use of respiratory cardiovascular responses of rainbow trout (*Salmo gairdneri*) in developing fish acute toxicity syndromes: Part II. Malathion, carbaryl, acrolein and benzaldehyde. *Environ. Toxicol. Chem.*, 6: 313 – 328.
8. Hanazato T (1991). Effects of long-term and short-term exposure to carbaryl on survival, growth and reproduction of *daphnia ambigua*. *Environ. Pollut.*, 74(2): 139-148.
9. Sinha N, Lal B, Singh TP (1991). Carbaryl-induced thyroid dysfunction in

- the freshwater catfish clama batrachus. *Ecotoxicol. Environ. Safety*, 21: 240 – 247.
10. Harverns K E (1995). Insecticide (carbaryl, 1-naphthol-N-methyl carbamate) effects on a freshwater plankton community: zooplankton size, biomass and algal abundance. *Water, Air Soil Pollut.*, 84(1-2): 1-10.
  11. Beyers DW, Keefe TJ, Carlson CA (1994). Toxicity of carbaryl and malathion insecticide to two federally endangered fishes, as estimated by regression ANOVA. *Environ. Toxic. Nad. Chem.*, 13: 101 – 107.
  12. Beauvais SL, Jones SB, Parris JT, Brewer SK, Little EE (2001). Cholinergic and behavioral neurotoxicity of carbaryl and cadmium to larval rainbow trout (*Oncorhynchus mykiss*). *Ecotoxicol. Environ. Safety*, 49(1): 84-90.
  13. Barahona MV, Sanchez S (1999). Toxicity of carbamates to brine shrimp *Artemia salina* and the effect of atropine, Bw284c51, ISC-OMPA and 2-PAM on carbaryl toxicity. *Environ. Pollut.*, 104(3): 469-476.
  14. Todd NE, Van Leenwen M (2002). Effects of sevin (carbaryl) on early life stages of zebrafish (*Danio rerio*). *Ecotoxicol. Environ. Safety*, 53(2): 267-272.
  15. Ferrar A, Venturino A, Pechen de D'Angelo AM (2007). Effects of carbaryl and azinphos methyl on juvenile rainbow trout (*Oncorhynchus mykiss*) detoxifying enzymes. *Pesticide Biochemistry and Physiology.*, 88(2): 134-142.
  16. Beyer DW, Sikoski PJ (2009). Acetylcholinesterase inhibition in federally, endangered Colorado squawfish exposed to carbaryl and malathion, *Environ. Toxicol. Chem.*, 13(6): 935-939.
  17. Duel Jr. LE, Brown KW, Price JD, Turner FT (1985). Dissipation of carbaryl and 1-naphthol metabolite in flooded rice fields. *J. Environ. Qual.* 14(2): 349 - 354.
  18. Edwards, C.A. *Persistent Pesticides in the Environment*, CRC Press, Cleveland, Ohio, 1975
  19. Brown D.S, Flagg EW (1981). Empirical prediction of organic pollutant sorption in natural sediments. *J. Environ. Qual.*, 10(3): 382 – 386.
  20. Karickhoff SW, Brown DS, Scot TA (1979). Sorption of hydrophobic pollutants on natural sediments. *Water Res.*, 13: 241-248.
  21. Zaranyika MF Mandizha NT (1998). Adsorption of amitraz by a river sediment: Apparent thermodynamic properties. *J. Environ. Sci Health*, B33: 235-251.
  22. Spalding RF, Cassada DA, Burbach ME (1994). Study of pesticides in two closely spaced lakes in Northwest Nebraska. *J. Environ. Qual.*, 23: 571-578.
  23. Hance RJ (1965). The adsorption of urea and some of its derivatives by a variety of soils. *Weed Res.*, 5(2): 98-107.
  24. Bowman BT and Sans WW (1977). Adsorption of parathion, fenitrothion, methyl parathion, amino parathion and parooxon by  $\text{Na}^+$ ,  $\text{Ca}^{2+}$  and  $\text{Fe}^{3+}$  montmorillonite suspension. *Soil Sci. Soc. Am. J.*, 41: 541 – 519.
  25. Parkpian P, Anurakpongsatorn P, pokkong P, Patrick WH Jr (1998). Adsorption, desorption and degradation of  $\alpha$ -endosulfan in tropical soils of Thailand. *J. Environ. Sci. Health*, B33(3): 211-233.
  26. Piccolo A, Celano G, Arienzo M, Mirabella A (1994). Adsorption and desorption of glyphosate in some European soils. *J. Environ. Sci. Health*, B29(6): 1105-1115.
  27. Singh N, Wahid PA, Murty MVR, Sethunathan N (1990). Sorption-Desorption of methyl parathion, fenitrothion and carbofuran in soils. *J. Environ. Sci. Health*, B25(6): 713-728.
  28. Extensions Toxicology Network (EXTOXNET) (1993). Pesticide information profile. [Pmep.cce.cornell.edu/profiles/.../carbaryl.html](http://Pmep.cce.cornell.edu/profiles/.../carbaryl.html)
  29. Gerstl Z, Kluges L (1990). Fractionation of the organic matter in soils and sediments and their contribution to the sorption of pesticides. *J. Environ. Sci. Health*, B25(6): 729-741.

30. Jackson MI. Soil Chemical Analysis. Prentice-Hall, New Delhi, 1967.
31. Black CA. Methods of Soil Analysis, Part 2 (1965). American Society of Agronomy, Madison, Wis.
32. Handa SK, Dikshit AK (1979). Spectrophotometric method for the determination of residues of carbaryl in water. *Analyst*, 104, 1185-1188.
33. Alva AK, Singh M (1991). Sorption-desorption of herbicides in soil as influenced by electrolyte cations and ionic strength. *J. Environ. Sci. Health*, B26(2): 147-163.
34. Hermosin MC, Roldan I, Cornejo J (1991). Adsorption-desorption of maleic hydrazide on mineral soil components. *J. Environ. Sci. Health*, B26(2): 165-183.
35. Spieszlski WW, Niemczyk HD, Sheltar DJ (1994). Sorption of chlorpyrifos and fonofos on lawn soils and turfgrass thatch using membrane filters. *J. Environ. Sci. Health*, B29(6): 1117-1136.
36. Burchill S, Greenland DJ, Hayes MHB (1981). Adsorption of Organic Molecules. In *The Chemistry of Soil Processes*, Greenland, D.J., Hayes, M.H.B., Eds.; Wiley & Sons, New York.
37. Atkins, P.W. *Physical Chemistry*, Oxford University Press, Oxford, 4<sup>th</sup> Ed., 1990, p. 938.
38. Zaranyika MF, Nyandoro GM (1993). Degradation of Glyphosate in the Aquatic Environment: An Enzymatic Kinetic Model that takes into account Microbial Degradation of both Free and Colloidal (or Sediment) Particle adsorbed Glyphosate. *J. Agric. Food Chem.*, 41(5): 838-842.
39. Singh RP, Nabi SA, Singh S (2010). Adsorption and movement of carbaryl in soils: A verification of cosolvent theory, and comparison of batch equilibrium and soil thin layer chromatography results. *Toxicol. Environ. Chem.*, 92(4): 721-735.
40. Hamaker JW, GarnyCAI, Youngson CR (1966). Sorption and leaching of 4-amino-3,5,6-trichloropicolinic acid in soils. *Adv. Chem. Ser.* 60: 23-27.



## ESTIMATION OF BINDING RATIO BETWEEN COLLOIDAL GOLD PARTICLES AND THIOUREA FROM SURFACE STUDIES

S. A. Mbogo<sup>1</sup>; A.Y. Ngenya<sup>2</sup>; L. L. Mkayula<sup>2</sup>; J. M. Pratt<sup>3</sup> Ramón Vilar-Compte<sup>3</sup>

<sup>1</sup>Open University of Tanzania, <sup>2</sup>University of Dar es Salaam, Department of Chemistry, P. O. Box 35061, Dar es Salaam, Tanzania, <sup>3</sup>Imperial College London.

### Abstract

Several emerging applications of colloidal gold are attributable to properties of nanoscale size particle, such as their ability to bind to neutral molecules. In this paper we report the results of work carried out to estimate the binding ratio between colloidal gold particles and neutral thiourea molecules. Gold colloids with mean particle size of 14 nm were obtained from freshly prepared aqueous gold colloid preparation. The particle concentration studies for the forward titration between fresh aqueous colloids and neutral thiourea (TU) molecules showed that the 640 nm product (first blue product) may contain three thiourea molecules per colloidal monomer. Studies on the same reaction using a Stopped-Flow spectrometer (SF) showed that the reaction could be of second order kinetics with respect to gold monomer (GM) concentration, suggesting a formula  $(GM)_2(TU)_2$ . The rate constant ( $k_2$ ) of the reaction was estimated to be approximately  $7.4 \times 10^8 \text{ M}^{-1}\text{s}^{-1}$ .

### Introduction

Colloidal dispersions of many metals, particularly at the nanoscale size, display properties and attributes that make them important materials for numerous nano-technology related products and processes [1]. This is in contrast with the bulk form of their metallic counterparts. For gold, in bulk form, is inert to air and most reagents, it is soft, yellow coloured, with a face centred cubic structure and a melting point of 1068°C. Many of the current applications of bulk gold are based on its physical properties, these including low electrical resistivity, high thermal conductivity and corrosion resistance where it has its major attributes.

Properties of gold at nanoscale size accounts for its ever increasing importance for its future uses. At the nanoscale size, gold does not necessarily display those observations/properties of the bulk material. Neat gold colloidal particles are relatively stable towards aggregation because the electrostatic repulsive forces between them are stronger enough to resist the attractive van der Waals forces, hence its stability [2, 3]. However, when this balance of forces is reversed the stability is broken and particles aggregate. For example, the addition of small quantities of strong absorbing neutral molecules such

as pyridine and thiourea would cause the metallic gold colloidal particles to aggregate into a network-like pattern consisting of strings [4].

The optical properties of gold at the nanoscale size are exciting; they have colour varying from red to purple depending on the particle size, a property that has been successfully exploited in a range of biomedical related applications [5]. Colloidal gold is also known to be catalytically active for a range of commercially important reactions and they also have a surface chemistry particularly suited to the attachment of sulphur containing molecules such as the thiols, which permits the “bottom-up” assembly of interesting and useful structures [5, 6]. Recognition of gold as a useful catalyst requires preparation of gold of very small particle size (less than 5 nm) on an appropriate oxide support material. Apart from the chemical and optical properties of gold, which have been extensively studied, very little is known about the thermodynamic and kinetic properties of these nanoscale sized gold particles; for example why particles aggregate, their binding ratio and the kinetics of their aggregation with neutral molecules.

Attempts to produce single sized colloidal particles have been made over the years



[7,8,9,10,11], but due to the lack of understanding of the physico-chemical factors that influence the process; it has until to date been difficult to come up with a synthetic method that would ensure the generation of uniform-sized particles [12]. In 1973 Frens showed how strict control of synthetic conditions can give a nearly mono-dispersed product [9]. Hence, working with colloidal particles appears to be shrouded with uncertainties making it difficult to obtain truly quantitative results.

This paper reports on the work that was undertaken in order to estimate the binding ratio between colloidal gold particles and neutral thiourea. Colloidal particles were synthesized and characterized following established standard protocols. Data obtained, such as size was used in estimating the approximate particle concentration. Particles were then reacted with known concentration of thiourea. Using a combination of techniques including UV-visible spectrometer and Stopped-Flow spectrometer, the binding ratio between the particles and neutral molecules was estimated.

## Experimental

### Materials and reagents

Sodium citrates and chloroauric acid used for the preparation of aqueous Au colloids were Analytical Reagent Grade from Fisher Scientific. Other chemicals were standard Grade (Fisher). All chemicals were used as received without further purification. Water purified through an ultra pure water system (MILLI-Q, Millipore Co. Inc.) was used without further purification.

### Preparation and Characterization of Aqueous Gold Colloidal Particles

Aqueous gold colloids were prepared by the reduction of chloroauric acid solution with sodium citrate; Turkevich's method for the preparation of a standard sodium citrate sol was used [8]. The prepared colloid samples were then characterized using UV-visible and Transmission Electron Microscope (TEM - JEOL 2000 EX) operating at 200 kV (figure 1 TEM image). This was done by casting a single drop of the freshly prepared sample onto a standard carbon-coated (200-300 Å) formvar films on a 400 mesh copper grid, leaving the sample to dry in air for at least one hour before acquiring the images.



**Figure1:** TEM of a freshly prepared Gold Colloid ( $\lambda_{\text{max}} = 520 \text{ nm}$ ).

In order to get the average particle size, the diameters of about three hundred particles from the acquired micrograph images were measured using a defused light microscope fitted with a standard scale. The average diameter of the particles was found to be about 14 nm with a standard deviation of 2.8 nm.

A 5 ml sample of the freshly prepared solution of gold colloids was titrated with 5 mM thiourea (TU) by initially adding 1 $\mu$ l TU, followed by adding increments of 0.5  $\mu$ l to make a total volume of 3.0 $\mu$ l TU added. The resulting product was scanned over the UV-visible spectrum between 800-400nm.

### Kinetic Studies of Aqueous Gold Colloids with TU using Stopped-Flow methods

Freshly prepared gold colloid sample and 1.0 mM TU solutions were used for kinetics studies. The experiment was carried out using a Stopped-Flow UV-visible spectrometer; the reaction chamber was thermostated at 25  $^{\circ}$ C.

Reactions between the gold colloids and TU were monitored at five different wavelengths on the UV-visible spectrum so as to check for the identity of the intermediate products of the reaction, the direction and the magnitude of changes in absorption.

Results obtained are given in parentheses (+/-) indicating an (increase/decrease) in absorbance respectively: 520 nm (-), 540nm (0), 600 nm (+), 640 nm (+) and 700 nm (+).

The kinetics of the reaction was followed using the Stopped-Flow spectrophotometer set at 520 nm (i.e. monitoring the disappearance of the monomer).

## Results and Discussion

### Estimation of the concentration of the colloid

Figure 2 is a UV-visible spectrum of a freshly prepared aqueous colloidal solution titrated with TU. A band is observed at 520 nm and a second band appearing at approximately 640 nm., these bands are associated with a visible colour change of the colloids from red (fresh colloid) to blue (aggregated particles; TEM image figure 3). An isosbestic point can be observed at about 540 nm that seems to break as the second maximum band moves to longer wavelengths. This suggests that one major species was formed under equilibrium conditions followed by one or more overlapping equilibria and/or reactions.

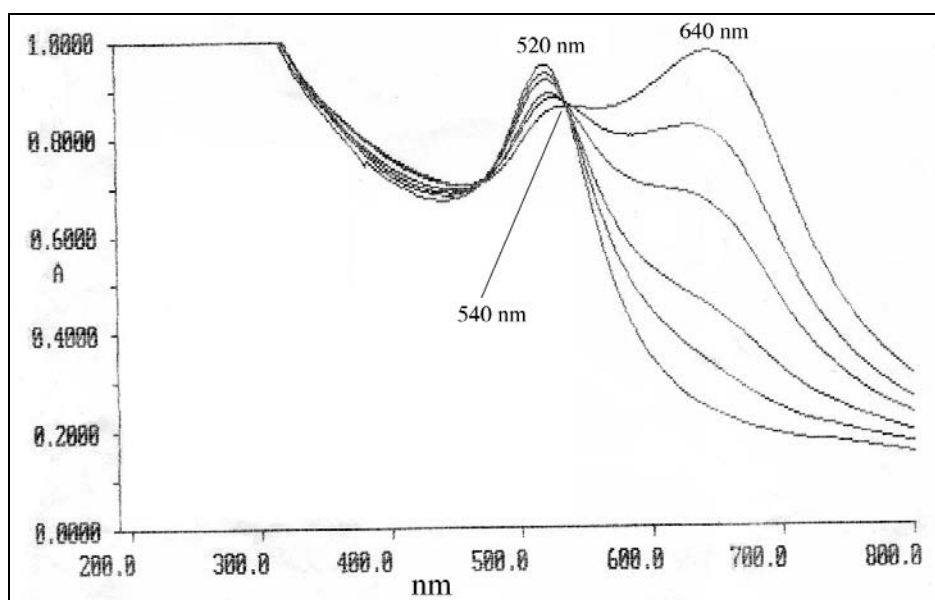


**Figure2:** A typical UV-Visible spectrum of Aqueous Gold Colloid titrated with TU, at 520 nm  $\lambda_{\max}$  for fresh red gold particles, 640nm Blue product and 540nm the isosbestic point.

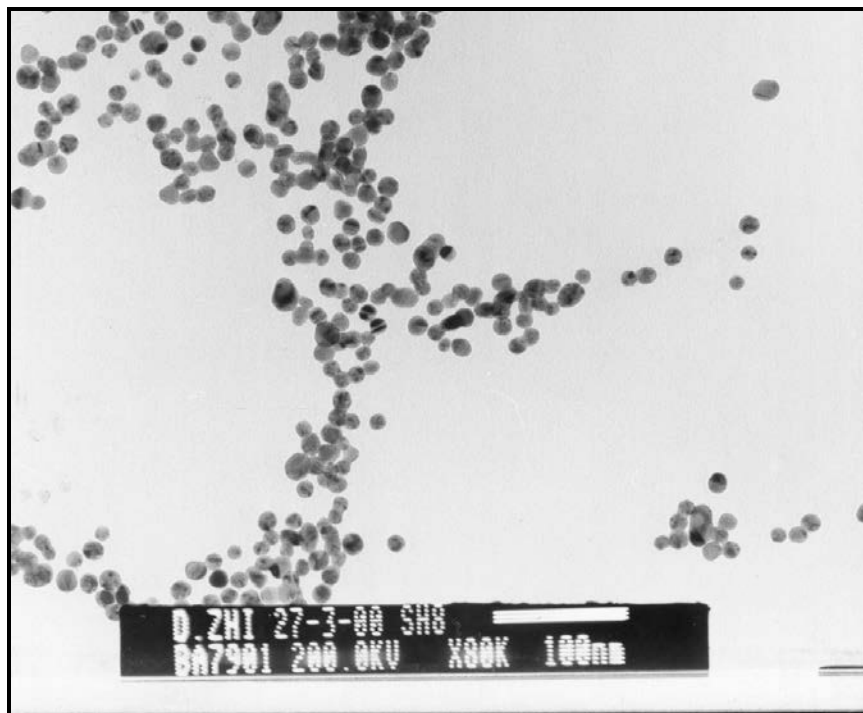


**Figure 3:** TEM of aqueous Gold Colloid + TU ( $\lambda_{\max} = 640 \text{ nm}$ )

Based on the average particle diameter of the fresh colloid preparation (14 nm), the concentration of the gold colloidal prepared was estimated using the following equation:

$$V = 4/3 (r^3) \pi$$

Where  $V$  is the volume of a sphere and  $r$  is the atomic radius which is 0.144 nm. [9]. Therefore the average number of gold atoms per particle will be equal to:

$$\frac{\text{Volume of the particle (Vp)}}{\text{Volume of the atom (Va)}}$$

Taking into consideration of the packing fraction in a particle as 0.74 of the total volume, therefore; the average number of gold atoms was:

$$0.74 \times V_p / V_a = 0.74 \times (7^3) / (0.144^3) = 8.6 \times 10^4 \text{ Au atoms per particle.}$$

The concentration of gold colloid particles  $[\text{Au}]_{\text{coll}}$  was therefore determined accordingly:

Concentration of Au of all forms:

$$(2.5 \times 10^{-4} \text{M} \{ \text{from total weight of reduced Au} \}) / \text{Number of Au atoms per particle} (8.6 \times 10^4).$$

Hence, the concentration of the gold colloidal particles in the stock solution could be estimated to be about:

$$[\text{Au}]_{\text{coll}} = 3 \times 10^{-9} \text{ M.}$$

Table1. Data for the Forward Titration of gold colloid with TU at 640 nm.

Absorption Intensity at 650nm	[TU] $10^{-6}/M$	[TU] $10^{-12}/M^2$	[TU] $10^{-24}/M^3$	[TU] $10^{-48}/M^4$
0.250	0	0	0	0
0.325	1.00	1.00	1.00	1.0
0.450	1.50	2.25	3.37	5.06
0.675	2.00	4.00	8.00	16.00
0.850	2.50	6.25	15.62	39.02

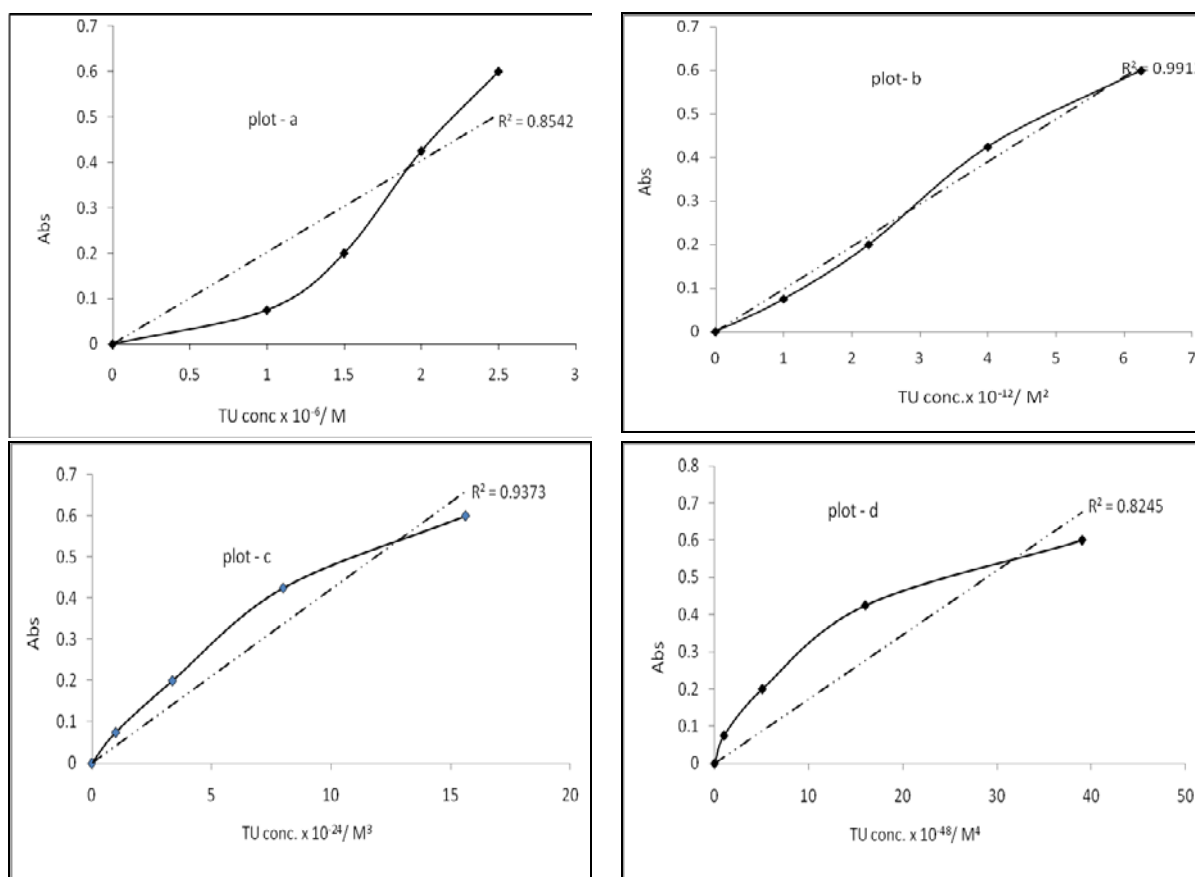


Figure 4 : Absorbance changes :- plot- a Vs [TU]<sup>1</sup>, plot- b Vs [TU]<sup>2</sup>, plot- c Vs [TU]<sup>3</sup> and plot- d [TU]<sup>4</sup> 640 nm.

**Table2. First and Second Half-Life of two Aqueous Colloidal Gold Concentrations with varying [TU],  $\lambda=520$  nm.**

	1st $t_{1/2}$ (sec)	2nd $t_{1/2}$ (sec)	Ratio 2 <sup>nd</sup> : 1st
$\text{Au}_{\text{coll}} + 10^{-6}$ TU	1.4	3.0	2.1
	1.6	2.9	1.8
$\text{Au}_{\text{coll}} + 10^{-5}$ TU	1.3	2.6	2.0
	1.4	2.8	2.0
$\text{Au}_{\text{coll}} + 10^{-4}$ TU	1.4	3.0	2.1
	1.4	2.8	2.0
$2\text{Au}_{\text{coll}} + 10^{-6}$ TU	0.9	1.8	2.0
	1.0	1.9	1.9
$2\text{Au}_{\text{coll}} + 10^{-5}$ TU	0.8	1.5	1.9
	0.8	1.8	2.2
$2\text{Au}_{\text{coll}} + 10^{-4}$ TU	1.1	2.2	2.0
	0.9	1.8	2.0

Further analysis of the spectrum for the forward titration of the gold colloids with varying concentrations of thiourea was carried out and the results are as presented in Table: 1 and subsequent figures that follow. Figure 4 (a-d) show plots of absorption intensity at 640 nm against [TU] raised to the power of one, two and three and four, respectively. All but one plot- b  $[\text{TU}]^2$  show distinct curvatures. This is proved by regression analysis of the plots where by the  $R^2$  value of plot-b is close to unit. This trend is observed for as long as the isosbestic point remains unbroken. These results suggest that in spite of all existing reactions, the major “640 nm” product includes two (2) TU molecules per colloidal monomer, i.e.  $(\text{GM})_n(\text{TU})_2$

(where GM= gold colloid monomer). Four similar experiments were performed, all showed similar trend.

Analysis of the kinetic traces at 520 nm (table 2) gave a good second order plot for the first three half lives (i.e.  $1^{\text{st}} t_{1/2} = 2^{\text{nd}} t_{1/2} = 3^{\text{rd}} t_{1/2}$ ), however, mixed kinetics were observed at 640 nm which may arise from the overlap of the formation and further reaction(s) of the first product. The rates and orders of formation of the “640 nm” blue product from red monomer (520 nm) and TU were therefore derived from the decrease in absorption at 520 nm. The experiment involved the use of two colloid concentrations that varied in strength by a factor of two (i.e.  $[\text{GM}] = \text{Au}_{\text{coll}} = [\text{M}]$  and  $[\text{GM}] = 2\text{Au}_{\text{coll}} =$

[2M]), and three concentrations of thiourea  $10^{-6}$  M,

The data in table 2 shows that in all cases the ratio of the second to the first half-life is close to 2.0, indicating a reaction with a second-order dependence on the gold colloidal concentration. The fact that doubling the initial gold concentration does not completely halve the half-life reflects the fact that the faster rate means a larger fraction of the reaction is complete before the trace is sufficiently stable to be analyzed reliably. The data also show that a 100-fold change in TU concentration has no effect on the half-life. The rate of formation of the “640 nm” product therefore shows a second-order dependence on gold concentration, but a zero-order dependence on TU concentration. Logical conclusion that can be drawn is that the “640 nm” product contains two colloid particles. The titration data earlier studied suggested that the product contained two molecules of TU. Therefore, a probable formula of the first blue product with a band at 640 nm (ignoring the associated citrate and sodium ions) can be written as:  $(GM)_2(TU)_2$ , where GM represents a gold colloid monomer. However, the kinetics does not indicate whether the attachment of the first TU or the additional molecules occurs after the observed rate determining dimerization or as a very fast pre-equilibrium process.

For a second order reaction in the same initial species, the rate constant of reaction is given as:

$$k_2 = 1/(t.a)$$

where  $t$  is half-life of the reaction and  $a$  is the initial concentration (table 2).

This gives  $k_2 = 1/(1.4 \times 1.5 \times 10^{-9}) = 7.4 \times 10^8 \text{ M}^{-1}\text{s}^{-1}$ .

Where  $t_{1/2}$  is 1.4 seconds and initial colloidal gold concentration =  $1.5 \times 10^{-9}$  M.

## Conclusion

The method used for the synthesis of the aqueous gold colloids developed by Frens is of great importance in that it has been shown to produce colloids of highly uniform and controllable size. The average particles size obtained in this experiment using TEM (14.4 nm) falls within the reported expected range i.e., 12 - 64 nm [12].

$10^{-5}$  M and  $10^{-4}$  M, respectively.

The average particle size data from TEM have been used to estimate the concentration of the aqueous colloids in the preparation; and the calculations show that the preparation produces concentrations of gold colloids of approximately  $0.3 \times 10^{-8}$  M. The calculated concentration of colloids during titration is far less than that of TU; so that the total added TU does not appear to need correction for any colloid-bound TU.

Kinetic studies using SF provide evidence that the blue “640 nm” product could be a dimer consisting of two colloidal particles. Four plots of Abs vs  $[TU]^n$  (where  $n = 1$  to 4) show that the plot of Abs vs  $[TU]^2$  gave a better linear plot than the other three. In view of the above mentioned facts it is therefore reasonable to assume that the main “640 nm” species contains two TU molecules per two colloid monomers suggesting the following formula;  $(GM)_2(TU)_2$ . However, further work is underway to ascertain this relationship and others between neutral thiourea and gold colloids of different particle sizes.

## Acknowledgement

The authors gratefully acknowledge the Department for International Development (DFID) of the UK government and the University of Dar es Salaam for supporting this study. The authors also thank Dr P. Wilde of Imperial College London for his guidance all along the study period.

## References

1. Thompson, D. T. 2001, Chemistry in Britain, 37, p 43
2. Mulvaney, P. Langmuir 1996, 12, p 788-800
3. Goodwin, J. W. Colloidal Dispersions, Royal Society of Chemistry, 1981, p 1-23
4. Blachford, C. G.; Campbell, J. R.; Creighton, J. A. 1982. Surface Science, 120, p 435
5. Corti, W. C.; Holliday, R. J.; 2004, Gold Bulletin, 37, p 25

6. Maye, M. M.; Luo, J. Han, L.; Kariuki, N. N.; Zhong, C.J. 2003, Gold Bulletin, 36, p 3.
7. Murray, C. B.; Norris, J.; Bawendi, M. G. 1993, J. Amer. Chem. Soc., 115, p 8706
8. Turkevich, J.; Stevenson, P. C.; Hillier, J. 1951, Discuss. Faraday soc., 11, p 55
9. Frens, G.; 1973, Nature Physical Science, 20. p 244
10. Ahmadi, T. S.; Wang, Z. L.; Green, T. C.; Hengelein, A.; El-Sayed, M. A. Surface Science, 1996, 272, p 1924.
11. Quinn, M.; Mills, G. 1994, J., Phy. Chem., 98, p 9840
12. Hayat, M. A., Colloidal Gold: Principles Methods and Applications 1989, Vol. 1, Academic Press, San Diego, p 54
13. Aylward, G. H.; Findlay, T. J. V. SI Chemical data, 2<sup>nd</sup> Ed.; John Wiley and Sons: NewYork; 1974; p 9.

# MODEL FOR THE ESTIMATION OF INITIAL CONDITIONS IN A CONFLICT ENVIRONMENT

V.O. Omwenga, M.M. Manene and \* C.B. Singh

University of Nairobi, School of Mathematics, P.O. Box 30197 Nairobi, Kenya

## Abstract

Conflict can be described as a condition in which actions of one person prevent or compel some outcome at the resistance of the other. Quite often this can be seen as “two or more competing, often incompatible, responses to same event”. Model-based predictions and formulations of trends are becoming more commonly used by researchers in the field of conflicts. These models to a great extent rely on fundamental or empirical models that are frequently described by systems of differential equations. In this paper, we have developed the dynamic time varying model for estimating control variables (initial conditions) which play a significant role in the success of conflict resolution estimated using a logistic probability model. A real conflict data set, from International Peace Institute, Oslo (PRIO), was used to test on the workability of the model.

**Key words:** *Bayesian theory, Conflict, dynamic state, Initial conditions, Logit model, Ultimatum game*

## 1.0. Introduction

The application of formal models and quantitative analysis techniques have come a long way towards explaining how strategic actors bargain in a variety of conflict settings. For instance, in the political setting or international relations, bargaining plays a central role in understanding and solving any conflict and thus the mastery of the concept of bargaining is very important, [1, 2, 3, 4, 5 and 6].

The basics of logic of bargaining in the face of conflicting interests have been explained by Game theory. Political scientist have employed for instance, bargaining models based on the Game theory to analyze effects of open and closed rules on the distributive politics of legislative appropriation to the study of war initiation and termination, [7, 8 and 9].

Understanding the interplaying factors in a conflict is very important in solving the conflict. In the likelihood that the factors are not known, a reliable model can be used to predict them. Most conflicts are generally triggered by the differences in opinions and interpretation of an idea, [6]. It is therefore, important that these differences are understood in terms of their magnitude in a conflict. In this paper, we categorize these factors into two broad distinct variables, that is, control variables and state variables. Control variables are the most critical factors to any conflict. According to [6], the control variables are represented as reservation values. In general, it is important to understand the effects of these substantive variables (control variables) on the bargaining process.

The control and state variables can be represented in a model that describes a conflict situation using statistical and numerical models of the system dynamics. The fundamental or empirical models that are frequently described by systems of ordinary differential equations (ODEs) can also be used to describe a conflict situation, [10, 11]. The systems of ordinary differential equations can be used to predict the future behaviour/dynamics of the conflict, provided that the initial states of the conflict are known. An account on the modelling of a conflict from the perspective of social welfare theory and social choice theory has been given by [12]. A complete data defining all of the states of a conflict system at a specific time are, however, rarely available. This challenge can however, be handled using missing data analysis techniques, [13, 14 and 15].

In a conflict, for instance, there are some underlying issues that can be described to be private and as such may not be available. Moreover, both the models and the available initial data/information contain inaccuracies and random noise that can lead to significant differences between the predicted states of the system and the actual states of the system. In this case, observations of the system over time can be incorporated into the model equations to derive improved estimates of the states and also to provide information about the uncertainty in the estimates.

The popularity of model-based algorithms in a number of systems and situations like control and process



optimization has consequently led to an increased interest in developing fundamental models with precise parameter estimates [16, 17]. It is therefore, crucial for researchers to develop models in a dynamic conflict system that responds to these needs reliably and efficiently.

In this paper, we present a model for the estimation of initial conditions of a conflict situation based on the state dynamics using ordinary differential equations (ODEs). The initial conditions estimated are to be integrated in the linear and exponential dynamic models to predict on the future trends of a conflict. A method for estimation of the initial conditions (initial control conditions) in a dynamic state system is given in section (3).

A brief description of the linear and exponential dynamic system models is provided where the estimated initial conditions can be used to form a predictor model.

**1.1. Linear model:**

In the dynamic system continuous time formulation, it is assumed that the absolute change with respect to time of the series is equal to a constant. That is, the average growth is constant during the period. Hence, the dynamics can be represented by

$$\frac{dy}{dt} = \phi, \quad y(0) = \theta, \quad \dots\dots\dots(1)$$

where  $\theta$  is the initial condition of the series. This is

equivalent to assuming that  $\frac{d^2y}{dt^2} = 0$  and  $\frac{dy(0)}{dt} = \phi$  are the initial conditions.

The solution to this equation is given by

$$y_t = \theta + \phi t, \quad \dots\dots\dots(2)$$

which is the linear model in time. Thus, we can view the estimation of the parameters in (1) as fitting the solution (2) to a discrete data set.

**1.2. Exponential model:**

The dynamics in this case can be modelled by

$$\frac{dy}{dt} = \phi y, \quad y(0) = y_0 = e^\theta, \quad \dots\dots\dots(3)$$

That is, the percent growth rate is equal to a constant or that the absolute change is proportional to the current value of the series. We denote by  $y_0$  the initial condition for the problem with a solution given by,

$$y_t = e^{(\theta + \phi t)}, \quad \dots\dots\dots(4)$$

This is the exponential model of time used in estimating trends and growth rates in dynamic environments like economic setting. Its advantage is that the estimated coefficient is the average growth rate.

The linear and exponential functions of time are often used for forecasting for instance in economics, business, and finance.

**2.0. Dynamic representation of the system models**

Purely linear and exponential functions of time can be used for trend estimation as a solution to their corresponding time dynamics equations, that is, equations used to describe how systems change or evolve over time. This is important because understanding the relationships can be very useful to researchers in a conflict situation. It is often the case that reality necessitates the relaxation of the linearity assumptions in a number of situations like conflict and economic environments giving rise to nonlinear dynamic systems. Analytical solutions of these systems are in general unattainable for some relatively more complicated dynamics and the only method of estimation may be the dynamic approach.

In a static state, the initial data point is used as the initial condition of the differential equation, while in the dynamic option; the initial condition(s) is estimated as an additional parameter. The nice thing about this procedure is that the dynamics are written as they occur in the model equations. It is very important to understand the difference between the static and dynamic options when fitting dynamic models to data. The model developed in this paper, can be used for the estimation of the initial conditions for both static and dynamic systems.

**3.0. Model for the estimation of initial conditions**

In modelling any conflict, control variables play a crucial role. Control variables can be any private information that is relevant to the party's decision making in a conflict environment. In the context of this paper, the control variable is modelled to constitute the following components:

1. Demand to the other parties.
2. Demands from the other parties.

The two components are the conditioning variable to a probability of one another.

Suppose we have a conflict control variable  $\ell_i$ , it can be defined by a Bayes probability distribution which is drawn independently and identically distributed (i.i.d) from a logistic distribution function  $F_i(\cdot)$  with a corresponding everywhere positive density  $f_i(\cdot)$ ,

mean  $\mu_i = 0$  variance  $\sigma_i^2 < \infty$ , and assuming that  $f_i$ 's are continuously differentiable.

It is also assumed that a conflict is most likely to arise if the demands from one party are not met by the other party. These demands are usually private information/reservation. Understanding these demands is critical for success of a bargaining game towards the resolution of a conflict, since they constitute a greater part of the control variables of a conflict.

The private reservations  $R_i$  usually will lead to a conflict in opinion. As a consequence of conflict of opinion, a conflict state described by these divergent opinions is developed. This conflict state is characterised by initial conditions (control variables) which must be understood and quantified to successfully model and solve any conflict. In most cases, the initial conditions might be known or unknown and therefore a good model for the estimation of these conditions is paramount. The estimation of the initial conditions in a conflict situation can be compared to the estimation of types in a Bayesian game theory.

Suppose the initial conditions are the state set,  $\theta$ , (current state), they can be represented by:

$$\theta = X_{i \in N} \theta_i, \dots \dots \dots (5)$$

where N is a set of parties to a conflict, X is the state vector,  $\theta_i$  is the state of the system at  $i$ .

Initially, state is assigned a prior belief  $P(\theta)$  which reflects existing knowledge about the conflict state environment. As the system evolves, some new information and data say  $D$  will become available. To estimate these new outcomes, the available beliefs can be updated using the Baye's rule.

$$posterior = p(\theta / D) = \frac{p(D / \theta)p(\theta)}{\int_N p(D / \theta)p(\theta)d\theta} = \frac{likelihood \times prior}{normalizer} \dots \dots \dots (6)$$

Equation (6) gives a new set of initial conditions.

**3.1. Conflict and Ultimatum game**

Suppose in a conflict the first party has made an offer  $y$  based on the state set  $\theta$  given by (5), then the second party will chose between the offer and her reservation value given by  $R_2 + \ell_2$ . Equilibrium and hence settlement of a conflict can be achieved if the second party will play the cut-point strategy given by:

$$s_2(y, \ell_2) = \begin{cases} accept & \text{if } y \geq R_2 + \ell_2 \\ reject & \text{if } y < R_2 + \ell_2 \end{cases} \dots \dots \dots (7)$$

From a negotiation stand point, the first party does not observe  $\ell_2$ , but must assess the probability that the second party will accept or reject his offer, where;

$$\begin{aligned} Pr(accept / y) &= Pr(y \geq R_2 + \ell_2) \\ &= Pr(\ell_2 \leq y - R_2) \dots \dots \dots (8) \\ &= F_{\ell_2}(y - R_2) \end{aligned}$$

Considering the optimization problem for the first party, given the second part's strategy (8), then the expected utility for the first party is:

$$Eu_1(y/Q^*) = F_{\ell_2}(y - R_2). (Q^* - y) + (1 - F_{\ell_2}(y - R_2)). (R_1 + \ell_1); \dots \dots \dots (9)$$

By the first order condition (F.O.C) and the log-concavity of  $f_{\ell_2}$ , the first party's optimal offer is the unique  $y^*$  that implicitly solves

$$y^* = Q^* - R_1 - \ell_1 - \frac{F_{\ell_2}(y^* - R_2)}{f_{\ell_2}(y^* - R_2)}, \dots \dots \dots (10)$$

However,  $0 \leq y^* \leq Q^*$  and sometimes  $y^*$  will be outside the feasible set. We can then show that an end-point (0 or  $Q^*$ ) is optimal and in any perfect Bayesian equilibrium (PBE), the first party will have the strategy:

$$s_1(\ell_1 / R_1, R_2, Q^*, F_{\ell_2}(\cdot)) = \begin{cases} Q^*, & \ell_1 \leq -R_1 - \frac{F_{\ell_2}(Q^* - R_2)}{f_{\ell_2}(Q^* - R_2)} \\ y^*, & -R_1 - \frac{F_{\ell_2}(Q^* - R_2)}{f_{\ell_2}(Q^* - R_2)} < \ell_1 < Q^* - R_1 - \frac{F_{\ell_2}(-R_2)}{f_{\ell_2}(-R_2)} \\ 0, & \ell_1 \geq Q^* - R_1 - \frac{F_{\ell_2}(-R_2)}{f_{\ell_2}(-R_2)} \end{cases} \dots \dots \dots (11)$$

Taking variables  $\delta_k, k \in \{0, y, 1\}$  such that  $\delta_0 = 1$ , if  $y = 0$ ,  $\delta_y = 1$ , if  $0 < y < Q^*$  and  $\delta_1 = 1$ , if  $y = Q^*$  that is, a censored model with a "latent" best offer in the constraint set. Otherwise, there is the best feasible offer, at, a boundary point.

Taking the second party's acceptance as  $\delta_{accept} = 1$ , if she accepted the offer and  $\delta_{accept} = 0$ , if she rejected the offer and assuming we have data on both parties actions (i.e.,  $y$  and  $\delta_{accept}$ ) from the state set,  $\theta$ , then the likelihood would be

$$L = \prod_{i=1}^n Pr(y^* < 0)^{\delta_0} . Pr(y^* = y)^{\delta_y} . (1 - Pr(y^* < Q^*))^{\delta_1} . Pr(accept)^{\delta_{accept}} . Pr(reject)^{1 - \delta_{accept}} \dots \dots \dots (12)$$

Equation (12) is based on the existing control variables in  $\theta$ . It gives the log-likelihood function for our data in

terms of distributions already derived, which are functions of regressors.

Using equation (12), the Likelihood,  $P(D/\theta)$ , which is a measure of the probability of seeing particular realization of the state  $\theta$ , can therefore be estimated, where  $y$  =ultimatum offer from the first party to the conflict,  $Q^*$  =upper bound of the contested prize,  $\delta_i$  = actions,  $\sigma_i : \ell_i \rightarrow A^i, i = \{1, 2\}$ , where  $A^i$  defines the action set for the  $i^{th}$  party.

Since, party 1 is making the ultimatum offer,  $A^1 = \{y: y \in [0; Q^*]\}$ , the second party is then left to accept or reject the offer, so  $A^2 = \{\text{accept; reject}\}$ .

$$\Pr(\text{accept} / y) = \wedge(y - Z\gamma), \dots\dots\dots (13)$$

Suppose the public portion of the parties' reservation values are  $R_1 = \beta X$  and  $R_2 = \gamma Z$ , where  $X$  and  $Z$  are sets of substantive regressors.

Then, for party 1, logistic distribution of  $y^*$  implies that

$$y^* = Q^* - \beta X - \ell_1 - \frac{\wedge(y^* - \gamma Z)}{\lambda(y^* - \gamma Z)}, \dots (14)$$

which is the optimal offer, where  $\wedge(\cdot)$  is the logit cumulative distribution function (c.d.f) and  $\lambda(\cdot)$  is the logit p.d.f.. Solving for  $y^*$  gives

$$y^* = Q^* - \beta X - \ell_1 - 1 - \omega \left( e^{(Q^* - \beta X - \gamma Z - \ell_1 - 1)} \right) \dots\dots (15)$$

where  $\omega$  is Lambert's  $\omega$ , which solves transcendental functions of the form  $z = \omega e^z$  for  $\omega$ . Lambert's  $\omega$  is useful here because it is known to have nice properties. First, Lambert's  $\omega$  is single valued on  $R_+$ . Second,  $\omega$ 's first and second derivatives exist and are well behaved, making it easy to show that  $y^*$  is a monotonic function of  $\ell_1$  and allowing for the derivation of the probability density function for equilibrium offers.

From (6), the new initial conditions estimates of  $\theta$  in a dynamic system, estimated as posteriors can then be given by:

$$\hat{\theta} = \frac{LP(\theta)}{\int_N P(D/\theta)p(\theta)d\theta}, \dots\dots\dots (16)$$

where  $\int_N P(D/\theta)p(\theta)d\theta$  is used to ensure that the values of  $P(D/\theta)$  sum up to one and thus define a proper probability distribution.

**3.2. Application of the model to an armed conflict**

We examine the application of the model in the estimation of initial conditions in an armed conflict situation. Modelling the initial conditions in this situation can be

compared to the modelling of the risk related to the previous conflict, [18].

It is believed that countries that have experienced an armed conflict are more prone to another conflict in the future and thus their risk levels of an armed conflict are high. We have developed a model that estimates the initial conditions which can act as the pointer to the current risk levels using the past and current state control variables. The estimates of the initial conditions can be used to make predictions for the future trends of a conflict in a dynamic state system.

Assuming that all countries in the world are a universal set  $\Psi$  and the countries that are likely to be in a conflict are its subset denoted by  $Q^*$ . Our concern is on the subset which can be described as the "prize". A country becomes an element (member) of  $Q^*$  if it has experienced an armed conflict at any time in the period of interest. The set  $Q^*$  is described as a semi-open space since it allows individuals to become members but does not allow them to get out.

We can therefore define an indicator variable  $X_{tc}$ , such that

$$X_{tc} = \begin{cases} 0 & \text{if } c \text{ is not in conflict in year } t \\ 1 & \text{if } c \text{ is in conflict in year } t \end{cases} \dots\dots\dots (17)$$

Thus,

The total number of countries in a conflict in year  $t$  is:

$$S_t = \sum_{c=1}^n X_{tc} \dots\dots\dots (18)$$

The number of countries that are at conflict in year  $t$  and have experienced at least one armed conflict in the past is:

$$m_t = \sum_{c=1}^n X_{tc} \quad \text{if } X_{tc} = 1 \text{ and } \exists y < t / X_{yc} = 1 \dots\dots (19)$$

The number of countries that have experienced an armed conflict before year  $t$ , they are not at conflict in year  $t$ , but are reported to have experienced another conflict later is:

$$z_t = \sum_{c=1}^n X_{tc} + 1 \quad \text{if } X_{tc} = 0 \text{ and } \exists y < t, j > t / X_{yc} = 1, X_{jc} = 1 \dots\dots\dots (20)$$

The number of countries at conflict in year  $t$  that are reported to be still at conflict at any later period is:

$$r_t = \sum_{c=1}^n X_{tc} \quad \text{if } X_{tc} = 1 \text{ and } \exists y > t / X_{yc} = 1 \dots\dots\dots (21)$$

The total of armed conflicts in a country which is subset of  $Q^*$  is:

$$a_c = \sum_{c=1}^n X_c \dots\dots\dots(22)$$

The probability,  $P(D/\theta)$ , given by equation( 12) that an armed conflict is likely to occur given that a country is a member of  $Q^*$  in  $t$  can be estimated by:

$$P(D/\theta) \equiv L = \frac{m_t r_t}{m_t r_t + s_t z_t} \dots\dots\dots (23)$$

And the prior belief  $P(\theta)$  can be obtained as:

$$P(\theta) = \frac{a_c}{s_t} \dots\dots\dots(24)$$

Using the PRIO/Uppsala Conflict Data Project, data set that can be obtained from <http://www.prio.no/cwp/ArmedConflict> and estimated values by equation (23) and (24), our estimated initial condition  $\hat{\theta}$ , for the various conflict situations in the various countries in the year 2000, 2003 and 2004 can be estimated using equation (16). These estimates are shown in table 1 below:

**Table1: Estimated initial conditions as posterior.**

Country	2000		Country	2003		Country	2004	
	$\hat{\theta}$	No. of conflicts		$\hat{\theta}$	No. of conflicts		$\hat{\theta}$	No. of conflicts
India	0.68	8	India	0.69	7	India	0.74	6
Nepal	0.60	1	Nepal	0.60	1	Nepal	0.67	1
DRC	0.50	1	DRC	0.34	-	DRC	0.56	-
Colombia	0.68	1	Colombia	0.68	1	Colombia	0.74	1
Peru	0.14	0	Peru	0.14	0	Peru	0.18	0
Pakistan	0.49	1	Pakistan	0.49	1	Pakistan	0.56	2
Ethiopia	0.68	3	Ethiopia	0.69	2	Ethiopia	0.74	2
Turkey	0.68	1	Turkey	0.69	1	Turkey	0.74	1
Indonesia	0.55	1	Indonesia	0.55	1	Indonesia	0.52	1
Mali	0.25	0	Mali	0.25	0	Mali	0.31	0
Nigeria	0.14	0	Nigeria	0.14	0	Nigeria	0.18	1
Niger	0.37	0	Niger	0.25	0	Niger	0.31	0
Thailand	0.55	0	Thailand	0.55	1	Thailand	0.62	1

The estimated initial conditions for the various countries based on the past armed conflicts and the current state conditions are given in table 1 as  $\hat{\theta}$ . The estimates reflect the risk level predictions of an occurrence of an armed conflict and can give a pointer to the future trends of the existing conflict. The initial conditions which estimate the likelihood of an occurrence of a conflict have been compared with the actual occurrence of a conflict for various countries. For DRC, there was no data available to indicate any new conflict and thus it was indicated as a dash. From the table, there is a direct relation

between the initial conditions and the actual occurrence of a conflict for most countries.

**4.0. Conclusion**

The model gives initial conditions based on the previous and available conditions for the country in conflict. The estimated initial conditions gives the probability of the occurrence of an armed conflict and can thus form the basis for further investigation and prediction of the trend that a conflict is likely to take as other new interplaying factors come into play. The model is dynamic in the sense it can be adjusted

over the time under investigation. The threshold of the initial conditions upon which a conflict must occur needs to be investigated.

## References

1. J.S. Banks, Equilibrium Behavior in Crisis Bargaining Games. *American Journal of Political Science* .34(3):579-614 (1990).
2. P. K. Huth, L. A. Todd, The Democratic Peace and Territorial Conflict in the Twentieth Century. New York, NY: Cambridge University Pres. (2002).
3. T.R. London, Leaders, Legislatures, and International Negotiations: A Two-Level Game with Different Domestic Conditions. Ph.d Thesis University of Rochester (2002).
4. R. Powell, Bargaining in the Shadow of Power. *Games and Economic Behavior*. 15:255-289 (1996).
5. R. Powell, Crisis Bargaining, Escalation, and MAD. *American Political Science Review*. 81(3):717-736 (1987).
6. V.O. Omwenga, P.N. Mwita, Conflict resolution using statistical approach. *African Journal of Mathematics and Computer Science Research* Vol. 3(2), pp. 026-030 (2010).
7. D.P. Baron, F. John F, Bargaining in Legislatures. *American Political Science Review*. 33(4). (1989).
8. D.P Baron, A Noncooperative Theory of Legislative Coalitions. *American Political Science Review*. 33(4) (1989).
9. E.D. Mansfield, V.M. Helen, B.P. Rosendorff, Tree to Trade: Democracies, Autocracies, and International Trade. *American Political Science Review*. 94:305-321 (2000).
10. C. Signorino, Strategy and Selection in International Relations. *International Interactions*. 28(1):93-115 (2002).
11. C. Signorino, Strategic Interaction and the Statistical Analysis of International Conflict. *American Political Science Review*. 93(2):279-297 (1999).
12. S. Gordon, "Solidarity in choosing a location on a cycle," *Social Choice and Welfare*, Springer, vol. 29(1) (2007)
13. D.B. Rubin, Multiple Imputation after 18+ years. *Journal of the American Statistics*, Vol. 91, 473-48 (1996).
14. T. Harzog, D.B. Rubin, Using multiple imputations to handle nonresponse in sample surveys. *Incomplete data in sample surveys*. New York, Academic press, Volume II, 209-245 (1993).
15. V. Omwenga Singular Value Decomposition of a matrix as an Imputation technique. Msc. Thesis. Egerton University. Njoro. Kenya (2004).
16. L.T. Biegler, I.E. Grossman, Retrospective on optimization. *Computers and Chemical Engineering*. 28, 1169-1192 (2004).
17. N.H. El-Farra, P.D. Christofides, Bounded robust control of constrained multivariable nonlinear processes. *Chemical Engineering Science*. 58, 3025-3047 (2003).
18. B. Clementine, B. Dirk, K. Francois Quantitative global model for armed conflict risk assessment. *JRC Scientific and Technical Reports*. EUR 23430 EN-2008 (2008).

## INITIAL CORRELATIONS AMONG THE LEVELS OF VARIOUS NUTRIENT SPECIES IN WATER FROM NAIROBI DAM, KENYA

P. G. Muigai<sup>1</sup>, P. M. Shiundu<sup>2</sup>, F. B. Mwaura<sup>3</sup> and G. N. Kamau<sup>2</sup>

<sup>1</sup> Department of Chemistry, Jomo Kenyatta University of Agriculture and Technology, P.O. Box, 62000 – 00200, Nairobi, Kenya, E-mail Address: muigaigitita@yahoo.com. <sup>2</sup>Department of Chemistry and <sup>3</sup>School of Biological Sciences; College of Biological and Physical Sciences, University of Nairobi, P.O. Box 30197, Nairobi, Kenya

### Abstract

Research work on Nairobi Dam, Kenya, and its tributaries has revealed that during the first trial sampling period, the  $R^2$  value, i.e., the square of linear regression correlation coefficient was poor between the nutrients:  $(\text{PO}_4^{3-} + \text{Hydrolysable}) - \text{Phosphorous}$  and nitrate-nitrogen (0.0133). But excellent or fairly good correlation was obtained between other pairs of bulk inorganic nutrients in the same groups or blocks of the Periodic Table, or having the same physiological or environmental roles. The results for correlation in descending order are as follows: K & Na (0.9782), Ca & Mg (0.9468), Mn & Fe (0.6357) and Zn & Cu (0.5373). On the other hand, the second sampling results showed that the  $R^2$  value between 'Total' phosphorous and 'Total' Nitrogen ((Total Kjeldahl + nitrate) - nitrogen) (0.8587) was far much higher than that involving phosphorous and nitrate-nitrogen for the first sampling, while that between the other nutrient pairs remained fairly satisfactory as follows:- K & Na (0.9875), Ca & Mg (0.6047), Mn & Fe (0.5147) and Zn & Cu (0.554). This was as expected for elements in the same group or those close to one another like copper and zinc, thus indicating possibility of a common source for most of these inorganic nutrients, such as the domestic sewage effluents. The correlation data for nitrogen and phosphorus demonstrated the fact that it is the total amount of these elements which matters when dealing with eutrophication.

### INTRODUCTION

Two decades ago, Nairobi Dam, Kenya, used to be a very attractive scene for recreation, as well as to offer certain services, such as domestic use, fishing and Church Baptism by immersion. As a result, tourists and local visitors would flock there. The water was then clear and plant growth minimal. In the closing years of the 20<sup>th</sup> Century, the dam was infested with aquatic weeds, especially the water hyacinth, leading to its imminent partial "death", and the former recreational activities were no more. This was a probable consequence of Eutrophication. The current apparent Eutrophication in Nairobi Dam has been postulated to be mainly due to the abundance of phosphorous as a result of use and disposal of anionic surfactants, in domestic sewage effluents. The element, which is most essential for the growth of the (fresh-aquatic) water-hyacinth in the shallow dam, was therefore expected to be the limiting element in the growth

and proliferation of the water hyacinth in the dam and its environs [1].

In Eutrophication work, by plotting phosphorous versus nitrogen concentrations during various seasons, a straight-line relationship can usually be established. It is assumed that the limiting nutrient will be exhausted first, and will show as a negative intercept of the line on the axis of the limiting nutrient. The one which is not limiting will remain in solution, yielding a positive intercept of the line of best-fit [2].

It is worth noting that both nitrogen and phosphorous, which are major nutrients required by all organisms for the basic processes of life, are in the same group of the Periodic Table. They possess similar chemical properties and are expected to interact similarly in various biological and environmental systems. This also applies to the other nutrient elements in the same groups or blocks of the Periodic Table. This can be demonstrated by various similar biological



functions for these elements as given in the literature [3].

Previously, no detailed work had been done on the Eutrophication of lakes, rivers and dams in the East African region, especially in Kenya and particularly in Nairobi Dam with regard to seasonal variations. The Nairobi Dam water mass has in the recent years, since 1998, been largely covered with aquatic weeds, particularly water hyacinth [1]. However, the dam and its environs have attracted many Non Governmental Organizations (NGOs) and researchers in pursuit of information, data and solutions to inherent problems. Information and data on geological and chemical pollution assessment have been compiled in a report on the Nairobi River basin edited by Okoth and Otieno [4]. Related work on environmental impact of urbanisation on Nairobi Dam was conducted by Iole [5].

It was reported [4] that although Biological Oxygen Demand (BOD) levels were relatively low, total coli form counts at Nairobi Dam, Kibera Station (inlet to Nairobi Dam) were

quite high. This was attributed to direct sewage inputs to the river from the large informal Kibera settlement due to lack of a municipal sewage disposal infrastructure [4].

The current research work was therefore meant to complement what has been reported on the pollution of Nairobi River basin, especially with regard to seasonal influence [4, 6].

## **METHODOLOGY**

### **SAMPLING**

A map of the part of the City of Nairobi showing Nairobi Dam, its tributaries and environs and the sampling points is shown in Figure 1. The area of the dam is approximately 0.274 Km<sup>2</sup>. The water samples collected and analyzed were from Nairobi Dam and from its two main tributaries, Motoine and Ngong Rivers. Sampling was mainly done near the bridges, shores or where the dam and the rivers were easily accessible. Water samples were drawn in duplicate using cleaned High Density Polyethylene (HDPE) plastic containers of 1L and 2L capacities, at the surface of various points of the

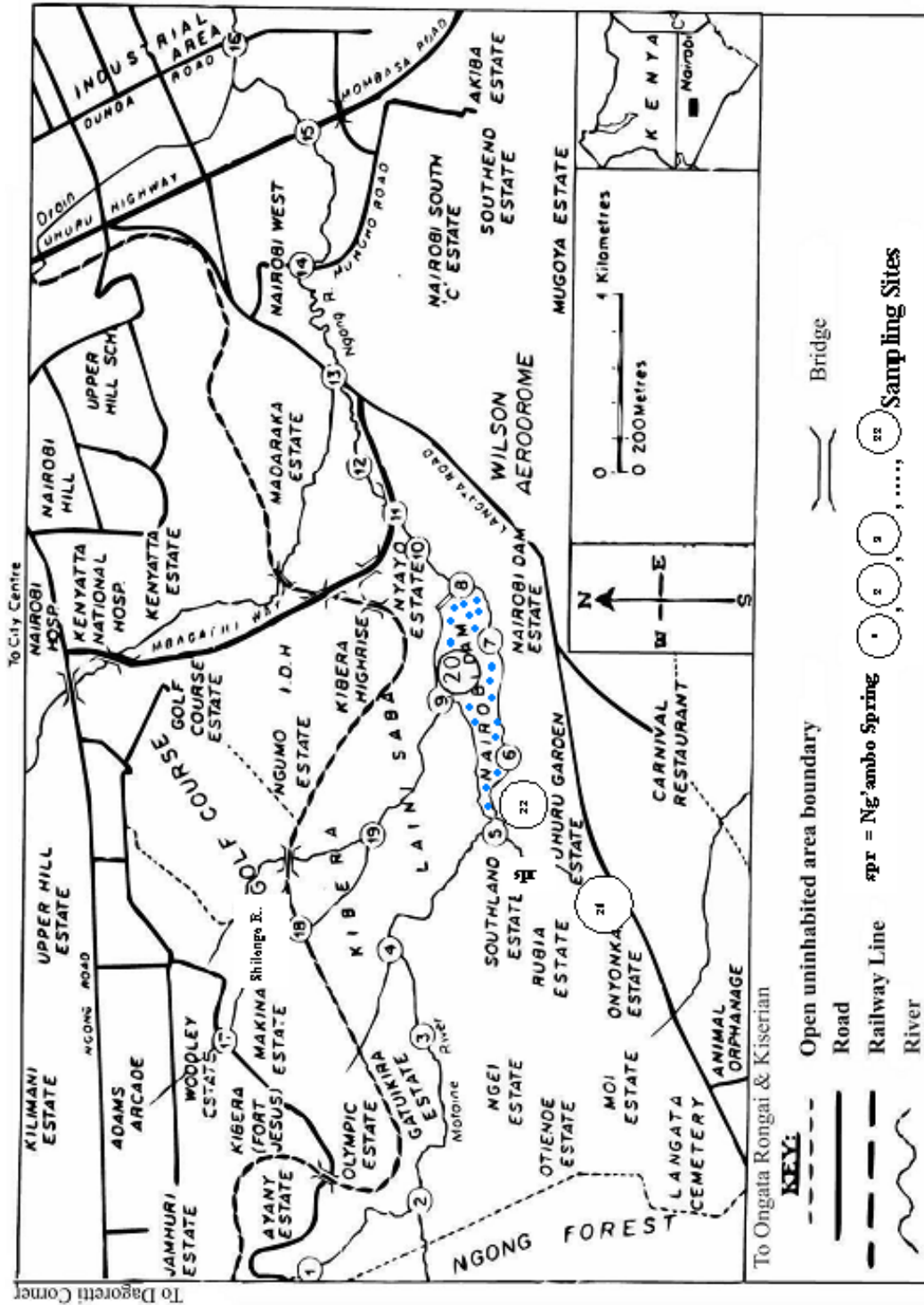


**Figure 1.** Map of Nairobi Dam, its major tributaries and environs, showing the sampling points



dam and its two tributaries almost simultaneously. This was done by three well coordinated teams to avoid time variation effects. For every pair of samples, one was acidified by addition of 2ml of conc.  $H_2SO_4$  (96-98% m/m) per litre of sample and stored at room temperature until the time of analysis. The untreated samples were stored in the fridge at 4° C until the time of analysis. The two sampling periods involved in the current publication were on 2<sup>nd</sup> October 2004 and 12<sup>th</sup> February 2005.

## SAMPLE ANALYSIS

### *Determination of Phosphorous*

Standard International methods were used [7]. For the determination of phosphorous, the acidified water samples were filtered through No. 40 or 540 filter papers. 40 ml of the water filtrate had its pH adjusted to 3-10, using 2M sulphuric acid or 1M sodium hydroxide. To this was added 1 ml of ascorbic acid solution (10 % (m/v)) followed by 2 ml of acid molybdate solution (13 g of ammonium heptamolybdate tetrahydrate  $[(NH_4)_6Mo_7O_{24} \cdot 4H_2O]$  and 0.35 g antimony potassium tartrate hemihydrate  $[K(SbO)C_4H_4O_6 \cdot \frac{1}{2} H_2O]$  were transferred into a clean glass container. To this mixture was added 200 ml of water followed by 300 ml of 9 M sulphuric acid with continuous stirring and mixing well). This was made to the 50 ml mark with distilled water, mixed well and left to stand for at least 30 minutes and diluted if necessary for analysis. For calibration, 0.0; 1.0; 3.0; 5.0; 8.0; 10.0 and 15.0 ml of the orthophosphate standard solution (2 mg of phosphorous per litre) were transferred by means of pipette to a series of 50 ml volumetric flasks, diluted to about 40 ml with distilled water and the same reagents used in the colour development for the samples added before diluting to 50 ml with distilled water and treating as for the samples. The absorbance for the standards and sample solutions were read at 880 nm with CADAS 100 UV/Visible Spectrophotometer. A calibration graph of absorbance against the phosphorous content, in mg/l, of the calibration solutions was plotted and linear correlation coefficient ascertained to be  $\geq 0.99$  and sample phosphorous

contents calculated. Spiked water was treated in the same way for Quality Control checks.

### *Determination of Total Kjeldahl (Proteinaceous and Ammoniacal) Nitrogen – (TKN):*

#### *Automated Distillation & Titration*

For the determination of Total Kjeldahl Nitrogen (TKN), 30 ml of liquid (water, liquid blank and recovery) samples were weighed into clean dry digestion tubes. 0.8 g of  $CuSO_4 \cdot 5H_2O$  and 7 g of  $K_2SO_4$  were added to each of the digestion tubes. 10 ml of (96%) conc. Sulphuric acid was added from a dispenser and mixed carefully by swirling the tube by hand. The rack with digestion tubes containing the samples was placed besides the automated digester and fitted with the exhaust manifold on top. The vacuum source (scrubber) was turned on to maximum air flow. The tubes and exhaust manifold were placed in the pre-heated digester at 420° C and the heat shields hooked on the stand. The tube contents were digested for 3-5 minutes with maximum air flow through the manifold. The flow was then adjusted until the fumes were just contained. The digestion was continued until all samples were clear with a blue green solution. This was normally about 30 minutes, depending on sample type. The stand with the tubes and exhaust manifold were removed and the entire assembly cooled sufficiently at room temperature, but avoiding solidification. However, if formed, any solid was dissolved by placing the digestion tube in the pre-heated digester for a short time.

The Automated Distillation / Titration – 2300 Kjeltex Analyzer Unit, Foss Tecator (Computerized) was started up (according to the instrument's operating manual), using boric acid solution (1% (m/v) containing 0.0007% methyl red indicator, 0.001% bromocresol green indicator, 1.7% methanol (m/v) and 0.0005 M NaOH) as receiver solution. The suitable Kjeldahl programme was selected for reading the nitrogen content in %, m/m. One or two blanks were run, their display noted and their value recorded. The prepared digestion tube was placed in position and the safety door closed. When the cycle was over, the results were noted and the safety door opened to remove the

digestion tube ready to insert the next sample digestion tube and the cycle repeated. These included the liquid and solid spikes and House Reference Materials (HRM) [8, 9].

**Calculation of results:**

$$\text{Total Kjeldahl Nitrogen (TKN), \% , m/m} = \frac{1.401 \times (V_2 - V_1) \times N}{B}$$

Where  $V_2$  = Volume of hydrochloric acid required for the sample;

$V_1$  = Volume of standard hydrochloric acid required for the blank;

$N$  = Normality of hydrochloric acid used in titration;

$B$  = Mass in grams of the sample taken for determination.

**Determination of Nitrate - Nitrogen**

50 ml of the calibration standard solutions and acidified water samples, including their respective blanks and spiked Quality Control sample solutions were transferred into 100 ml plastic beakers. 2 ml of sodium salicylate solution (0.5% (m/v)) was added and evaporated to near dryness in the air oven at  $105 \pm 2^\circ$  C. The residue was cooled at room temperature. 2 ml of conc. Sulphuric acid was added and the solution allowed to stand for about 10 minutes. 15 ml of distilled water was added followed by 15 ml of mixed solution containing sodium hydroxide (400 g/L) and potassium sodium tartrate (16 g/L). This was cooled to room temperature and transferred to 100 ml volumetric flask and made to the mark with distilled water. These were stirred and mixed well. The absorbance of the calibration standard (0.0, 1.0, 3.0, 6.0, 9.0 and 12.0 mg/l) and sample solutions, their respective blanks and recovery spikes were measured, using a calibrated CADAS 100 UV / Visible Spectrophotometer at 420 nm after taking the zero reading using a blank test solution and operated as per manufacturer's instructions. A calibration graph of absorbance against the concentration was plotted and its linear correlation coefficient, i.e.  $r$  ascertained to range from 0.99 to 1.00. Using the linear regression

equation, the sample nitrate was calculated. This value was multiplied by the stoichiometric conversion factor 0.226 to obtain the corresponding  $\text{NO}_3^-$ -N concentration [10].

The total amount of nitrogen was estimated by the following formula:

$$\text{'Total' Nitrogen content} = \text{Total Kjeldahl Nitrogen (TKN)} + \text{Nitrate - Nitrogen}$$

**Determination of Metallic Nutrients in Water**

Determination of sodium and potassium was done using Corning 400 Flame Photometer. Calibration was done using 0, 1, 2, 4, 6, 8 and 10 mg/l sodium and potassium standards. The filtered water samples were aspirated directly into the flame and diluted if necessary, using distilled water. Their emission intensities were read using a sodium filter at wavelength of 589.0 nm and a potassium filter at 766.5 nm and their sodium and potassium concentrations calculated from the respective calibration graphs.

Atomic Absorption Spectrometry (AAS) was used for determination of Ca, Mg, Mn, Fe, Zn and Cu in water samples. The theory and applicability of Flame Photometry and AAS are well documented in the literature [11-13].

Samples were aspirated directly into the AAS, with appropriate dilutions, for the determination of available Ca, Mg, Mn, Fe and Cu, without need for digestion or extraction, using standard procedures, as cited in the literature above. For the determination of calcium and magnesium, when using air/acetylene flame, caesium chloride solution (as an ionization buffer) was added (so that one litre of the final solution contained 2.5 gram of CsCl and 0.8 ml of conc. (37%) hydrochloric acid) and when using nitrous oxide/ acetylene flame, lanthanum oxide ( $\text{La}_2\text{O}_3$ ) was added, so that one litre of the final solution contained 1000 mg of lanthanum and 20 ml of conc. (37%) hydrochloric acid [7, 14]. In the current work, the oxidant/ fuel mixtures indicated below were

used for the following techniques: (a) AAS for Ca and Mg - Nitrous oxide/ acetylene flame, (b) AAS for other metals – Air/ acetylene flame and (c) Flame Photometer for Na and K – Air/ n-butane flame. The water samples were diluted where necessary. Spiked recovery samples were

also included for reference and analytical Quality Control. Metals were analyzed using the recommended standard wavelengths and conditions in AAS as listed in Table 1.

**Table 1: AAS INSTRUMENTAL CONDITIONS EMPLOYED**

METAL ANALYTE AND SYMBOL	WAVELENGTH, $\lambda$ , in nm	BAND PASS, nm	CALIBRATION Standard Solution Concentrations, mg/l	SOURCE OF STD. STOCK SOLUTION, 1000 mg/l
CALCIUM, Ca	422.7	0.5	0.0, 0.2, 0.4, 0.6, 0.8, 1.0	Panreac Quimica SA
MAGNESIUM, Mg	285.2	0.5	0.0, 0.2, 0.4, 0.6, 0.8, 1.0	Panreac Quimica SA
MANGANESE, Mn	279.5	0.2	0.0, 0.5, 1.0, 1.5, 2.0, 2.5	Panreac Quimica SA
IRON, Fe	248.3	0.2	0.0, 0.5, 1.0, 1.5, 2.0, 2.5	Panreac Quimica SA
ZINC, Zn	213.9	0.5	0.0, 0.2, 0.4, 0.6, 0.8, 1.0	Panreac Quimica SA
COPPER, Cu	324.8	0.5	0.0, 0.2, 0.4, 0.6, 0.8, 1.0	Panreac Quimica SA

N.B. Appropriate dilutions were made from the Standard stock solution to obtain the calibration standard solutions required.

## RESULTS AND DISCUSSIONS

Comparison between correlation data from all sampling points for different pairs of nutrient levels for water from Nairobi Dam and its inlet and outlet tributaries during the first two samplings of 2<sup>nd</sup> October 2004 and 12<sup>th</sup> February 2005 (Seasons nos. 1 & 2) are as shown in Figures 2 – 6. These results show that the

correlations between the elements in each pair were positive and relatively high ( $R^2 > 0.5000$ ), except between orthophosphate-phosphorous and nitrate-nitrogen, which was relatively very low, with  $R^2 = 0.0133$ . This shows that except for the two combined nutrients ( $\text{NO}_3^-$  &  $\text{PO}_4^{3-}$ ), the other nutrients could have originated from the same source, most likely the domestic sewage effluents.

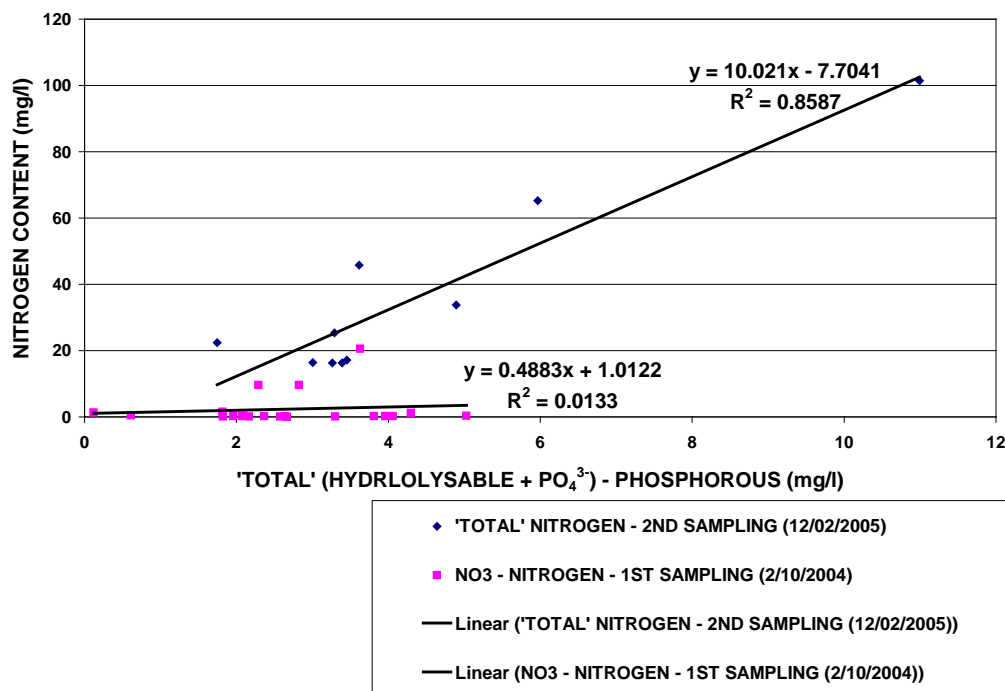


**Figure 2:** Graphs of Nitrogen versus Phosphorous Concentrations in Nairobi Dam Basin Water (1<sup>st</sup> & 2<sup>nd</sup> Samplings).

The notably fair positive linear correlation between phosphorous and 'Total' Nitrogen ((Total Kjeldahl + nitrate) - nitrogen), i.e. ( $R^2 = 0.8587$ ), which was found to be significantly higher than 0.5000, can be explained by the fact that the nutrient balance (in aquatic systems) is a product of at least five phenomena. These include carbonate cycle, the nitrogen cycle, the phosphate cycle, the level of photosynthesis and the maintenance of aerobic processes [15]. There are optimal ratios of  $\text{NO}_3^-/\text{N}$  and  $\text{PO}_4^{3-}/\text{P}$  for varied regimes. As the

balance becomes tipped, some species become tipped, some species become predominant and the environment becomes unfavourable for many others [15]. In the current work, for existence of suitable correlation between these two nutrients (nitrogen and phosphorous), all possible environmental forms of nitrogen had to be considered. When these parameters were thus determined, Nitrogen (from nitrates,  $\text{NH}_3$  and Proteins) and Phosphorous (mainly from  $\text{PO}_4^{3-}$  species), both of which are in the same group of the Periodic Table, correlated very well.

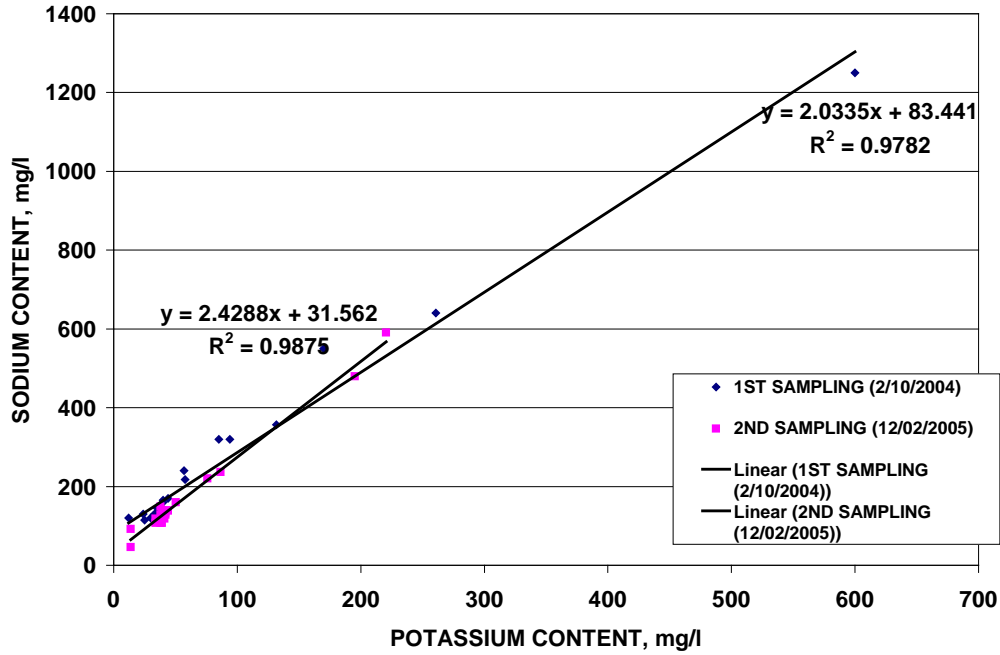


**Figure 3:** Correlation Graphs of Sodium vs. Potassium Concentrations in Nairobi Dam Basin Water (1<sup>st</sup> & 2<sup>nd</sup> Samplings).

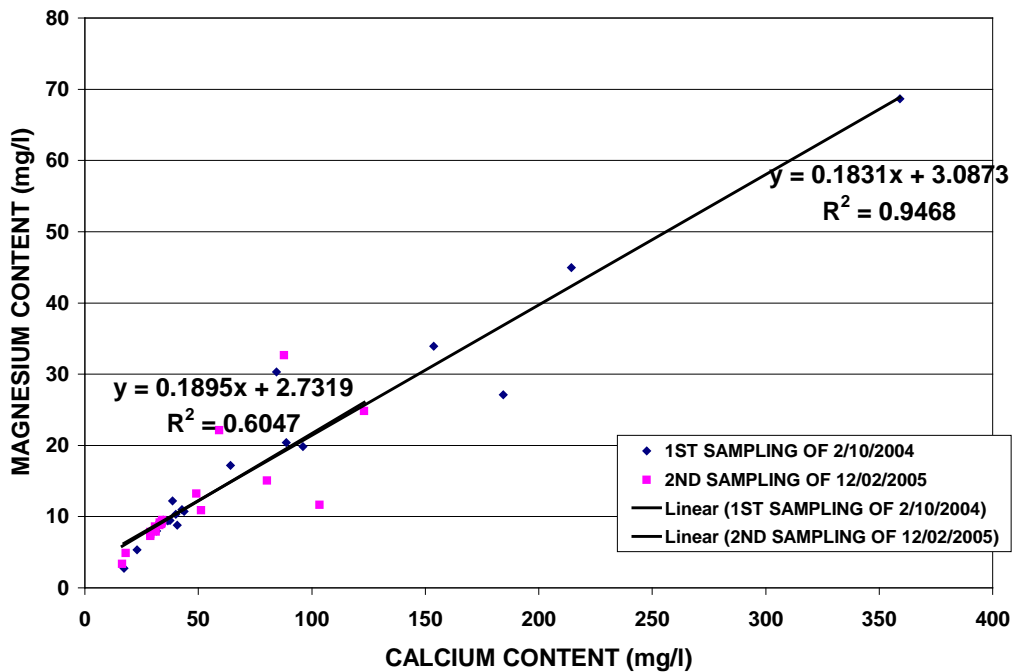


**Figure 4:** Graphs of Magnesium versus Calcium Concentrations in Water (1<sup>st</sup> & 2<sup>nd</sup> Samplings).

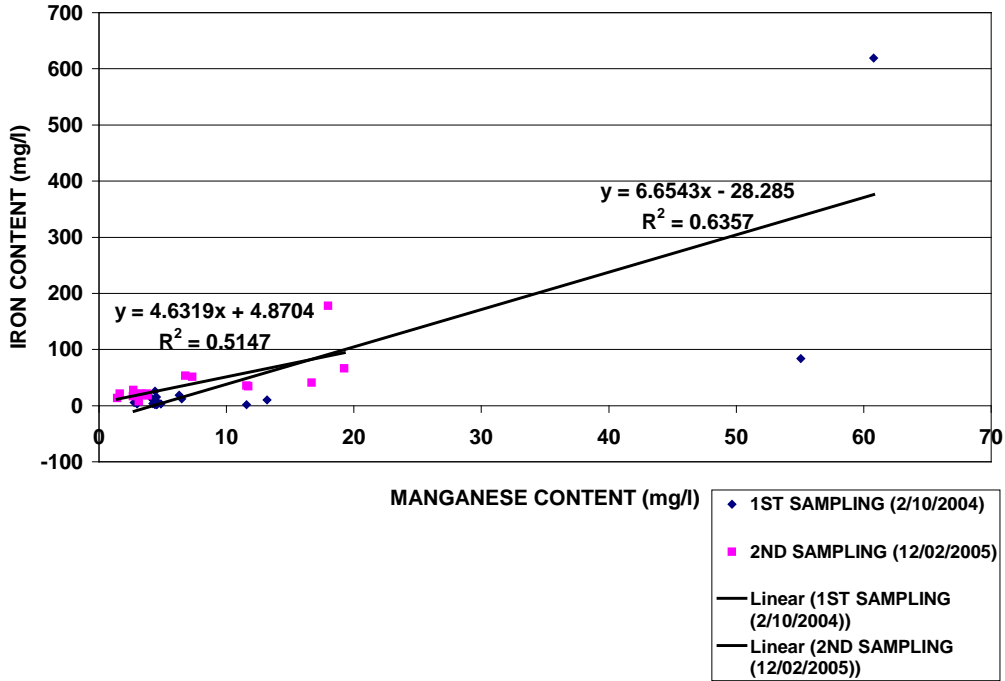


Figure 5: Correlation Graphs of Iron vs. Manganese Concentrations in Nairobi Dam Basin Water - All Points (1<sup>st</sup> & 2<sup>nd</sup> Samplings).

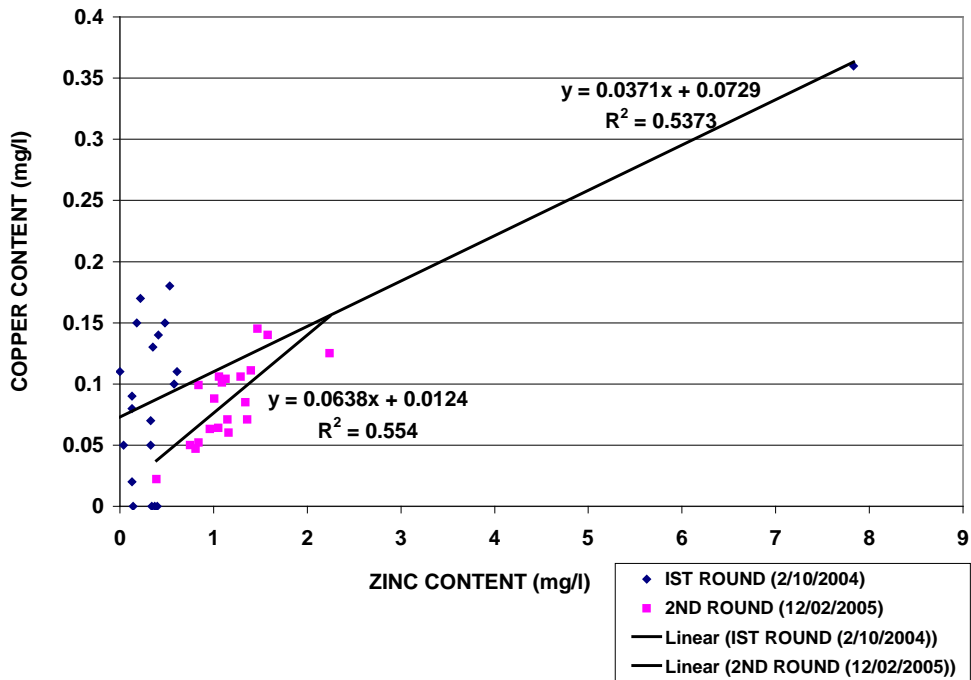


Figure 6: Correlation Graphs of Copper vs. Zinc Concentrations in Nairobi Dam Basin Water (1<sup>st</sup> & 2<sup>nd</sup> Samplings).

The above results (for metals) show that on average, the pairs zinc-copper) and manganese-iron) had lower linear correlation coefficients as compared to potassium- sodium and calcium-magnesium in that order. This evidently suggested that species in the same group of the Periodic Table exhibited much higher correlation than the ones in the same row of the periodic table. This was expected because the bonding and hence chemical characteristics between species of the same charge or group, say potassium and sodium are relatively identical, compared to those pertaining to different charges or groups, though the same row (transition metals). Charges of a particular sign, such as Group I or II cations will have comparably higher interaction with the oppositely charged ions, such as chloride or sulphate respectively, than dissimilar ones.

The above concept, behaviour of elements in the same group of periodic table, which was apparent in the current study, was demonstrated the appreciable correlation between 'total' orthophosphate-phosphorous and 'total' nitrogen ((Organic + Inorganic) – N). This can be explained by recalling from the literature review that Phosphorous is present in lakes (including dams) only in the form  $\text{PO}_4^{3-}$ , with phosphorous exhibiting an oxidation number of 5, so that the complications regarding oxidation and reduction discussed with Nitrogen do not arise [16]. Therefore, for existence of suitable correlation between these two nutrients (nitrogen and phosphorous), all possible environmental forms of nitrogen had to be considered but for phosphorous, it was sufficient to consider the (hydrolysable + orthophosphate) – phosphorous. This was done by simple preservation with 2 ml of concentrated  $\text{H}_2\text{SO}_4$  for every litre of water sample and then determines the orthophosphate – phosphorous amount in the resulting supernatant liquid.

Nevertheless, the overall fair correlation encountered between manganese and iron ( $R^2 > 0.5000$ ) can be explained by the fact highlighted by Cole [17]: manganese is very close to iron in the redox transformations of lakes and behaves in much the same manner, both being soluble in the bivalent oxidation state. Manganese has four major valence states (+II, +III, +IV and +VII), alternating between reduced soluble and oxidized (less soluble) conditions. Being soluble in the bivalent state, manganese is reduced and mobilized at a higher redox voltage than iron. Under strong oxidizing conditions, manganese is part of the colloidal micro

zone seal and it serves with iron as a barrier between deeper sediment and supernatant water probably in the tetravalent or trivalent condition [17].

On average, the metallic nutrient pair with the overall lowest linear correlation coefficient (with  $R^2$  value greater than, but close to 0.5) was that between zinc and copper. This can be explained by the fact that although both these two are d-block elements, zinc exists exclusively as  $\text{Zn}^{2+}$ , which is usually very stable, with filled d orbitals ( $d^{10}$ ). On the other hand, copper can exist as  $\text{Cu}^{2+}$  ( $d^9$ ) as well as  $\text{Cu}^+$  ( $d^{10}$ ), of which the cupric (+II oxidation) state is relatively much more stable. Also, these two nutrients are trace elements and any excessive levels beyond the threshold safe limit become toxic to the aquatic plants, leading to their imminent death. The overall levels of these two nutrients, zinc and copper, were generally found to lie below their maximum limits of 5 and 0.1 mg/l respectively for drinking water, set by the Kenya Bureau of Standards [18]. This showed minimal toxicity with respect to these metallic nutrients. In addition, zinc was generally found to be higher than copper in the water samples from the water-hyacinth growing zone. This showed that the water hyacinth and other aquatic plants in the environment studied could tolerate relatively higher levels of zinc than copper. This is also supported by the fact that the major sources of zinc in the area were rain (containing levels from 2.5 to 12  $\text{mg/m}^3$ ) [17] and its use in the manufacture of galvanized iron sheets [19] which were rampant in the sprawling settlements of the area studied.

It is also evident that the linear regression equations for most of the above nutrient pairs, except between 'Total' nitrogen-'Total' phosphorous in the second sampling and between manganese-iron in the first sampling, the intercepts for the vertical axis were positive. The above correlation data could also form a good solid basis for further future work especially in the determination of the limiting nutrient element in Nairobi Dam and other aquatic bodies of the world, in line with the 'limiting nutrient' definition [2].

## CONCLUSIONS AND RECOMMENDATIONS

The current initial research work on Nairobi Dam, Kenya, has revealed that there was



biological activity as demonstrated by proliferation of aquatic plant growth, mainly the water hyacinth, coupled with existence of linear correlations among difference nutrients pairs, which was a good indicator of possible eutrophication. Moreover, during the first sampling, there was very poor positive correlation between the nutrients nitrate/nitrogen and ( $\text{PO}_4^{3-}$  + Hydrolysable) - Phosphorous ( $R^2 = 0.0133$ ), which indicated that the sources of these two nutrients ( $\text{NO}_3^-$  &  $\text{PO}_4^{3-}$ ) were most likely different. Nitrate is a product of microbial activity by nitrogen fixing bacteria, while phosphate could have originated from the sewage effluent and (most probably) from use of phosphorous-containing surfactants (such as detergents) as permitted in the relevant Kenya Standard [20]. During the second sampling, the linear correlation between 'Total' Phosphorous and 'Total' Nitrogen ((Total Kjeldahl + nitrate) - nitrogen) was positive and far much better, i.e. ( $R^2 = 0.8587$ ) than that involving phosphorous and nitrate-nitrogen for the first sampling. The relatively high correlation value obtained clearly demonstrated that it is the total nitrogen and total phosphorus which are important for eutrophication of water bodies. Nitrogen is from nitrates ( $\text{NO}_3^-$ ), ammonia ( $\text{NH}_3$ ) and Proteins) and Phosphorous is mainly from  $\text{PO}_4^{3-}$  species. In addition, the following pairs of elements in same group or block of the periodic table or similar physiological or environmental roles gave fairly good correlations ( $R^2 > 0.5000$ ): K & Na ( $R^2 = 0.9782, 0.9875$ ), Ca & Mg ( $R^2 = 0.9468, 0.6047$ ), Mn & Fe ( $R^2 = 0.6357, 0.5147$ ) and Zn & Cu ( $R^2 = 0.5373, 0.554$ ). This suggests that these nutrients could have originated from the same source, most probably the domestic sewage effluents.

Based on the above results and conclusions the authors recommend that studies on eutrophication of aquatic bodies be carried out aimed at investigating existence of possible linear correlations among various nutrients as indicators of possible eutrophication.

## ACKNOWLEDGEMENTS

The authors wish to thank Kenya Bureau of Standards for allowing the main analytical work to be conducted at their Laboratories, Jomo Kenyatta University of Agriculture and Technology and University of Nairobi for technical assistance.

The additional help from field assistants is also highly acknowledged.

## REFERENCES

1. P.G. Muigai. Extent of Eutrophication of Nairobi Dam, Kenya and Possible Implications on the Surrounding Environment. Ph. D. Thesis, University of Nairobi, Department of Chemistry, P.1-219 (2007).
2. P.A. Krenkel and V. Novotny. Water Quality Management. Academic Press, Inc., New York, P.509-553 (1980).
3. R.W. Hay. Bio-inorganic Chemistry, Ellis Horwood Ltd., Chichester, England, P.1-210 (1984).
4. P.E. Okoth and P. Otieno (eds.). Pollution Assessment Report of the Nairobi River Basin. Africa Water Network & UNEP, P.1-81 (2000).
5. I. Iole. Environmental impact of urbanisation on water resources – A case study on Nairobi Dam, Kenya. M.Sc. Dissertation Abstract, ICSTM, CET, University of London, P.1 (2000).
6. S.M. Kithiia, M.Sc. (Hydrology) Thesis, University of Nairobi, Department of Geography, P.1-192 (1992).
7. International Organisation for Standardisation. ISO Standards Compendium: *Environment*, Water Quality, Vol. 2 - Chemical Methods, 1<sup>st</sup> ed., P.1-343 (1994).
8. Kenya Bureau of Standards. Kenya Standard Methods of Test for Animal Feed Stuffs. Part 1, KS 01-63: Part 1, P.1-13 (1990).
9. ISO Standards: Animal Feeding Stuffs. Determination of Nitrogen Content and Calculation of Crude Protein Content – Kjeldahl Method, ISO-5986:1983, P.1-5 (1983).



10. W. Fresenius, K.E. Quentin and W. Schneider (eds.). Water Analysis. Springer-Verlag, P.226-230 (1988).
11. H.H. Willard, L.L. Merritt (Jr.), J.A. Dean and F.A. Settle (Jr.). "Instrumental Methods of Analysis", CBS Publishers & Distributors, New Delhi-15, P.127-153 (1986).
12. B. Welz. Atomic Absorption Spectroscopy. Verlag Chemie, Weinheim, New York, P.64-71, 158-159 (1976).
13. A.E. Greenberg, R.R. Trusselli and L.S. Clesceri. Standard Methods of Examination of Water and Wastewater, 16<sup>th</sup> edition American Public Health Association, Washington, P.151 (1985).
14. Perkin Elmer. Atomic Absorption Spectroscopy Analytical Methods. The Perkin Elmer Corporation, P.132-145 (1996).
15. E.T. Chanlett. Environmental Protection. McGraw-Hill, Kogakusha, P.124-125 (1973).
16. T.D. Brock. A Eutrophic Lake, Lake Mendota, Wisconsin. Springer-Verlag New York, Inc., P.43-83 (1985).
17. G.A. Cole. Textbook of Limnology, C.V. Mosby Company, U.S.A., P. 1-283 (1975).
18. Kenya Bureau of Standards. Kenya Standard Specification for Drinking Water. Part 1 – The Requirements for Drinking Water and Containerized Drinking Water, 1<sup>st</sup> Revision, KS 05-459: Part 1, P.1-11 (1996).
19. Kenya Bureau of Standards. Kenya Standard Specification for Galvanized Plain and Corrugated Iron Sheets. 4<sup>th</sup> edition, KS 2, P.1-10 (2003).
20. Kenya Bureau of Standards. Kenya Standard Specification for Synthetic Detergents. Part 1: Household Hand Use, KS 92-1, P.1-12 (2003).

# CREATION OF THE UNIVERSE FROM A NON CLASSICAL SPACE-TIME STATE

M. G. Okeyo, M. N. Maonga, M. J. Otieno

Department of Physics, School of Physical Sciences, University of Nairobi, P.O. Box 30197-00100 Nairobi, Kenya

## Abstract

Creation of the universe from the initial hot state is studied topologically. It is found that the universe emerges from the initial compact state with a finite size to a symmetric state and later evolves inflationary to its asymmetric global minimum. The tunneling probability from this compact state to a classical state rapidly approaches unity at very high temperatures in the radiation dominated phase. This indicates that the initial hot state is necessary for the spontaneous creation of our universe. The big bang singularity prevalent in the standard cosmological model is non-existent in this model.

## I. Introduction

Nonlinear classical field theories possess extended solutions known as solitons that represent configurations with well-defined energies that are nowhere singular. One of the solutions that appear interesting is that of instantons. An instanton is a solution to the equations of motion with a finite, non-zero action, either in quantum mechanics or in quantum field theory. More precisely, it is a solution to the equations of motion of the classical field theory on a Euclidean space-time. In such a theory, solutions to the equations of motion may be thought of as critical points of the action. These critical points can be local maxima of the action, local minima or saddle points. Hence, instantons are important in quantum field theory because they can describe solutions of the gauge field equations in which, as the time coordinate evolves along the entire time axis, a vacuum belonging to one homotopy class evolves into another vacuum belonging to another homotopy class with the pontryagin index taking the value unity<sup>1</sup>. In between these vacua is a region where the field tensor is non-vanishing with positive field energy. The Yang-Mills vacuum is thence infinitely degenerate consisting of an infinite number of homotopically non-equivalent vacua and the instantons solution will represent a transition from one vacuum state to another.

The idea of instantons can be very interesting to the study of the particle physics of the big bang cosmology. In particular, in the standard big bang cosmology, the universe started from a big bang and continued to expand. When extrapolated backwards, the universe is found to be very dense in the past and the average energy per particle is much higher<sup>2</sup>. This extrapolation predicts a singularity at zero moment of time. As we approach this instant, the volume of the universe vanishes and the Hubble constant increases rapidly being infinite at zero time. This epoch indicates violent activity and is normally referred to as the big bang singularity<sup>3</sup>. Quantitatively, zero volume and time implies a breakdown of the concept of space-time geometry and has been recognized as an inevitable feature of Einstein's general theory of relativity. Qualitatively, it is a feature that prevents one from investigating what happened at zero volume and time or prior to it. This abrupt termination of the past signifies the inadequacy of the general theory of relativity. This leads one to pause and question: Where and how did it start? This paper attempts to answer the first part of the question. The second part will be communicated in our subsequent publication.

Now, in any big bang model, one must deal with the problem of creation. This problem has two aspects: One is that the conservation laws of physics forbid

the creation of something from nothing. The other is that even if the conservation laws were inapplicable at the moment of creation, there is no apparent reason for such an event to occur. The prevailing attitude towards creation is that our universe is probably undergoing merely one in an infinite sequence of expansions with intervening contractions. According to this view, the universe has always existed, so that its origin lies in the infinite past. The preceding viewpoint may indeed be correct but it leaves some unanswered questions. First by what mechanism does the universe bounce back from each contraction? No satisfactory mechanism has ever been proposed. Second, why does the universe have its particular values for energy, electric charge, baryon and lepton numbers and so on? Still no satisfactory explanation has ever been found.

Edward Tryon<sup>4</sup> has suggested that our universe did appear from nowhere about  $10^{10}$  years ago, an event that violates none of the conventional laws of physics. He argues that the laws of physics merely imply that a universe which appears from nowhere must have certain specific properties. In particular, such a universe must have a zero net value for all conserved quantities. In this paper a cosmological model in which the creation of the universe from a non-classical space-time state is studied topologically. To first order, our calculations show that the universe emerges with a finite size that may not be totally stable as a result of thermal, gravitational or quantum effects. The Euclidean equation of motion is solved and the transition probability evaluated. The results obtained are topological in nature, an indication of the usefulness of the soliton solutions especially instantons to the study of the very early universe. They may be a suitable candidate for quantum cosmology.

The paper is organized as follows: Section I contains the introduction and section II briefly reviews the evolution of the inflationary universe. An elementary example from condensed matter physics is also discussed to aid in understanding the concept of spontaneous pair creation of matter-antimatter states in a given field. Section III calculates the Euclidean action for the equation of motion and evaluates the tunneling probability of the false vacuum. The action

is a soliton-like solution which is also the aim of the paper. Section IV contains our conclusions and further research work.

## II. Evolution of the Universe

A universe that starts in the symmetric vacuum state is described by the Friedmann-Limatre-Robertson-Walker metric<sup>5,6,7,8,9,10</sup>

$$d\tau^2 = dt^2 - S^2(t) \left[ \frac{dr^2}{1-kr^2} + r^2 d\Omega^2 \right] \quad (1)$$

and the Friedmann evolution equation<sup>11,12,13</sup>

$$\frac{\dot{S}^2 + k}{S^2} = \frac{8\pi G}{3} \rho_o \quad (2)$$

where  $d\tau$  is the invariant line element between two space-time points,  $dt$  is the proper time interval,  $S(t)$  is the scale factor related to an observable say the red shift of a receding object,  $dr$  is the proper three-space interval between two points,  $d\Omega$  is the angular space interval,  $\dot{S}$  is the time derivative of  $S$ ,  $k$  is the curvature parameter that may take the values  $-1, 0$  or  $+1$ ,  $G$  is the gravitational constant and  $\rho_o$  is the critical energy density. We use the natural units where  $c = \hbar = 1$ . The equation can be solved<sup>14</sup> to get the de Sitter solution

$$S(t) = H^{-1} \cosh(Ht) \quad (3)$$

where  $H = \left( \frac{8\pi G}{3} \rho_o \right)^{1/2}$ . Solution (3) describes a universe that is contracting at  $t < 0$ , reaches its minimum size  $S_{\min}(0) = H^{-1}$  at  $t = 0$  and is expanding at  $t > 0$ . This behavior is equivalent to that of a particle bouncing off a potential barrier at  $S(t) = H^{-1}$  where  $S$  plays the role of the particle coordinate<sup>4</sup>. Since particles can tunnel through potential barriers quantum mechanically, then the

creation of the universe can be visualized as a quantum tunneling effect where it emerges having a finite size ( $S(0) = H^{-1}$ ) and zero velocity. Its subsequent evolution is described by equation 3 with time  $t > 0$ .

A semiclassical<sup>1</sup> description of quantum tunneling can be given by the solution of equation 2 with  $t$  replaced by  $it$ , where  $it$  is the complex imaginary time. If the potential energy ( $V$ ) is greater than the kinetic energy ( $E$ ) of the particle ie

$$V > E \quad (4)$$

Then, naturally, the process is classically ( $\hbar = 0$ ) forbidden, but the actual tunneling amplitude is

$$\exp\left\{-\hbar^{-1} \int_a^b 2m\sqrt{V-E} dx\right\} = \exp(-\hbar^{-1} A_E) \quad (5)$$

where  $A_E$  is defined by the integral in the bracket and  $a$  and  $b$  are the classical turning points. In the case where

$$E > V \quad (6)$$

the transition is classically allowed. In this case the wave function oscillates and the number of oscillations is given by

$$\hbar^{-1} \int_a^b p dx = \hbar^{-1} \int_a^b [2m\sqrt{E-V} dx] \quad (7)$$

It is a well known fact that

$$\int_a^b p dx = \int_a^b p \dot{x} dt = \int_a^b (H+L) dt = \int_a^b (E+L) dt \quad (8)$$

If the total energy is normalized to zero, then

$$\int_a^b p dx = \int_a^b L dt = A \quad (9)$$

which is the total action for the motion from one quantum state to another quantum state. The only difference between equation 4 and 6 is that the sign of  $E - V$  is reversed. However the sign of  $V$  in the classical equation of motion of a particle given below:

$$m \ddot{x} = -\frac{\partial V}{\partial x} \quad (10)$$

is reversed  $\left(m \ddot{x} = \frac{\partial V}{\partial x}\right)$  if we replace  $t$  by  $it$ ,

where  $it$  is complex imaginary time,  $m$  is the mass of the particle,  $\ddot{x}$  is the acceleration of the particle and  $\frac{\partial V}{\partial x}$  is the potential gradient. Hence  $A_E$  is the action for imaginary times so that the Euclidean version of equation 2 is

$$\frac{k - \dot{S}^2}{S^2} = \frac{8\pi G}{3} \rho_o \quad (11)$$

whose solution is:

$$S(t) = H^{-1} \cos(Ht) \quad (12)$$

The equations 3 and 12 describe a four-sphere  $R^4$  which is the deSitter instanton. Solution 12 is seen to bounce at the classical turning point  $S = H^{-1}$  but it does not approach any initial state at  $t \rightarrow \pm\infty$ .  $R^4$  is a compact space and the solution 12 is defined only for  $t$  taking values less than  $\frac{2\pi}{H}$  in magnitude.

We interpret the solution 12 as describing the tunneling to the de Sitter space 3 from a non classical space-time state<sup>4</sup>. To make the concept of the universe being created from a non classical space-time state more familiar, we consider the pair creation of an electron-positron in a constant field say the electric field  $\vec{E}$ . The electrons that are emitted from the emitter surface do not all of them have the same energy. They are emitted from varying depths of the emitter-bulk hence lose different amounts of energy before emanating from the emitter surface<sup>15</sup>. When the potential between the emitter and the collector is equal to the stopping potential, then even the most energetic electron would just fail to reach the collector. If  $v_{\max}$  is the maximum velocity of the emitted electrons at the emitter, then their kinetic energy at the emitter is  $\frac{1}{2}m_e v_{\max}^2$  where  $m_e$  is the mass of the electron. As the electron travels from the emitter to the collector, its kinetic energy decreases and its potential energy increases such that its total energy is conserved. For those electrons that just manage to reach the collector, the velocity, and hence the kinetic energy becomes zero. The energy conservation law then implies that:

$$\frac{m_o}{\sqrt{1-v^2}} = q\vec{E}\Delta\vec{x} \quad (13)$$

where  $c^2 = 1$  and  $m_o$ ,  $v$  and  $q$  are the rest mass, velocity and the charge of the electron respectively. Equation (13) can be solved as follows. First we let

$$v = \frac{\Delta x}{\Delta t}, \quad \Delta x = x - x_o \quad \text{and} \quad \Delta t = t - t_o \quad \text{so that}$$

$$m_o^2 \Delta t^2 - (qE\Delta x\Delta t)^2 + (qE\Delta x^2)^2 = 0 \quad (14a)$$

We then let  $\Delta x^2 = x$  from which we have

$$q^2 E^2 x^2 - q^2 E^2 \Delta t^2 x + m_o^2 \Delta t^2 = 0 \quad (14b)$$

To first order, equation (14b) gives

$$(x - x_o)^2 + (t - t_o)^2 = R^2 \quad (14c)$$

$$\text{where } R^2 = -\frac{m_o^2}{q^2 E^2}.$$

The equation (14c) describes a circular trajectory which we consider as a compact instanton. This can schematically be represented as in figure 1 below

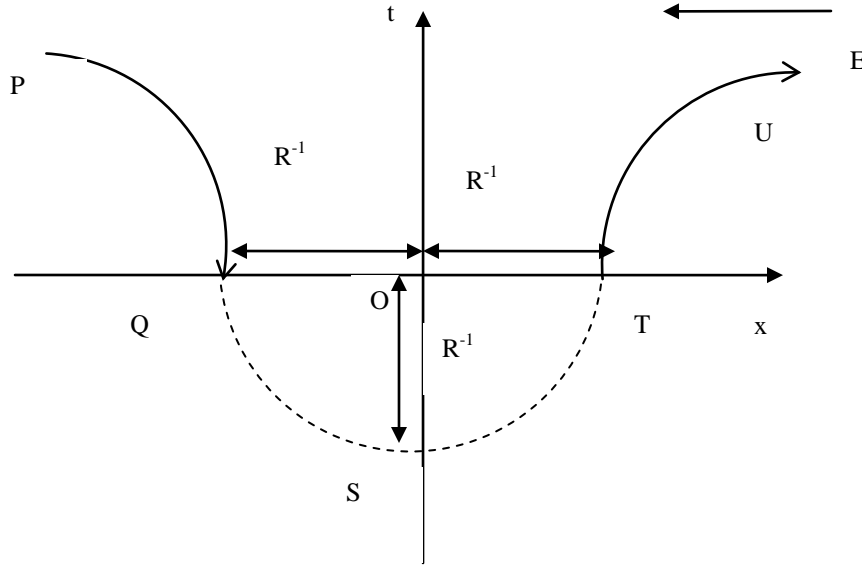


**Figure 1:** particle-antiparticle pair creation in a constant electric field  $\vec{E}$ .

PQ and TU are the classically allowed trajectories: PQ describes a particle moving backwards in time (positron), the semicircle QST represents the instanton and TU describes a particle moving forwards in time (electron).

### III. Decay rate of the false vacuum

Since the vacuum is an infinitely degenerate state consisting of an infinite number of homotopically non-equivalent vacua<sup>1</sup>, the instanton will represent a transition from one vacuum class to another ie the probability amplitude for the transition. Classically it is zero since the particle cannot penetrate the energy barrier. But quantum mechanically, there is a barrier penetration factor. The instanton solution can then be Equation 16 is solved in polar coordinates to obtain:

$$A_E = \frac{\pi m_o^2}{|q\vec{E}|} \quad (17)$$

$$\text{so that } P_b \propto \exp\left(-\frac{\pi m_o^2}{|q\vec{E}|}\right) \quad (18)$$

used to estimate the barrier penetration amplitude since

$$P_b \propto e^{-A_E} \quad (15)$$

where  $P_b$  is the probability of barrier penetration and  $A_E$  is the Euclidean action for imaginary time given as

$$A_E = \int \left[ \frac{m_o}{\sqrt{1 + (\Delta \dot{x})^2}} - q\vec{E}\Delta x \right] dt \quad (16)$$

which is a familiar result from the theory of neutrino oscillations propagating in matter of varying density

Big bang scenarios predict that at very early <sup>16</sup> times the universe was extremely hot and has since then cooled down to the presently observed temperature of 2.726K. The analysis of the finite effective potential shows that initially, the expectation value of the scalar field  $\bar{\phi} = 0$  is the only ground state of the theory. As time increases, the temperature of the universe will decrease and at some critical temperature  $T = T_c$  the symmetric vacuum will cease to be stable and a new energetically favored ground state will appear. Thermal, gravitationally induced or quantum fluctuations will tend to force the theory into the new asymmetric ground state, the true vacuum. The relevant quantity that must be computed is the decay rate per unit volume of the false vacuum.

with the adiabaticity parameter  $\gamma_r = \frac{2m_0^2}{qE}$ .

To study temperature effects <sup>17</sup>, we consider a real scalar field  $\phi$  described by the Lagrangian

$$L = \frac{1}{2}(\partial_\mu\phi)(\partial^\mu\phi) - V(\phi) \quad (19)$$

where the first term is the kinetic energy part and the second is the potential energy part given by

$$V(\phi) = -\frac{1}{2}M^2\phi^2 + \frac{1}{4}\lambda\phi^4 \quad (20)$$

If we assume that  $m = \lambda = 1$ , then the potential can be sketched as in figure 2 below.

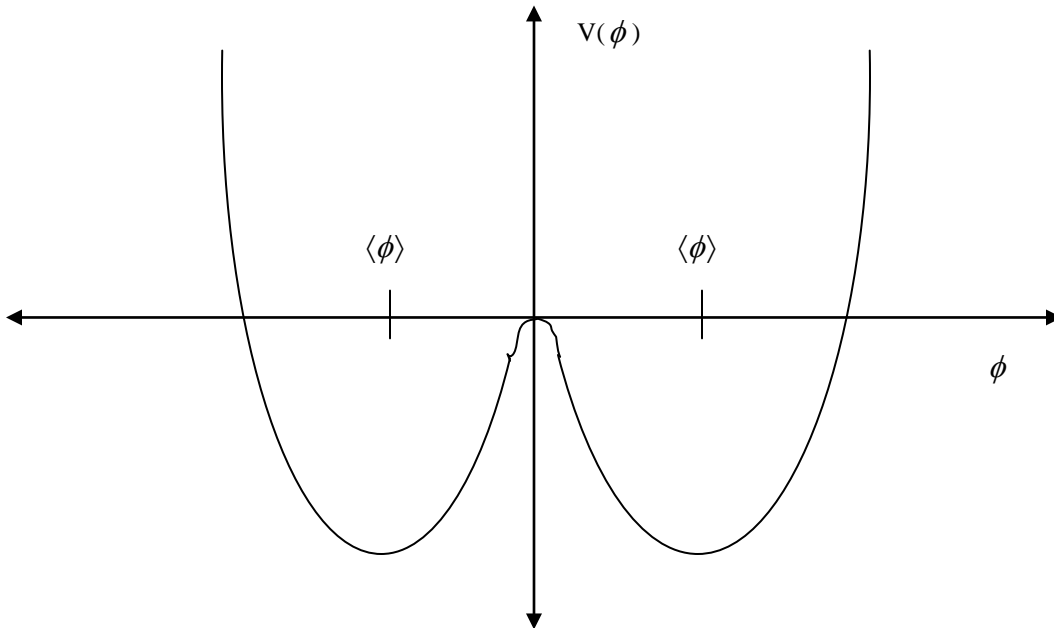


**Figure 2:** An example of the potential for a model with spontaneous symmetry breaking<sup>17</sup>.

By the condition  $\partial V/\partial\phi = 0$ , the minimum of the potential and the value of the potential at the minimum are given by

$$\langle\phi\rangle = \pm\sqrt{\frac{M^2}{\lambda}} \quad (21)$$

$$V(\langle\phi\rangle) = -\frac{M^2}{4\lambda}$$

The ground state of the system is either  $+\langle\phi\rangle$  or  $-\langle\phi\rangle$  and the reflection symmetry  $\phi \leftrightarrow -\phi$  present in the Lagrangian is not respected by the vacuum state and is called spontaneous symmetry breaking. From the definition of the stress-energy tensor in terms of the Lagrangian

$$T_{\mu\nu} = -\partial_\mu\phi\partial_\nu\phi - Lg_{\mu\nu} \quad (22)$$

the energy density of the vacuum is

$$\langle T_{00} \rangle = \rho_V = -L = V(\phi) = -\frac{M^4}{4\lambda} \quad (23)$$

The contribution of the vacuum energy to the total energy density today must be smaller than the critical density<sup>18,19</sup>  $\rho_c = 1.88 \times 10^{-29} h^2 gcm^{-3}$ . Since this number is quite small, it is appropriate to require that  $\rho_V = 0$ . This can be accomplished by adding to the

Lagrangian a constant factor of  $\frac{+M^4}{4\lambda}$ . The constant term will not affect the equations of motion but will only cancel the present vacuum energy density.

High-temperature symmetry restoration requires that we express the effective finite temperature mass  $M_T$  of  $\phi$  as the zero-temperature mass  $-M^2$  and a plasma mass,  $M_{plasma} \approx \alpha\lambda T^2$ , where  $\alpha$  is a constant of order unity. If  $M_T^2 = -M^2 + M_{plasma}^2 < 0$ , the minimum of the potential will be at  $\phi \neq 0$  (SSB), while if

$M_T^2 = -M^2 + M_{plasma}^2 > 0$  the effective mass term will be positive and the minimum of the potential will be at  $\phi = 0$  (symmetry restored). There

is a critical temperature  $T_c = \frac{M}{\sqrt{\alpha\lambda}}$  above which  $\langle\phi\rangle = 0$ .

A detailed approach to symmetry restoration is to account for the effect of the ambient background gas in the calculation of the higher-order quantum corrections to the classical potential. The finite temperature potential  $V_T(\phi)$  will include a temperature-dependent term that represents the free energy of  $\phi$  particles at temperature T. To one loop, the full potential is

$$V_T(\phi) = V(\phi) + \frac{T^4}{2\pi^2} \int_0^\infty dx x^2 \ln \left[ 1 - \exp \left\{ - (T^{-2}(x^2 + \mu^2))^{\frac{1}{2}} \right\} \right] \quad (24)$$

where  $V(\phi)$  is the zero-temperature one-loop potential and  $\mu^2 = -M^2 + 3\lambda\phi^2$  is the effective finite temperature mass. At high temperature, equation 24 has the expansion

$$V_T(\phi) = V(\phi) + \frac{\pi^2}{90} T^4 + \frac{\lambda}{8} T^2 \phi^2 + \dots \quad (25)$$

The term proportional to  $T^4$  is minus the pressure of a spinless boson which should be the leading contribution to the free energy and the second term is the plasma mass term for  $\phi$ . The phase transition from the symmetric to the broken phase can either be first order or higher order. If, at the critical temperature  $T_c$  there is a barrier between  $\phi = 0$  and the spontaneous symmetry breaking minimum  $\phi = \sigma$ , the change in  $\phi$  will be discontinuous signaling a first order transition. If no barrier is present at  $T_c$ , the change in  $\phi$  will be continuous signaling a higher order transition. The particular order of the phase transition will be studied in greater details and the findings shall be reported elsewhere.



At some temperature  $T \leq T_c$ , the  $\phi = 0$  phase is a metastable phase and this phase will be terminated by the decay of the false vacuum by quantum or thermal tunneling.

The tunneling occurs by the nucleation of bubbles of the new phase and the probability for bubble nucleation is calculated by solving the Euclidean equation of motion

$$\Delta_E \phi - V'(\phi) = \frac{d^2 \phi}{dt^2} + \nabla^2 \phi - V'(\phi) = 0 \quad (26)$$

with boundary conditions  $\phi = 0$  at

$$r^2 = x^2 + t^2 = \infty \text{ and } \frac{d\phi}{dr} = 0 \text{ at } r = 0. \text{ The}$$

probability of bubble nucleation per unit volume per unit time is

$$\Gamma = C \exp(-A_E) \quad (27)$$

where  $A_E$  is the Euclidean action for the solution of equation 26

$$A_E(\phi) = \int d^4 x \left[ \frac{1}{2} \left( \frac{d\phi}{dt} \right)^2 + \frac{1}{2} (\nabla \phi)^2 + V(\phi) \right] \quad (28)$$

and C is a constant. Of the many possible solutions to equation 26, the one with least action is the most important. The least action solution has O(4) symmetry and the Euclidean equation of motion becomes:

$$\frac{d^2 \phi}{dr^2} + 3r^{-1} \frac{d\phi}{dr} - V'(\phi) = 0 \quad (29)$$

There are no general solutions to equation (29). In the approximation where the difference in energy between the metastable and true vacua are small compared to the height of the barrier the damping term can be neglected. Then the solution for the action  $A_E$  is found as follows. For  $\frac{d\phi}{dr} = 0$ , we have

$$\frac{d^2 \phi}{dr^2} = \frac{dV(\phi)}{d\phi} \quad (30a)$$

We then rewrite equation (30a) as

$$\frac{d}{dr} \left( \frac{d\phi}{dr} \right) = \frac{dV}{dr} \frac{dr}{d\phi} \quad (30b)$$

so that

$$\frac{d\phi}{dr} d \left( \frac{d\phi}{dr} \right) = dV \quad (30c)$$

We then let  $\frac{d\phi}{dr} = x$  from which

$$x dx = dV \quad (30d)$$

With the integration constant being equal to zero, we obtain

$$\left( \frac{d\phi}{dr} \right)^2 = 2V(\phi) \quad (30e)$$

after substituting for  $x$ . In the static case, equation (28) gives

$$\begin{aligned} A_E(\phi) &= \int dr \left\{ \frac{1}{2} \left( \frac{d\phi}{dr} \right)^2 + V(\phi) \right\} \\ &= \int dr \left\{ \left( \frac{d\phi}{dr} \right)^2 \right\} \end{aligned} \quad (30f)$$

In terms of  $V$ , we then have

$$A_E(\phi) = \int_0^\sigma d\phi \sqrt{2V(\phi)} \quad (30g)$$

which is an instanton-like solution to the classical

$$\text{equation of motion } m \ddot{x} = -\frac{\partial V}{\partial x}.$$

## IV. Conclusion

By using simple topological methods, the universe is seen to emerge with a finite size  $2R$  at  $t = 0$  and later expands exponentially to its presently observed size. At very high temperatures, where the particle masses vanish, the tunneling probability rapidly approaches unity. The instanton with the smallest value of Euclidean action is seen to correspond to the most probable universe so that our universe is one of the rare universes that tunneled to the symmetric vacuum state. The tunneling probability is similar to the probability of neutrino oscillations that occur in matter of varying density. Also bubble nucleation rate is proportional to probability of barrier penetration in the decay rates of a false vacuum. After the tunneling, the structure and evolution of such a configuration is totally determined by the laws of physics. The creation of the universe is a spontaneous event associated with a phase transition from a non-classical configuration through a quantum fluctuation to formation of masses. The foreseeable difficulty is to account for the origin of the initial hot state. This issue and the second part of the question that we posed earlier will be the subject of our next communication.

## Acknowledgements

The authors are extremely grateful to the Higher Education Loans Board (Kenya) for the Research Grant Number HELB/LD/PSA/VOLUME 1/15 2006/07 S/NO.731 and the University of Nairobi, where the research works was carried out.

## References

1. Lewis H Ryder, *Quantum Field Theory*, Cambridge University Press 2001 page 423.
2. Utpal Sarkar, *Particle and Astroparticle Physics-series in High Energy Physics, Cosmology and Gravitation*, CRC Press Taylor & Francis Group 2008 page 389
3. Narlikar J V, *Introduction to Cosmology*, 2<sup>nd</sup> Edition Cambridge University Press, 1993 page 135.
4. Alexander Vilenkin, *Creation of the Universe from Nothing*, Phys Lett 117B, 25-28 (1982).
5. Edward P Tryon, *Is the Universe a Vacuum Fluctuation?* Nature Volume 246, 396-400 (1973).
6. Brout R, et al, *The creation of the universe as a quantum phenomenon*, Annals of Physics 115, 78-106 (1978).
7. Burcham W E and Jobes M, *Nuclear and Particle Physics*, LongmanGroup Ltd 1995 page
8. Hughes I S, *Elementary Particles*, 3<sup>rd</sup> Edition Cambridge University Press 1991 page 336.
9. Mohapatra R N and C H Lai, *Selected papers on Gauge Theories of Fundamental Interactions*, World Scientific Singapore 1981 page 36.
10. Michael S Turner, *Towards the Inflationary paradigm*, Summary of Lectures given at Gauge Theories and the Early Universe-Erice May 1986.
11. Padmanabhan T, *Structure Formation in the Universe*, Cambridge University Press, 1998 page 51
12. Ruth M Williams, *Curved Space-times*, CERN preprint 91-06 Geneva 1991 page 35.
13. Keith Olive, *Cosmology and GUTS*, Fermilab Conf-84/59-A 1984 page5.
14. Peccei R D, *The Physics of Neutrinos*, Fed Rep Germany UCLA/89/TEP 12 page 58.
15. Hawking S W and Moss I G, *Supercooled Phase Transitions in the Very Early Universe*, Physics Letters 110B 1982 page 35.
16. Maumba G O, Monyonko N M and Malo J O, *The Flatness Problem as a Natural Cosmological Phenomenon*, accepted for publication in the International Journal of Pure and Applied Physics (IJPAP) 2008.
17. Mani H S and Mehta G K, *Modern Physics*, Affiliated East-West Press private Limited 1988 New Delhi page 7.
18. Robert H Brandenberger, *Quantum Field Theory Methods in Cosmology*, HUTMP 82/8122 page 34.

19. Edward W Kolb, *Particle Physics and Cosmology*, FermiLab-Conf-86/146-A 1986 page 40
20. Wick C Haxton and Barry R Holstein, *Neutrino Physics*, Am J Phys 68 (1) 2000 page 15.

21. Coughlan G D, *The Ideas of Particle Physics*, CambridgeUniversity Press 1991 page 194.

# ELECTRON TRANSFER PROPERTIES OF 2-ACETYLFERROCENYL-2-THIOPHENECARBOXYLSEMICARBAZONE AND ITS COPPER (II) COMPLEX

P. M. Guto<sup>1</sup>, J. M. Kiratu<sup>1</sup>, L. S. Daniel<sup>2</sup>, E. M. R. Kiremire<sup>2</sup>, G. N. Kamau<sup>1</sup>

<sup>1</sup>Department of Chemistry, University of Nairobi, P. O. Box 30197-00100, Nairobi, Kenya

<sup>2</sup>Department of Chemistry and Biochemistry, University of Namibia, Private Bag 13301, Windhoek, Namibia

## Abstract

This work is aimed at obtaining the electrochemical properties of 2-acetylferrocenyl-2-thiophenecarboxylsemicarbazone (LH) and Copper (II) complex of 2-acetylferrocenyl-2-thiophenecarboxylsemicarbazone (CuL<sub>2</sub>), which were there earlier found to have different biological activities against malaria parasites. Cyclic voltammetric studies on these compounds (LH and CuL<sub>2</sub>) mainly gave one peak for each of the cathodic and anodic scans. These reduction/oxidation responses were attributed to Fe<sup>III</sup>/Fe<sup>II</sup> for LH and Cu<sup>II</sup>/Cu<sup>I</sup> for CuL<sub>2</sub> redox couples. The mid-point potentials were found to be +0.536 V for LH and -0.350 V for CuL<sub>2</sub> versus Ag/AgCl. Literature shows that more positive redox potentials than negative potentials are associated with higher biological activities. The average peak separations for LH and CuL<sub>2</sub> were found to be ~48 mV and ~363 mV between the scan rates of 0.01 V/s and 0.1 V/s while their diffusion coefficients were 5.21 x 10<sup>-7</sup> cm<sup>2</sup>/s and 2.67 x 10<sup>-7</sup> cm<sup>2</sup>/s, respectively. This difference in diffusion coefficients was attributed partially to the differences in their molecular weights and the overall geometry, whereby CuL<sub>2</sub> was almost double that of LH. The rates of electron transfer constants were also found to be 12.3 cm/s for LH and 1.0 cm/s for CuL<sub>2</sub>.

## Introduction

Thiosemicarbazones and semicarbazones and their metal complexes are a class of compounds which have drawn attention to researchers due to their notable biological activities. In particular, they have been reported to have a wide range of biological properties including antitumor, antiviral and antimalarial [1, 2]. Their biological activities are mediated through binding to a metal in cells leading to blocking of DNA synthesis through inhibition of ribonucleoside diphosphate reductase enzyme. Studies have shown that the metal complexes especially those containing Copper II and Iron II are more bioactive than uncoordinated thiosemicarbazone and semicarbazone molecules. Redox potentials of these metal complexes have been correlated with their biological properties [1]. The more positive the redox potential the higher the biological activity. This means that the ability to control their redox potentials can in turn be used to control their biological activities. Hence the interests in the current research work.

Recently, we reported the synthesis, the Fourier Transform Infrared (FT-IR) spectroscopic and malarial biological studies of complexes derived from the reactions of 2-acetylferrocenyl-4-

phenylthiosemicarbazone, 2-acetylferrocenyl-4-methylthiosemicarbazone, 2-acetylpyridine-2-thiophenecarboxylsemicarbazone and 2-acetylferrocenyl-2-thiophenecarboxylsemicarbazone with copper (II) chloride [3]. We found that the biological activities of these compounds against malaria parasites were more enhanced for the copper (II) complexes than their respective ligands. We associated the enhanced biological activities of the copper (II) complexes with the increase in their lipophilic nature which favored their penetration through the membrane walls of the malarial parasites. But the opposite trend was observed with the 2-acetylferrocenyl-2-thiophenecarboxylsemicarbazone and its copper(II) complex where the ligand was found to be more biologically active towards falcipain-2 (FP-2) than its copper(II) complex. The present research work employs electrochemistry, aimed at understanding the electron transfer behavior of 2-acetylferrocenyl-2-thiophenecarboxylsemicarbazone (LH), shown in figure 1.1, and Copper (II) complex of 2-acetylferrocenyl-2-thiophenecarboxylsemicarbazone (CuL<sub>2</sub>), shown in figure 1.2. The electrochemical results obtained may explain the observed biological activities of

these compounds against malarial parasites. The electrochemical technique used in the current work was cyclic voltammetry (CV), which is one of the

most frequently used electrochemical methods because of its relative simplicity and its high performance content [4, 5].

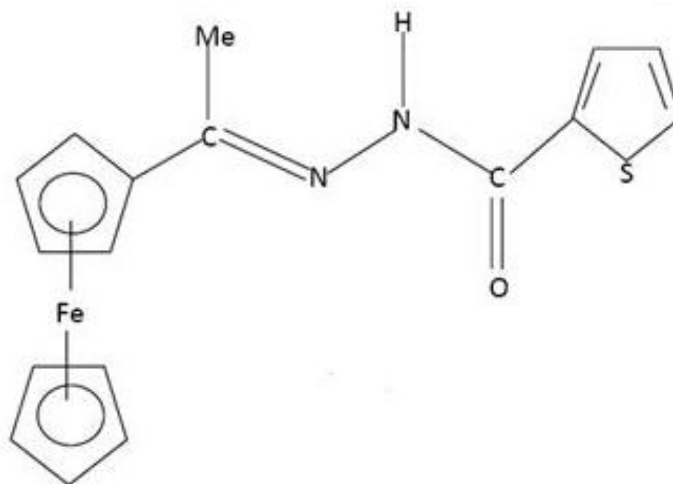


**Figure 1.1:** 2-acetylferrocenyl-2-thiophenecarboxylsemicarbazone (LH).

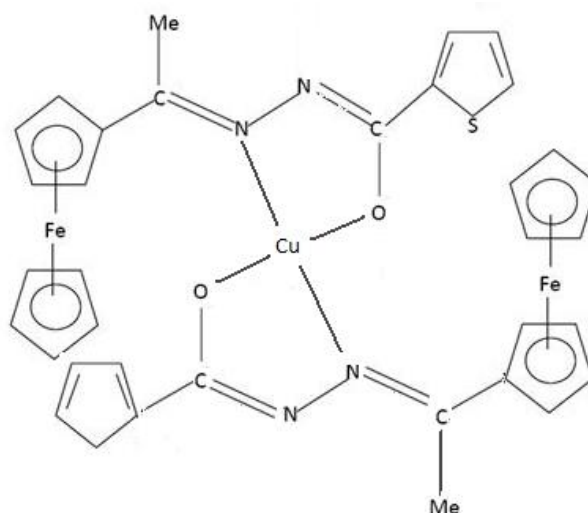


**Figure 1.2:** Copper (II) complex of 2-acetylferrocenyl-2-thiophenecarboxylsemicarbazone ( $\text{CuL}_2$ ).

## Experimental

**Chemicals and Solutions:** Tetraethylammoniumbromide (98%), sodium dodecylsulfate (SDS), ferrocene (98%) and potassium chloride were from Aldrich and acetonitrile was obtained from Kobian. The samples 2-acetylferrocenyl-2-thiophenecarboxylsemicarbazone abbreviated as LH and Copper (II) complex of 2-acetylferrocenyl-2-thiophenecarboxylsemicarbazone abbreviated as  $\text{CuL}_2$  of molecular weights 351.85g and 765.55g, respectively, were synthesized in the Department of Chemistry, University of Namibia. The synthetic methods of the complexes are given below [6, 7, 8, 9, 10, 11, 12, 13, 14, 15, 16, 17, 18]. For voltammetry, the electrolyte was a mixture of water and acetonitrile in the ratio of 1:1 containing 0.1M tetraethylammoniumbromide (TEAB) and 3.5mM sodium dodecylsulfate (SDS). Water was purified and de-ionized by Elga water purification apparatus. All other chemicals were reagent grade and were used as received.

### *The synthesis of acetylferrocene-2-thiophenecarboxyl-semicarbazone (HL) ligand.*

The acetylferrocene-2-thiophenecarboxyl-semicarbazone ligand, HL was prepared by using equimolar quantities of  $7.0 \times 10^{-3}$  mole of 2-thiophenecarboxylic acid hydrazide (1.00 g, 99%) and acetylferrocene (1.60 g) in 100 mL ethanol. The reaction mixture was then refluxed for 3 hours. At the beginning of refluxing, 3 mL of acetic acid were added drop-wise. After refluxing, the mixture was transferred into a refrigerator at temperature of 5°C for 24 hours. The dark brown crystals of product were filtered off, washed with 10 mL of acetone, then again with 10 mL of ether and dried on a vacuum pump for 40 minutes. Percentage yield of unrecrystallized ligand was 53%. The complex was recrystallized from dimethylsulphoxide (DMSO) [6, 7, 8].

*The synthesis of the semicarbazone copper(II) complex,  $\text{CuL}_2$ .* The copper (II) complexes of HL was prepared according to the following procedure.

A solution of the copper(II) chloride hexahydrate (3.15 g, 0.01 mol) in water (100 mL) was added dropwise while stirring to a solution of the ligand HL (2.87 g, 0.001 mol) in DMSO (50 mL). The precipitation was separated by vacuum filtration, washed several times with ethanol, 20 mL of diethyl ether and dried on a vacuum pump. The copper complex was also recrystallized from DMSO. The complexes were characterized by elemental analysis, FT-IR,  $^1\text{H}$ NMR,  $^{13}\text{C}$ NMR and mass spectroscopy [9, 10, 11, 12, 13, 14, 15, 16, 17, 18].

**Voltammetry:** All experiments were done at room temperature. Ordinary basal plane pyrolytic carbon (PG) disk electrodes were polished on alumina slurry before every use, as reported previous [19]. Actual surface areas of these PG electrodes were determined by cyclic voltammetry using ferrocyanide oxidation and were found to be 0.16  $\text{cm}^2$ . This was confirmed by physical measurements. AUTOLAB PGSTAT 12 potentiostat was from Eco Chemie B. V. Silver-Silver Chloride electrode (Ag/AgCl) reference, a platinum (Pt) wire counter and the PG electrode as the working electrode were used. Pure nitrogen was purged into solutions for 20 min prior to voltammetric scans, then maintained over the solutions during the period the electrochemical measurements were undertaken. All the experiments were performed at ambient temperature of the room, which ranged from 20 to 24°C.

## Results and Discussions

The typical electrodes and relevant electrochemical cell used in the present research work were standardized using ferrocene which gave a well defined voltammogram (figure 2), and compares favorably with what was reported earlier by Kamau et. al [20, 21].

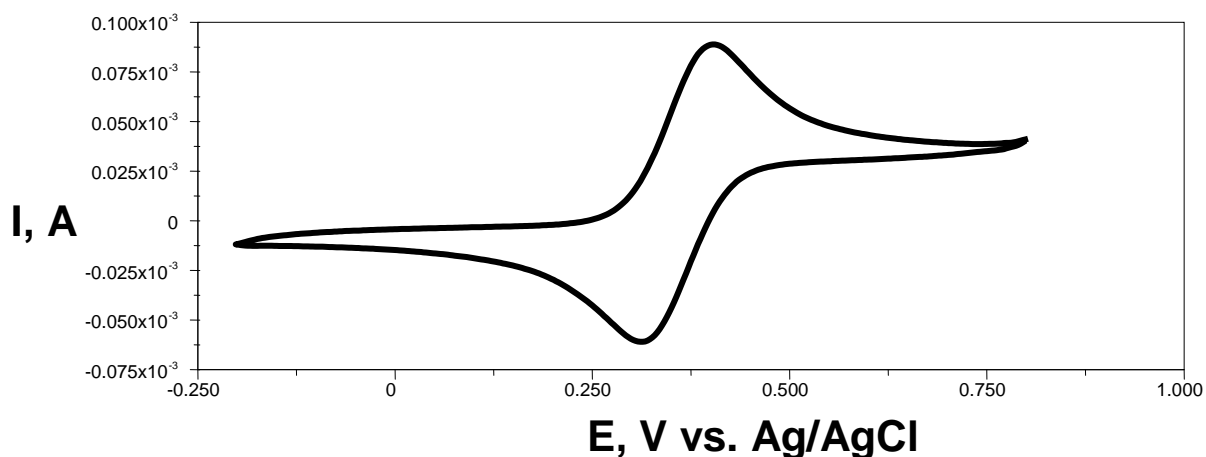


**Figure 2:** Cyclic voltammetry of 4mM ferrocene at scan rate of 0.03 V/s. The electrolyte was a mixture of water and acetonitrile (1:1) containing 0.1 M TEAB.

Cyclic voltammetry of 2-acetylferrocenyl-2-thiophenecarboxylsemicarbazone (LH) gave a one reduction peak centered around 0.511V and one oxidation peak around 0.561V versus Ag/AgCl (figure 3). On the other hand, CuL<sub>2</sub> gave a voltammogram with a reduction peak centered around -0.532V and an oxidation peak around -0.169V versus Ag/AgCl (figure 4). Both the reduction and oxidation peaks for the CuL<sub>2</sub> were well defined and larger than the LH peaks. Moreover, the reduction and oxidation peaks for

CuL<sub>2</sub> were far separated from one another by about 0.35V. But for LH the reduction and oxidation peaks had a separation of 0.050V. It is interesting to note that the reduction and oxidation potentials for the LH (0.511 V and 0.561 V) compares relatively with those of pure ferrocene. The slight difference, particularly with respect to the shape of the voltammogram, can be attributed to the additional hydrocarbons attached to the ferrocene moiety.



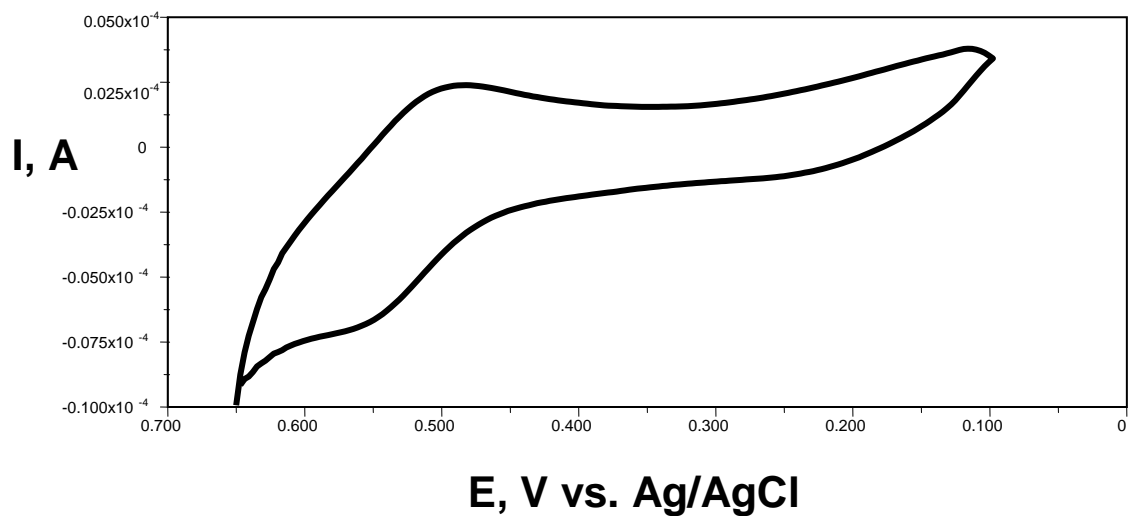


**Figure 3:** Cyclic voltammetry of 2-acetylferrocenyl-2-thiophenecarboxylsemicarbazone (LH) at scan rates of 0.01 V/s.

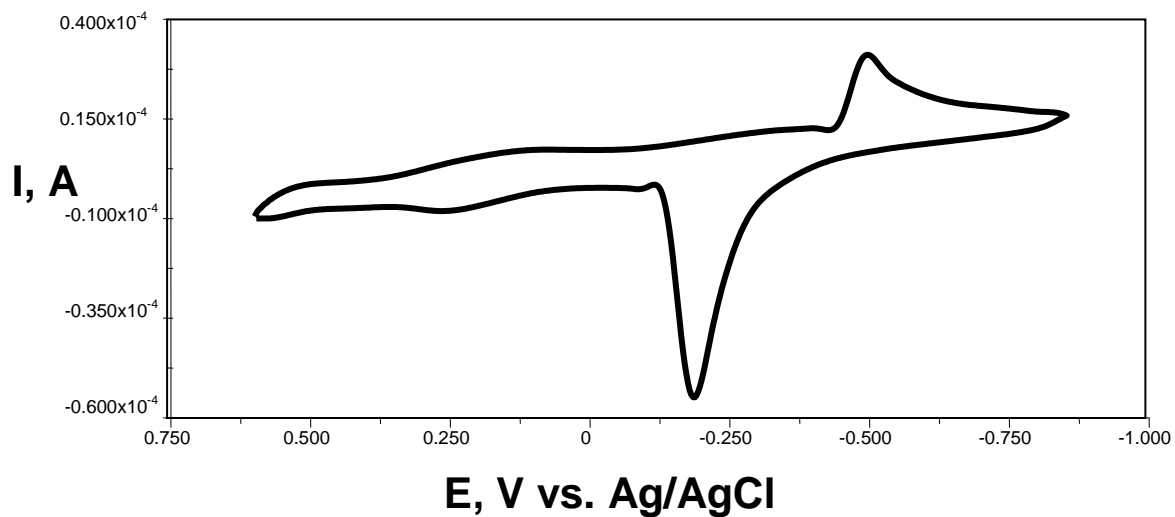


**Figure 4:** Cyclic voltammetry of Copper (II) complex of 2-acetylferrocenyl-2-thiophenecarboxylsemicarbazone ( $\text{CuL}_2$ ) at scan rates of 0.01 V/s.

The results for the reduction of CuL<sub>2</sub> compares favorably with the results of Libert [Error! Bookmark not defined.] and Pai [22], who found out that similarly related copper (II) complexes were reduced at potentials

ranging from -0.4 to -0.6 volts versus Ag/AgCl. These authors attributed the observed reduction/oxidation responses for the copper (II) complex to Cu<sup>II</sup>/Cu<sup>I</sup> redox couples.

**Table 1: Electrochemical properties of 2-acetylferrocenyl-2-thiophenecarboxylsemicarbazone (LH) and copper (II) complex of 2-acetylferrocenyl-2-thiophenecarboxylsemicarbazone (CuL<sub>2</sub>). The average ΔE and D were calculated from scan rates ranging between 0.01 and 0.1V/s.**

Sample	ΔE, <sup>a</sup> V	E <sup>o</sup> , <sup>b</sup> V vs. Ag/AgCl	D, <sup>c</sup> cm <sup>2</sup> s <sup>-1</sup>	κ, <sup>d</sup> cm s <sup>-1</sup>
LH	0.048 ± 0.05	+0.536 ± 0.09	5.21 x 10 <sup>-7</sup>	12.3 ± 0.4
CuL <sub>2</sub>	0.363 ± 0.04	-0.350 ± 0.06	2.67 x 10 <sup>-7</sup>	1.0 ± 0.02

<sup>a</sup>Peak separations; <sup>b</sup>Mid-point potentials; <sup>c</sup>Apparent values from the slopes of peak current vs. v<sup>1/2</sup> and the Randles-Sevcik equation; <sup>d</sup>Apparent standard electron transfer rate constant.

The reduction and oxidation voltammetric currents for both the ligand and its copper (II) complex increased with increase in scan rate. Considering the anodic to cathodic peak ratio (I<sub>a</sub>/I<sub>c</sub>), there was a tremendous difference between the ligand and its copper (II) complex. The I<sub>a</sub>/I<sub>c</sub> for the ligand is almost unity but the I<sub>a</sub>/I<sub>c</sub> for the copper (II) complex is in the range of 2 to 3. The significantly high ratio of oxidation to reduction currents of CuL<sub>2</sub> and the symmetry of the anodic peak, suggests that the reduced species is adsorbed on the electrode[4]. The number of electrons (n) involved in the redox responses for LH and CuL<sub>2</sub>

were obtained from the slope of the plots of potential, E, versus log[i/i<sub>d</sub>-i], equation 1.

$$E = E_{1/2} - \frac{0.0591}{n} \log\left(\frac{i}{i_d - i}\right) \dots \dots \dots (1)$$

Where E is the potential at any point on the wave, E<sub>1/2</sub> is the half-wave potential, i<sub>d</sub> is the peak current, i is the current at any point on the wave and n is the number of electrons exchanged in the redox process [4].

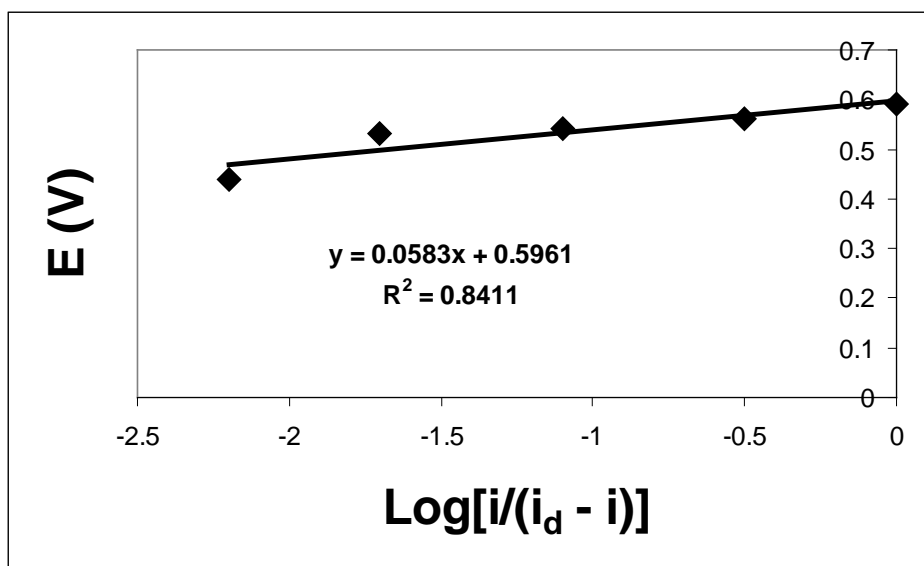


**Figure 5:** Plot of potential ( $E$ ) against  $\text{log } [i/i_d - i]$  for 2-acetylferrocenyl-2-thiophenecarboxylsemicarbazone (LH).

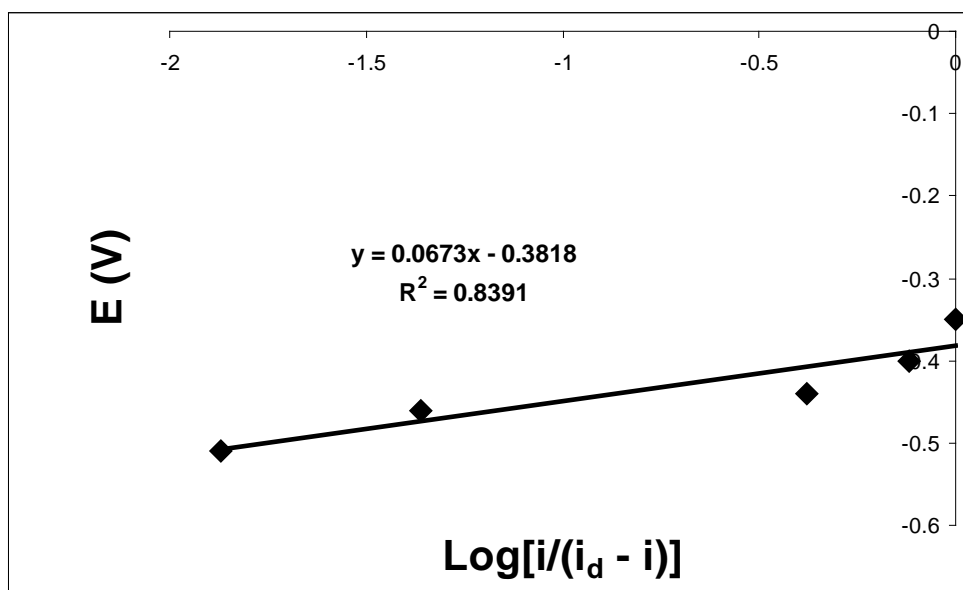


**Figure 6:** Plot of potential ( $E$ ) against  $\text{log } [i/i_d - i]$  for Copper (II) complex of 2-acetylferrocenyl-2-thiophenecarboxylsemicarbazone ( $\text{CuL}_2$ ).

According to figures 5 and 6, *n* was found to have a value of 1 for both the ligand (LH) and its copper (II) complex (CuL<sub>2</sub>). This in turn supports the single redox steps for LH (Fe<sup>III</sup>/Fe<sup>II</sup>) and CuL<sub>2</sub> (Cu<sup>II</sup>/Cu<sup>I</sup>) mentioned above.

The average peak separations between the cathodic and anodic potentials ( $\Delta E$ ) were found to be (0.048 ± 0.05) V for LH and (0.363 ± 0.04) V for CuL<sub>2</sub> between the scan rates of 0.01 V/s and 0.1 V/s (table 1). We applied methods developed by Laviron [23] and Hirst and Armstrong [24] to compute the rate of electron transfer between the electrode and the analyte. By compensating for the constant peak separations ( $\Delta E_p$ ) at low scan rates, we plotted the resulting data for the electron transfer between electrode and the diffusing analyte species. Assuming the electron transfer coefficient to be  $\alpha = 0.5$ , we estimated the apparent electrochemical electron transfer rate constants. The results obtained (table 1) show that the  $k_s$  value for the ligand is 12.3 cm/s and for the copper(II) complex is 1.0 cm/s. This indicates that the rate at which the electron is exchanged at the electrode surface is about 12 times faster for the ligand than for the copper(II) complex.

Following Randles-Sevcik equation 2 [4], plots of reduction currents ( $i_{pc}$ ) versus the square root of scan rates ( $v^{1/2}$ ) between 0.01 V/s and 0.1 V/s were made. Linear plots were obtained whose slopes were used to obtain the diffusion coefficients of LH and CuL<sub>2</sub>.

$$i_{pc} = (2.69 \times 10^5) n^{3/2} C^* A D^{1/2} v^{1/2} \dots\dots\dots(2)$$

Where  $i_{pc}$  is the diffusion peak current, *n* is the number of electrons exchanged in the redox process (obtained above),  $C^*$  is the concentration of LH and CuL<sub>2</sub>, *A* is the area of the electrode, *D* is the diffusion coefficient and *v* is the scan rate. The linear plots obtained indicate that the electrode processes for both LH and CuL<sub>2</sub> are diffusion controlled. From table 1, the *D* for LH and CuL<sub>2</sub> were found to be 5.21 x 10<sup>-7</sup> cm<sup>2</sup>/s and 2.67 x 10<sup>-7</sup> cm<sup>2</sup>/s, respectively. This difference can be ascribed to the differences in their molecular weights, where LH has a molecular weight of 351.85g and CuL<sub>2</sub> has a molecular weight of 765.55g.

Formal redox potential ( $E^0$ ) for a reversible system is taken to be the mid-point between the reduction ( $E_c$ ) and oxidation ( $E_a$ ) potentials. As shown from table 1, the  $E^0$  obtained were (+0.536 ± 0.09) and (-0.350 ± 0.06) V versus

Ag/AgCl for LH and CuL<sub>2</sub>, respectively. This data shows that the mid-point potential for the ligand is more positive while that of its copper (II) complex is more negative. Previous work done by West and co-workers [2] showed that the biological activities of copper (II) complex of 2-acetylpyridine-N<sup>4</sup>-dialkylthiosemicarbazones can be controlled through tuning their reduction potentials. In their work, complexes reduced at more positive potentials were found to be more biologically active than those reduced at more negative potentials. Compatible with their findings, one expect 2-acetylferrocenyl-2-thiophenecarboxylsemicarbazone (LH) to be more biologically active than its copper(II) complex (CuL<sub>2</sub>) based on their formal potentials. This is what we had observed in our previous work with no electrochemistry back up [3]. Hence electrochemical data can be used to correlate the bioactivity of LH and CuL<sub>2</sub> to their corresponding formal redox potentials.

### Conclusion

In summary, both 2-acetylferrocenyl-2-thiophenecarboxylsemicarbazone (LH) and copper(II) complex of 2-acetylferrocenyl-2-thiophenecarboxylsemicarbazone (CuL<sub>2</sub>) were found to be electrochemically active. The average diffusion coefficients for LH and CuL<sub>2</sub> were found to be 5.21 x 10<sup>-7</sup> cm<sup>2</sup>/s and 2.67 x 10<sup>-7</sup> cm<sup>2</sup>/s, while their estimated rates of electron transfer constants were 12.3 cm/s and 1.0 cm/s, respectively. Both LH and CuL<sub>2</sub> involves one electron transfer redox process. This work also indicates that CuL<sub>2</sub> involves adsorption for the reduced chemical species. Regardless of the exact mechanistic details of their biological activities, the more positive redox potentials associated with the ligand (LH) explains why it was previously found to be more biologically active against malaria parasites than its copper(II) complex (CuL<sub>2</sub>).

### Acknowledgments

The authors wish to extend their deep gratitude to the University of Namibia for providing the required funds for sample preparations. We also thank the department of Physics personnel, University of Nairobi, for availing the potentiostat.

## REFERENCES

1. A. S. Kumbhar; B. S. Padhye; X. D. West; E. A. Liberta. *Transition Met. Chem.*, 17, 247 (1992).
2. A. S. Kumbhar; B. S. Padhye; P. A. Saraf; B. H. Mahajan; A. B. Chopade; X. D. West. *Biol. Metals*, 4, 141 (1991).
3. L.S. Daniel; EMR. Kiremire; K. Kambafwile; K. Chibale; P.J. Rosenthal; T. M. Kiratu; P. M. Guto; G. N. Kamau; *International Journal of BioChemiPhysics*, 18(1), 8 (2010).
4. A. J. Bard; L. R. Faulkner; "Electrochemical Methods: Fundamentals and Applications", *John Wiley & Sons, New York*, 2nd Ed. (2004).
5. J. F. Rusling; S. L. Suib. *Adv. Mater.* 6(12), 922 (1994).
6. M. T. Cocco; C. Congiu; V. Onnis; M. L. Pellerano; A. De Logu. *Bioorganic and medicinal chemistry* 10, 501 (2002).
7. M. C. Cardia; M. Begala; A. Delogu; E. Maccioni; A. Plumitallo. *Farmaco*, 55, 93 (2000).
8. N. C. Kasuga; K. Sekino; C. Koumo; N. Shimada, N; M. Ishikawa; K. Nomiya, K. *Journal of inorganic and biochemistry*, 84, 55 (2001).
9. M. C. Rodriguez-Arguelles; E. C. Lopez-Silva; J. Sanmartin; P. Pelagitti; F. Zani. *Journal of inorganic and biochemistry*, 99, 2231 (2005).
10. O. E. Offiong; S. Martelli. *Farmaco*, 49, 513 (1994).
11. O. E. Offiong; S. Martelli. *Farmaco*, 48, 777 (1993).
12. O. E. Offiong; S. Martelli. *Farmaco*, 50(9), 625 (2006).
13. E. W. Ainscough; A. M. Brodie; W. A. Denny; G. J. Finlay; J. D. Ranford. *Journal of inorganic and biochemistry*, 70, 175 (1998).
14. M. Missbach; B. Jagher; I. Sigg; S. Nayeri; C. Carleberg; I. Wiesenberg. *Journal of biological chemistry*, 271, 13515 (1996).
15. R. R. Sharp. Paramagnetic NMR. *Royal society of chemistry*, 34, 553 (2005).
16. J. Shipman; S. H. Smith; J. C. Drach; D. L. Klayman. *Antiviral res.*, 6, 197 (2005).
17. T. Varadinova; D. Kovala-Demertzi; M. Rupelieva; M. Demertzis; P. Genova. *Acta Virology*, 45, 87 (2001).
18. A. Walcourt; M. Loyevsky; D. B. Lovejoy; V. R. Gordeuk; D. R. Richardson. *International Journal of biochemistry and cell biology*, 36, 401(2004).
19. P. M. Guto; J. F. Rusling. *Electrochem. Commun.*, 8, 455 (2006).
20. G. N. Kamau; T. M. Saccucci; G. Gounili; A. F. Nassar; J. F. Rusling. *Anal. Chem.*, 66, 994 (1994).
21. J. M. Kiratu. Electrochemical and Spectroscopic Characterization of Ferrocene- thiosemicarbazone Ligand and Copper Complexes. M.Sc thesis, University of Nairobi, (2009).
22. M. P. Sathisha; V. K. Revankar; K. S. R. Pai. *Metal-Based Drugs*, 2008, 1 (2007).
23. E. Laviron. *J. Electroanal. Chem.*, 101, 19 (1979).
24. J. Hirst; A. Armstrong. *Anal. Chem.*, 70, 5062 (1998).

## INFORMATION TO CONTRIBUTORS

### General:

International journal of BioChemPhysics is aimed at rapid processing and publication of papers dealing with Biological, medical, chemistry, physics, applied science and other related disciplines of science. The journal is charged with processing of original work in the specified fields. Papers submitted must be of sufficient competence in scientific work or active research and will be committed to three independence referees. Submitted papers must not have been published elsewhere and the authors must agree not to submit the same material for publication in a book or other journal unless authorized. Authors are encouraged to submit their papers to the appropriate regional editor, or in all other cases to the editor-in-chief.

### Manuscripts

Manuscripts should be clearly typed, double-spaced, and in continuous prose. The manuscript will include an abstract followed by an introduction, which contain objectives of the work and literature review of similar work. The introduction will then be followed by the following sections: experimental, results and discussion, conclusions and recommendations, where possible, legend to, tables, figure captions, figures and references and acknowledgement. The margins should be 2.5 cm top and sides and 1.5 cm bottom. A separate sheet of paper should be included indicating explicitly the name of the author(s), full address(es) and affiliations, telephone number, telex, fax and e-mail and where possible to whom correspondence should be made regarding corrections and proofs. All manuscripts should be submitted in quadruplicate (one should be original) and should include tables, figures and figure captions wherever possible. This will enable the papers to be sent to three referees simultaneously to assist in fast processing. All manuscripts should be typed in English on A4/21.5cm X 28cm paper.

### Abstract

Each paper submitted for publication must be preceded by an abstract (about 200 words), indicating clearly the essential findings of the work.

### Nomenclature

For usual terms and symbols, authors are advised to follow the report on Commission on Symbols, Terminology and units of the International Union of Pure and Applied Chemistry. The report is entitled "Manual of Symbols and Terminology for physiochemical Quantities and Units" and was published in Pure and Applied Chemistry 21, 3 (1970). Reprints are available from Butterworths of London.

### Tables

Tables should be kept to the minimum and not reproduced in both diagrammatic and tabular form. Tables should be have a brief title on top and numbered consecutively in Arabic numerals in the order of their citation in the text. The tables should not have vertical lines.

### Figures

Figures refer to graphs, maps, photographs and diagrams. They should be originals and supplied on A4/21.5cm X 28cm sized tracing paper, tracing cloth or photographic glossy paper in case

of photographs. Computer Scanned diagrams are highly recommended. Each figure should have a label pasted on its back bearing the name(s) of the author(s) and figure number. Legends to figures should be supplied separately from the text with Arabic numerals corresponding to the figure.

## Experimental

Identify the methods and the equipment used (Manufacturer's name in parenthesis) sufficiently so that other Researchers/Workers can reproduce the results.

## References

References should be numbered in the sequence in which they occur in the text, cited by numbers [with square brackets] and listed at the end of the paper. Attempts should be made to cite available published work. If unpublished or personal work must be mentioned, then these citations should be included in sequence with the normal literature references. If the material cited is not readily available, then one should also give, for example, the Chemical Abstract Reference. References should be listed as follows:

1. Z. G. Morang'a, G. N. Kamau, A. E. Nassar, J. Biochemphysics, 3, 41 (1994).
2. P. F. Russel, Man's Mastery of Malaria, Oxford University Press, London (1985).  
Journal titles must be abbreviated according to the system co-sponsored by the American Chemical Society and listed in the ACS style guide.

## Reprints

One reprint of each paper will be provided. Additional copies may be purchased on a reprint order form, which will accompany the proofs.

## Copyright

Upon acceptance of an article by the journal, the author(s) will be asked to transfer copyright of the article to the publisher. Copies of the publishing agreement are available in each issue of the journal, or from the editors and the publisher. A signed copy of this agreement should be submitted together with the revised manuscript.

## PUBLISHING AGREEMENT

---

Upon submission of the article, the authors will be requested to transfer the copyright of their article to the publisher. This should be confirmed by signing and returning the agreement below when submitting the paper. If the paper is rejected, this agreement is **null and void**. If you wish to publish any part of your article in connection with any other work by you, you can do so provided request is made prior to final write up and acknowledgements given regarding copyright notice and reference to the original publication.

If need arises, the author's employer may sign this agreement, and the employer/sponsor may reserve the right to use the article internally or for promotion purposes by indicating on this agreement.

By signing this agreement, the author so guarantees that the manuscript is the author's original work, and has not been published elsewhere. If section(s) from copyrighted works are included, the author should obtain a written permission from the copyright owners and show credit.

For the work prepared jointly, the author to whom page proofs should be dispatched agrees to inform the co-authors of the terms of the agreement prior to signing on their behalf.



I agree to abide with the above conditions and assign to the Publisher, the copyright of my article entitled:

---

---

---

for publication in the International Journal of BioChemiPhysics

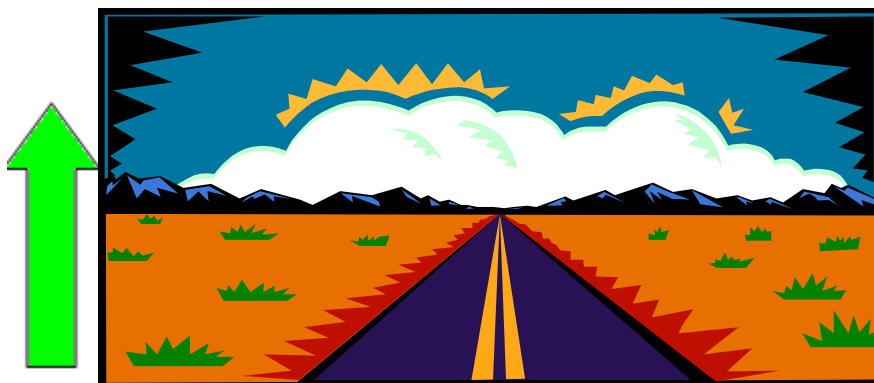
Signed: \_\_\_\_\_ Date: \_\_\_\_\_

## Energy mix for the Present World Order:

*The goal for any meaningful energy venture is to:*

- 1. Add value to human life,*
- 2. Alleviation of poverty,*
- 3. Environmentally hazard free,*
- 4. Affordable and environmentally friendly*

*Nuclear energy happens to have these Attributes. As Kenya plans to be industrialized by year 2030, nuclear electricity generation is one of the considerations earmarked to increase the national electricity output.*



**Highway to improved energy production**

## EXPRESS COLOURS



### **EXPRESS COLOUR & SCREEN LTD.**

SPECIALIST IN SCREEN ON T-SHIRTS, SCARFS, CAPS, METAL, WOOD, GLASS & PVC STICKERS  
P.O. BOX 31920 - 00600 NAIROBI, KENYA  
TEL: 6765345 FAX: 6761585

## RAS PAINTING & *RELIABLE ART SERVICES*



PRINTING ON: CANVAS, GLASS, CERAMICS, TEXTILE, WOOD  
& SCREEN PRINTING.

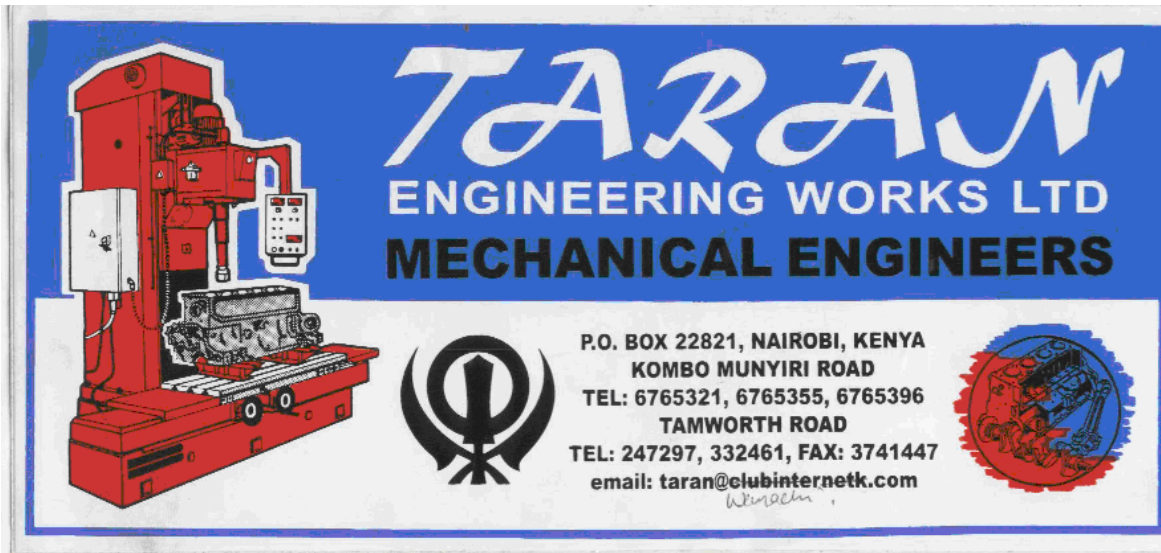
P.O. BOX 31095 - 00600  
TEL: 6763707

NAIROBI, KENYA  
FAX: 6761585

V.A.T Reg. No. 0510977Z

P.I.N. A001992144W

---



**TARA**  
ENGINEERING WORKS LTD  
MECHANICAL ENGINEERS

P.O. BOX 22821, NAIROBI, KENYA  
KOMBO MUNYIRI ROAD  
TEL: 6765321, 6765355, 6765396  
TAMWORTH ROAD  
TEL: 247297, 332461, FAX: 3741447  
email: taran@clubinternetk.com

# CRESTO WEARS

P.O. Box 32918 •  
Kombo Munyiri Road • Nairobi Kenya  
Tel: 760174 • Fax: 760174

Manufacturers of: Casual Wears & Industrial Clothings

*are proud to be associated with the*

**KENYA AIRFREIGHT HANDLING LTD.**



## **NELCO ENTERPRISES** **(GARMENT MANUFACTURES)**

Suppliers of: Mosquito Net, Express Larger Treated All Size and  
Diamoria Ne Round and Rectangle all Size, Nappy  
Liners, Baby West,  
Man's Boxer Shorts, Man's Briefs, All Children's  
Wear and Baby Nappies All Sizes

P.O. Box 32611 Nbi  
Popo Road, Gikomba

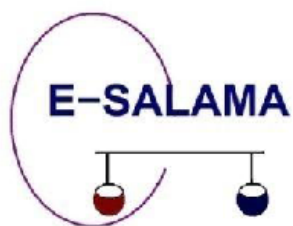
Tel.: 6767996  
Fax: 6764709 Nairobi-Kenya

**10<sup>TH</sup> AFRICALMA/EAST AND SOUTHERN AFRICA  
LABORATORY MANAGERS  
ASSOCIATION (E-SALAMA) WORKSHOP**  
To be hosted by the University of Zimbabwe  
Celebrating the International Year of Chemistry



**VENUE:** Elephant Hills Resort Hotel, Victoria Falls, Zimbabwe

5-9 December 2011



**THEME**

## ACCREDITATION FOR SUSTAINABLE INTERNATIONAL TRADE

### 1. Background

The East and southern Africa laboratory Managers Association (E-SALAMA) was established in 2002 with members from Kenya, Tanzania and Uganda. Since then others countries have joined and these include Zimbabwe, Botswana, Lesotho, Ethiopia and Sudan.

E-SALAMA was established with the aim of training laboratory managers in member countries towards achieving accreditation for their laboratories. To this end, the workshop is held annually and rotates from one member country to another. Prior to 2007, the workshop was held in Kenya, Tanzania and Uganda. In 2007 Zimbabwe hosted the workshop that was held 8 – 11 December 2007 at Victoria Falls. Subsequently the workshop was held in Kenya (2008), Ethiopia(2009) and Sudan (2010), while this year's workshop will be held in Zimbabwe.

### 2. Objectives

- To bring together African scientists for exchange of ideas in the areas of laboratory accreditation, proficiency testing, validation of laboratory measurements, and related fields.
- To foster Good Laboratory Practices (GLP) and Good Laboratory Management (GLM).
- To discuss problems facing laboratories in Africa.
- To foster collaboration among laboratories in Africa, e.g., in proficiency testing schemes.
- To foster collaboration between laboratories in academic institutions with those in industry and the public sector.

#### 4. Workshop Programme

The workshop programme will consist of 18 plenary lectures, and 3 panel discussions. The workshop programme is as follows:

Day	Time	Topic	Presenter(s)
Day 1	0800-0900	1. Registration	
	0900-1000	2. Opening Ceremony	
	1000-1030	3. Health Break	
	1030-1130	5. Plenary lecture 1: E-SALAMA: Historical, Aims and Vision	Prof. Geoffrey Kamau University of Nairobi, Kenya.
	11.30-12.30	1. Plenary Lecture 2: Accreditation	Dr. Wayne, USA.
	1230-1400	Lunch Break	
	1400-1530	6.E-SALAMA Country Chapter Reports	Mr. Koech, Kenya, Prof. Kishimba, Tanzania, Dr. Moges, Ethiopia, Prof. Bashir, Sudan, Prof. Zaranyika, Zimbabwe, Dr. Waswa, Uganda Botswana and Lesotho: Scientists to be named later,
	1530-1600	Tea Break	
	1600-1700	7. Plenary Lecture 3: Presentation by the Zimbabwe Standards Association	
Day 2	0800-0900	1. Plenary lecture 4: Uncertainties in laboratory Measurements: Fundamental definitions and relationships.	Prof. Mark Zaranyika University of Zimbabwe
	0900-1000	2. . Plenary lecture 5: Uncertainties in laboratory Measurements: Some practical examples and solutions	Prof. Geoffrey Kamau University of Nairobi, Kenya.
	1000-1030	3. Health Break	
	1030-1130	4. Plenary Lecture 6 Good Laboratory Practice (GLP) in the Analytical Chemistry Laboratory	1. Prof. N.I Bashir, Sudan 2. Mr. D. Koech, Kenya.
	1130-1200	5. Plenary Lecture 7 Good Laboratory Practice (GLP) in the Microbiological Laboratory.	Dr. Wayne, USA.
	1200-1230	6. Plenary Lecture 8: Waste disposal in Laboratories	Jane Mumbi/Nairobi Water company
	1230-1400	Lunch Break	
	1400-1500	7. Plenary Lecture 9 Laboratory Instruments: Purchasing, maintance and calibration	Prof. Mathew Nindi University of S. Africa, Pretoria, S. Africa
	1500-1530	Tea Break	
	1530-1700	8. Panel Discussion 1.	Prof. Kishimba, Kamau, Bashir, Zaranyika; Ms Kisulu
Day 3	0800-1000	1. Oral presentations (20 min. each)	Workshop participants, Instrument Vendors
	1000-1700	2. Excursion	
	1900-2000	3. Workshop Dinner	



Day 4	0800-0900	1. Plenary Lecture 10: Validation of laboratory measurements	Dr. Girma Moges ChemTest Consulting, Addis Ababa, Ethiopia.
	0900-1000	2. Plenary Lecture 11: SADC Proficiency Testing (PT) Scheme	
	1000-1030	3. Health Break	
	1030-1130	3. Plenary lecture 12: PT scheme: The Kenya Experience	Mr. David Keochi, Kenya Bureaux of Standards, Kenya.
	1130-1230	4. Panel Discussion 2	Dr. Moges, Mr. Koechi, Prof. Mbogo, Dr. Njiri
	1230-1400	Lunch Break	
	1400-1500	5. Plenary Lecture 13: Presentation by the Zimbabwe Medicines Control Authority Laboratory.	
	1500-1530	Tea Break	
	1530-1630	6. Plenary Lecture 14: Laboratory Measurements: Sampling and Sample pre-treatment	Prof. Mergesa University of Addis Ababa, Ethiopia.
Day 5	0800-0900	1. Plenary Lecture 15: Laboratory Measurements: Method Development and Validation: GC, GC-MS	Prof. M. Zaranyika University of Zimbabwe
	0900-1000	2. Plenary Lecture 16: Laboratory Measurements: Method Development and Validation: LC, LC-MS	Prof. Mathew Nindi University of S. Africa, Pretoria, S. Africa
	1000-1030	3. Health Break	
	1030-1130	3. Plenary lecture 17: Laboratory Measurements: Development and Validation: ICP, ICP-MS	Dr. Courtie Mahamadi
	1130-1230	4. Plenary Lecture 18 Managing a modern laboratory	Dr. Wayne
	1230-1400	Lunch Break	
	1400-1500	5. Panel Discussion 3.	Panel: Profs Kishimba, Bashir, Kamau, Zaranyika, Mergesa, Nindi; Drs Moges, Wasswa, Mahamadi, Ms ....
	1500-1600	Closing Ceremony.	

## 5. Call for abstracts

Invited speakers are invited to submit abstracts of their presentations. Abstracts should not exceed 300 words and must be submitted to the Workshop secretariat by e-mail. The name of the presenting author, if submitting with co-authors, should be underlined. The institution of author(s), postal address, e-mail, fax and telephone numbers should be included.

## 6. Registration

The deadline for registration is September 30, 2011. Registration fees are as follows:

Participants:	US\$350.00
Students:	US\$200.00

Registration fees will cover Conference room charges, morning and afternoon teas and lunch during the days of the conference.

## 7. Important dates

Deadline for abstracts: 31 August 2011  
Deadline for registration: 30 September 2011

## 8. Exhibitors

Companies interested in exhibiting their equipment or wares, or in holding vendor workshops, demonstrations or seminars, are invited to send their inquiries to the Conference Secretariat.

## 9. Excursion

Wednesday November 30, 2011, 1000 hrs onwards will be devoted to an excursion viewing the mighty Victoria Falls.

## 10. Traveling to Victoria Falls

Victoria falls can be reached by air from Johannesburg, Harare, Bulawayo. Workshop participants can make their own arrangements or contact the Workshop secretariat for assistance. Delegates from countries that are required to have Visas in order to enter Zimbabwe are advised to contact the Workshop Secretariat as soon as possible.

## 11. Accommodation at Victoria Falls

There are several hotels and lodges in Victoria falls Town. Charges range from about US\$45.00 to US\$250.00 for bed and breakfast. Self catering lodges are also available, delegates can contact the Workshop Secretariat for more information. The following hotels and lodges are offering special reduced rates for conference participants:

## 12. Contact Details

For further details, visit the conference website at <http://www.uz.ac.zw/science/chemistry/esaecc/index>

Or

Contact the Workshop Secretariat, e-mail address: [esalama@science.uz.ac.zw](mailto:esalama@science.uz.ac.zw)

Or

Prof. M.F. Zaranyika, Chairman, Local Organizing Committee,

E-mail address: [Zaranyika@science.uz.ac.zw](mailto:Zaranyika@science.uz.ac.zw)

Or

Ms M. Pagare, Secretary, Local organizing Committee,

E-mail address: [mpagare@science.uz.ac.zw](mailto:mpagare@science.uz.ac.zw)

## 9<sup>th</sup> East and Southern Africa Environmental Chemistry and Theoretical Chemistry in Africa Forum

3<sup>rd</sup> – 7<sup>th</sup> October, 2011

East and Southern Africa Environmental Chemistry and Theoretical Chemistry in Africa Forum will be hosting the 9th International conference from 3<sup>th</sup> to 7<sup>th</sup> October, 2011 in Mombasa, Kenya.



### 1<sup>st</sup> Announcement

**Preamble:** East and Southern Africa Environmental Chemistry (ESAEC) and Theoretical Chemistry in Africa (TCA) Forum is held bi-annually but rotate among the countries in the region. The overall objective of this forum is to address issues related to environment and theoretical chemistry in the region.

**Theme:** **SCIENCE AND TECHNOLOGY: SOLUTIONS FOR DEVELOPMENT IN AFRICA**

**Abstracts:** Those willing to present papers or posters should send an abstract of not more than 300 words in English, typed in Times New Romans, font 12 spacing 1.5. A soft copy in MS- word ('97- 2003) should be received by 30th May, 2009 via e-mail: [mdoe@chem.udsm.ac.tz](mailto:mdoe@chem.udsm.ac.tz) and copy to: [cmnguta@gmail.com](mailto:cmnguta@gmail.com) and [gnkamau@uonbi.ac.ke](mailto:gnkamau@uonbi.ac.ke)

The abstract should outline aims, content and conclusions. It should include the title, author's names, affiliated institutions, e-mail address and telephone numbers. Authors of accepted abstracts will be informed by 30<sup>th</sup> May, 2011. Full papers of accepted abstracts should be received by 30th June, 2009.

Look out for more details in the second call for papers.

## SPONSORS

**We welcome financial support from donors for partial or full support. The support of participants and sponsorship towards the organization of the conference will be highly appreciated. The organizers of the conference acknowledge support from:**  
[Public Universities](#)

## INTRODUCTION

The idea for the East and Southern Africa Environmental Chemistry Workshop (ESAECW) and the Sixth Theoretical Chemistry Workshop in Africa (TCWA) was first mooted in 1992 in Botswana during the International Conference in Chemistry in Africa (ICCA). The two first workshops were held in 1995, while subsequent ones were held in 1997, 1999, 2001 and 2003, 2005 and 2007. The two workshops are held simultaneously every two years. The last three workshops were held in Namibia: 5<sup>th</sup>-9<sup>th</sup> of December 2005 and Zimbabwe: 3<sup>rd</sup>-7<sup>th</sup> of December 2007 and Mombasa: 5<sup>th</sup> – 9<sup>th</sup> of October 2009.

### **Local Organizing Committee:**

To be announced later.

### **International Advisory Committee**

Dr. J.E.G. Mdoe, Tanzania  
Prof. Michael Kishimba, Tanzania  
Prof. E. Kiremire Namibia  
Prof. L. Mamino South Africa  
Prof. M. Zaranyika Zimbabwe  
Prof. Catherine Ngila, South Africa  
Prof. S. Mbogo Tanzania  
Dr. J. Mwaura U.S.A.  
Dr. C. Kivuti U.S.A.  
Prof. Jan Boeyens South Africa  
Dr. S. Nyanzi Uganda  
Dr. Nugussie Megersa, Ethiopia  
Prof. N. Basir Sudan  
Prof. S.M. Kagwanja, Kenya  
Prof. Z.M. Getenga, Kenya  
Prof. G.N. Kamau, Kenya

### **FIRST ANNOUNCEMENT AND CALL FOR ABSTRACTS**

**THE 9<sup>TH</sup> EAST AND SOUTHERN AFRICA ENVIRONMENTAL CHEMISTRY  
(ESAEC)  
AND  
THE 9<sup>TH</sup> THEORETICAL CHEMISTRY IN AFRICA  
CONFERENCE**

**VENUE:** Dar es Salaam, Tanzania  
**DATES:** 3<sup>rd</sup> – 7<sup>th</sup> October, 2011

### **THEME**

**SCIENCE AND TECHNOLOGY: SOLUTIONS FOR DEVELOPMENT AFRICA.**

#### **1. Objectives**

To bring together scientists, particularly from Africa, for exchange of ideas and research results in the fields of theoretical chemistry, environmental chemistry and related fields.

To foster collaboration among scientists from Africa and also enhance collaboration among scientists at international level.

**3. Areas to be covered:**

**All areas in Chemistry and related fields covered.**

## ***JOURNAL ARTICLES***

Adsorption of carbaryl by a river sediment from an acetone solution: Apparent thermodynamic properties  
*M. F. Zaranyika and P. Ncube*

Estimation of binding ratio between colloidal gold particles and thiourea from surface studies  
*S. A. Mbogo; A.Y. Ngenya; L. L. Mkayula; J. M. Pratt Ramón Vilar-Compte*

Model for the estimation of initial conditions in a conflict environment

*V.O. Omwenga, M.M. Manene and \*C.B. Singh*

Initial correlations among the levels of various nutrient species in water from Nairobi dam, Kenya

*P. G. Muigai, P. M. Shiundu, F. B. Mwaura and G. N. Kamau*

Creation of the universe from a non classical space-time state

*M. G. Okeyo, M. N. Maonga, M. J. Otieno*

Electron transfer properties of 2-acetylferrocenyl-2-thiophenecarboxylsemicarbazone and its copper (ii) complex

*P. M. Guto, J. M. Kiratu, L. S. Daniel, E. M. R. Kiremire, G. N. Kamau*

## **REFEREES**

Dr. K. AL-Sabati (Canada), Prof. J. Barongo (Kenya), Prof. C. R. Das (India), Prof. T. C. Davis (Nigeria), Dr. S. Derese (Kenya), Prof. R. O. Genga (Kenya), Dr. De. L. N. Gwaki (Kenya), Prof. S. M. Kagwanja (Kenya), Prof. C. N. Warui (Kenya), Prof. E. M. R. Kiremire (Namibia), Prof. M. Kishimba (Tanzania), Dr. M. Kumar (Kenya), Dr. H. M. Kwaambwa (Botswana), Prof. M. Mammino (South Africa), Dr. S. A. Mbogo (Tanzania), Dr. G. Morris (U. S. A), Dr. B. Munge (U. S. A), Prof. J. B. Mwaura (Kenya), Dr. J. C. Ngila (South Africa), Prof. L. W. Njenga (Kenya), Dr. N. C. Njoroge (Kenya), Prof. W. M. Njue (Kenya), Dr. F. Njui (Kenya), Dr. S. Nyanzi (Uganda), Dr. M. Schaible (U. S. A), Dr. R. Schulz (Australia), Prof. P. M. Shiundu (Kenya), Dr. J. B. Sreekanth (South Africa), Prof. A. H. S. El-Busaidy (Kenya), Prof. H. Ssekaalo (Uganda), Prof. Dr. A. K. Yagoub (Sudan), Dr. A. O. Yusuf (Kenya), Prof. A. Yenesew (Kenya), Prof. M. Zaranyika (Zimbabwe) and Prof. H. Zewdie (Ethiopia).